Interactions of Molecules and the Properties of Crystals

by

Thomas Daniel Leigh McConnell

A thesis submitted in partial fulfilment of the requirements of the University of London for the degree of Doctor of Philosophy.

The Christopher Ingold Laboratories

Department of Chemistry

University College London

September 1991

Abstract

In this thesis the basic theory of the lattice dynamics of molecular crystals is considered, with particular reference to the specific case of linear molecules. The objective is to carry out a critical investigation of a number of empirical potentials as models for real systems. Suitable coordinates are introduced, in particular vibrational coordinates which are used to describe the translational and rotational modes of the free molecule. The Taylor expansion of the intermolecular potential is introduced and its terms considered, in particular the (first-order) equilibrium conditions for such a system and the (second-order) lattice vibrations. The elastic properties are also considered, in particular with reference to the specific case of rhombohedral crystals. The compressibility and a number of conditions for elastic stability are introduced.

The total intermolecular interaction potential is divided into three components using perturbation methods, the electrostatic energy, the repulsion energy and the dispersion energy. A number of models are introduced for these various components. The induction energy is neglected. The electrostatic interaction is represented by atomic multipole and molecular multipole models. The repulsion and dispersion energies are modelled together in a central interaction potential, either the Lennard-Jones atom-atom potential or the anisotropic Berne-Pechukas molecule-molecule potential. In each case, the Taylor expansion coefficients, used to calculate the various molecular properties, are determined.

An algorithm is described which provides a relatively simple method for calculating cartesian tensors, which are found in the Taylor expansion coefficients of the multipolar potentials. This proves to be

particularly useful from a computational viewpoint, both in terms of programming and calculating efficiency.

The model system carbonyl sulphide is introduced and its lattice properties are described. Suitable parameters for potentials used to model the system are discussed and the simplifications to the Taylor expansion coefficients due to crystal symmetry are detailed. Four potential parameters are chosen to be fitted to four lattice properties, representing zero, first and second order Taylor expansion coefficients. The supplementary tests of a given fitted potential are detailed. A number of forms for the electrostatic interaction of carbonyl sulphide are considered, each combined with a standard atom-atom potential. The success of the molecular octupole model is considered and the inability of more complex electrostatic potentials to improve on this simple model is noted. The anisotropic Berne-Pechukas potential, which provides an increased estimate of the compressibility is considered as being an improvement on the various atom-atom potentials.

The effect of varying the exponents in the atom-atom (or molecule-molecule) potential, representing a systematic variation of the repulsion and dispersion energy models, is examined and a potential which is able to reproduce all of the given lattice properties for carbonyl sulphide is obtained.

The molecular crystal of cyanogen iodide is investigated. Superficially it is similar to the crystal of carbonyl sulphide and the potentials used with success for the latter are applied to cyanogen iodide to determine whether they are equally as effective models for this molecule. These potentials are found to be far less successful, in all cases yielding a number of unrealistic results. Reasons for the failure of the model are considered, in particular the

differences between the electrostatic properties of the two molecules are discussed. It is concluded that some of the simplifications which proved satisfactory for carbonyl sulphide are invalid for simple extension to the case of cyanogen iodide.

A first estimate of the differences in the electrostatic properties is attempted, calculating the induction energies of the two molecules. The assumption that the induction energy may be neglected is justified for the case of carbonyl sulphide but found to be far less satisfactory for cyanogen iodide.

Finally details of ab initio calculations are outlined. The amount of experimental data available for the electrostatic properties of the two molecules under consideration is relatively small and the experimental data which is available is supplemented by values obtained from these calculations.

Acknowledgements

I would like to thank my supervisor, Dr Stuart Walmsley for his encouragement, understanding and guidance during my time at University College London.

I would also like to thank my many friends, staff and students, for their teaching and friendship during my seven years in the Chemistry Department. In particular I must thank Prof. Max McGlashan for his award of a studentship from the Science and Engineering Research Council to fund this work.

I must express my gratitude to Janice Shackleton, Jonathan Jenkins and Mario Mariani. Their friendship, support and advice ensured that my days in G25 were always enjoyable and the many aspects of life kept in perspective.

Finally, I must offer my thanks to my parents and family for their love and support throughout the years. Whilst it has never been expected that I should consider this a debt to be repaid, I would like to dedicate this thesis to them as a token of my gratitude.

Contents

List of Figures

List of Tables

The primary objective of this thesis is to investigate a number of empirical potentials which are to be used as theoretical models for molecular crystals. The general procedure involves choosing a crystal for which a number of structural and vibrational properties have been experimentally measured and fitting the empirical potential to these properties. In general only a fraction of the potential parameters have been used in the fitting procedure, which has been carried out using least squares techniques. Similarly only a fraction of the molecular properties have been fitted directly by the procedure. Attempting to increase the number of parameters to be varied (and hence the number of properties to be fitted) would be a counterproductive procedure. For a larger set it would be unlikely that any successful fitting could be achieved and there would be no clear indication as to the reasons for the failure of the fitting procedure. It is more effective to fit a small number of parameters and then, using these fitted parameters, to calculate a number of other known molecular properties whose values provide a critical test of a given empirical potential.

The requirement that a small number of parameters (and properties) are to be used in the fitting procedure ensures that the crystals to be examined need to be relatively simple, so that the parameters chosen have realistic interpretation. Indeed, one of the conditions required of the empirical potentials is that their parameters should be physically realistic. The focus of attention in this thesis is on the molecular crystal of carbonyl sulphide and the objective is to find and critically analyse a number of empirical potentials acting as models for this system. Carbonyl sulphide is an ideal crystal, the

molecule is small enough to permit a relatively simplistic fitting procedure but a large number of the crystal properties have been experimentally measured and consequently provide a number of critical tests for an empirical potential.

The empirical potential is generally divided into a number of separate terms, each of which models a different interaction within the molecular crystal. This separation is derived from a general perturbation treatment of the overall interaction. A number of forms for each of these components is considered, the procedure employed being such that each of the individual interactions is investigated separately. In each case a standard form for the other components is employed so that a simple analysis may be performed.

The potentials obtained with varying success for carbonyl sulphide are then applied to the molecular crystal cyanogen iodide, whose structure is similar to the former so that the transferability of these potentials to other systems may be examined.

One problem which is encountered within this thesis is the relative lack of experimental data available concerning the electrical properties of the molecules under consideration. To this end a number of ab initio calculations have been performed using the now-defunct Amdahl 5890 supercomputer at the University of London Computer Centre with the aim of providing suitable values for properties such as the molecular multipole moments, distributed multipole analyses and molecular polarizabilities.

The lattice dynamical calculations detailed within this thesis have been performed using a number computer programs written, in the Fortran (77) language, specifically for this purpose. The calculations have been performed on a number of systems; the GEC 4100 series minicomputers (Euclid), the Pyramid 98x minicomputer and the Sun

Workstations all at the University College London Computer Centre plus the Amdahl 5890 previously mentioned. Although all of these computers are now defunct the programs may also be run on the Bloomsbury Computing Consortium Central Timesharing Service with a small number of modifications required to translate from non-standard Fortran 77. Development of these programs and algorithms for increase computational efficiency were a significant element of the work presented here. Much of the computational framework was based on earlier programs due to R.G. Della Valle and P.F. Fracassi, originally at the University of Florence.

2.1: Introduction

Lattice dynamics is a long established branch of solid state physics and its basic theories have been extensively described by Born and Huang[1]. In particular their work is concerned with crystals consisting of atomic and ionic units and when considering molecular crystals there are certain aspects which much be taken into account when constructing a suitable lattice dynamical theory. These basic theories have been developed by a number of authors[2-5] but the theory outlined in this thesis is based upon the work of Walmsley[2a,5a] and the only aspects of the theory which are outlined here are those which are relevant to the work presented within this thesis.

This chapter is divided into three sections, the first of which describes the approximations which are inherent to the theory. The second describes a number of coordinate systems which are used within the theoretical treatment while the third details the basic lattice properties with which this thesis is concerned.

2.2: Fundamental Approximations

Born Oppenheimer Approximation

The quantum mechanical basis of lattice dynamics rests on the Born-Oppenheimer approximation. For a system comprised of nuclei and electrons the Hamiltonian may be written:

$$H_c = T_N + T_E + V \qquad (2.2.1)$$

where T_N and T_E are the set of kinetic energy operators for the nuclei and electrons and V is the set of Coulomb interaction terms.

The first step in the Born-Oppenheimer approximation is to neglect the kinetic energy of the nuclei, on the basis that the kinetic energy is inversely proportional to the nuclear mass and thence solve the electronic problem for a fixed nuclear configuration. For example the variation of the lowest electronic energy with the nuclear configuration defines a function ϕ which under the scheme of the Born-Oppenheimer approximation acts as an effective potential energy function for the motion of the nuclei. It is this part of the procedure which is considered in detail within this thesis and the corresponding Hamiltonian may be written:

$$H = T_N + \phi \qquad (2.2.2)$$

with wavefunctions which are dependent upon the nuclear coordinates.

Rigid Molecule Approximation

The most outstanding feature of molecular crystals is that their component molecules persist virtually unchanged when the crystal melts, illustrating that the forces between the atoms within a single molecule (the intramolecular interactions) are much stronger than the forces between different molecules (the intermolecular interactions). The properties of molecular crystals tend to be divided into two subgroups dependent upon the type of interaction concerned. The first set are those molecular properties which are relatively unaffected by the state of condensation and the second set are those crystal properties which are characteristic of the solid state.

A similar situation exists for the molecular and crystal vibrations. Molecular vibrations are generally high in magnitude and are relatively unaffected by the state of condensation whereas the crystal vibrations, which arise through the loss of molecular translational and rotational degrees of freedom are much smaller in magnitude and

are modified greatly when the crystal melts.

With the significant differences in magnitude between the molecular properties and the crystal properties the interaction between the two types is relatively small and as a first approximation these interactions are set to zero, so that considerations of the crystal properties are effectively considerations of a lattice of rigid molecules.

In the basic Hamiltonian (2.2.2), T_N becomes the kinetic energy of the rigid molecules and ϕ is the intermolecular potential energy function.

Molecule Pair Approximation

To proceed further assumptions must be made about the form of the intermolecular potential energy function. As much of the information available concerning the interactions of molecules comes from experimental measurements on low temperature gases or theoretical calculations of pairs of molecules, the crystal potential energy is usually expressed as a sum of molecule-pair interactions, written as follows:

$$\phi = \frac{1}{2} \sum_{ij} \left[ij\right] \qquad (2.2.3)$$

where it is assumed that $\left[ii\right]$ is formally a function which is zero everywhere and whose derivatives are always zero.

Harmonic Approximation

Following the Born treatment the intermolecular potential energy function ϕ may be expanded as a Taylor Series. The precise form of the coordinates chosen is given in the next section but in general terms they may be written:

$$u_\alpha^i = X_\alpha^i - X_\alpha^{i0} \qquad (2.2.4)$$

where the superscript i labels the molecule with which the coordinate is associated and α labels the coordinate type within this molecule. X is the value of the coordinate, X^0 is the value of this coordinate at a given reference configuration and u is a displacement coordinate with respect to this reference.

In the case of a rigid molecule there are six coordinates, corresponding to the three translational and three rotational degrees of freedom of the isolated molecule. Throughout this thesis, attention is confined to linear molecules. The number of coordinates per molecule is reduced to five, there being only two rotational degrees of freedom for an isolated linear molecule. In the next section the choices for these five coordinates will be described. The Taylor expansion has the form:

$$\phi = \phi_0 + \sum_{\alpha i} \phi_\alpha(i)\, u_\alpha^i + \frac{1}{2} \sum_{\alpha i} \sum_{\beta j} \phi_{\alpha\beta}(ij)\, u_\alpha^i\, u_\beta^j + \ldots. \tag{2.2.6}$$

in which for example the term $\phi_\alpha(i)$ is defined by:

$$\phi_\alpha(i) = \left[\frac{\partial \phi}{\partial u_\alpha^i}\right]_0 \tag{2.2.7}$$

In the Harmonic Approximation terms other than quadratic are neglected. The effect of cubic and higher order terms is assumed to be small. Linear terms vanish provided that the reference configuration is at a minimum in the energy and the constant term is absorbed into the energy. In this way the Taylor expansion becomes:

$$\phi - \phi_0 = \frac{1}{2} \sum_{\alpha i} \sum_{\beta j} \phi_{\alpha\beta}(ij)\, u_\alpha^i\, u_\beta^j \tag{2.2.8}$$

2.3: Vibrational Coordinates

The work within this thesis concerns crystals comprised of linear molecules only and as discussed above these crystals possess only five degrees of vibrational freedom. The most logical representation of these degrees of freedom is to choose coordinates such that three represent changes of position (the three translational degrees of freedom) and two represent changes of orientation (the rotational degrees of freedom). The first set are chosen to be changes of the position of the molecular centre of mass and are represented by Cartesian displacements. The second set are more complicated and may be represented by a number of coordinate systems. Walmsley[2a] has outlined a number of systems but attention here is restricted to direction cosine coordinates.

Cartesian Displacement Coordinates

The displacement coordinates usually used to represent the three translational degrees of freedom associated with the isolated molecule are translational coordinates locating the centre of mass of the molecule. The three Cartesian displacement coordinates are introduced:

$$u_\alpha^i = R_\alpha^i - R_\alpha^{i0} \quad ; \quad \alpha = 1,2,3 \qquad (2.3.1)$$

where R locates the centre of mass of the molecule. These coordinates are often represented as t_α^i.

Direction Cosine Coordinates

Two further displacement coordinates are required corresponding to the two rotational degrees of freedom associated with the isolated molecule and these will represent the changes in orientation of the molecule within the lattice. Walmsley[6,7] has introduced a convenient method of representing the orientation of a molecule. This method uses the direction cosines relating the relative orientation of the

Cartesian crystal fixed (external) axes and the Cartesian molecule fixed axes.

The orientation of a linear molecule, labelled i, within a crystal may be described by the set of direction cosines represented by Λ_α^i, the direction cosine relating the α'th crystal fixed axis and the molecular axis (strictly the direction cosine Λ_α^i should be written as $A_{\alpha z}^i$ but the z subscript, which conventionally is the molecular axis, is normally dropped). A second set of direction cosines are introduced which are represented by λ_β^i, relating to the equilibrium direction of the β'th molecule fixed axis and the actual direction of the molecular axis. The two sets of direction cosines are related as follows:

$$\Lambda_\alpha^i = \sum_\beta \Lambda_{\alpha\beta}^{i0} \lambda_\beta^i \qquad (2.3.2)$$

where $\Lambda_{\alpha\beta}^{i0}$ is the value of the direction cosine relating the α'th crystal fixed axis and the β'th molecule fixed axis at the reference configuration. The direction cosines λ_β^i are related by the relation:

$$\lambda_\beta^i \lambda_\beta^i = 1 \qquad (2.3.3)$$

where the convention has been introduced that repetition of Greek suffices represents repeated summation over the three Cartesian axes (ie $\lambda_\beta^i\lambda_\beta^i \equiv \lambda_x^i\lambda_x^i + \lambda_y^i\lambda_y^i + \lambda_z^i\lambda_z^i$) and this convention should be assumed throughout this thesis. The three direction cosines of the form λ_α^i are not independent, noting (2.3.4) the direction cosine λ_z^i can be expressed in terms of the other two direction cosines such that:

$$\lambda_z^i = \left(1-\lambda_x^{i\,2}-\lambda_y^{i\,2}\right)^{1/2} \qquad (2.3.4)$$

The first and second derivatives of Λ_α^i with regard to λ_β^i at the reference configuration may be obtained and the expressions for these

are as follows:

$$\left(\frac{\partial \Lambda_{\alpha}^{i}}{\partial \lambda_{\beta}^{i}}\right)_{0} = \Lambda_{\alpha\beta}^{i0} \tag{2.3.5}$$

$$\left(\frac{\partial^2 \Lambda_{\alpha}^{i}}{\partial \lambda_{\beta}^{i} \partial \lambda_{\gamma}^{i}}\right)_{0} = -\delta_{\beta\gamma}\, \Lambda_{\alpha z}^{i0} \tag{2.3.6}$$

Finally it may be noted that at the reference configuration the direction cosines defined have the values:

$$\lambda_{x}^{i0} = \lambda_{y}^{i0} = 0; \tag{2.3.7}$$

$$\lambda_{z}^{i0} = 1 \tag{2.3.8}$$

As the direction cosines λ_{x}^{i} and λ_{y}^{i} are both zero at the reference configuration these are therefore the two remaining displacement coordinates required. Hence:

$$u_{\alpha}^{i} = \lambda_{\alpha}^{i} \quad ; \quad \alpha = 4,5 \tag{2.3.9}$$

Symmetry Coordinates

In lattice dynamics a crystal is considered as being comprised of a number of identical units which are referred to as unit cells. The regular arrangement of these units determines the symmetry of the crystal which may be described by a space group. The properties of space groups and their irreducible representations have been detailed by Califano, Schettino and Neto[3]. The symmetry of the crystal can be exploited when considering the Taylor expansion of the potential, as the Taylor series possesses the same symmetry as the configuration about which the expansion is being made.

A space group is described by subgroups of translational operators $\mathcal{T}$ which describe the periodic nature of the crystal lattice. These translational operators represent linear displacements of the crystal

and are defined relative to an externally fixed origin. These translational operators are defined as being combinations of the vectors which define the unit cell of the lattice and can be expressed as follows:

$$\underset{\sim}{T}_{n} = n_1\underset{\sim}{a}_1 + n_2\underset{\sim}{a}_2 + n_3\underset{\sim}{a}_3 \qquad (2.3.10)$$

where the vectors $\underset{\sim}{a}_i$ are the vectors defined by the sides of the unit cell of the lattice in question; n_i are integers and n represents the three integers which characterise a particular operator.

Born and von Karman[8] introduced cyclical boundary conditions which may written in terms of the elements of $\mathcal{T}$ as follows:

$$\underset{\sim}{T}_{n_1,n_2,n_3} \equiv \underset{\sim}{T}_{n_1+N_1,n_2,n_3} \equiv \underset{\sim}{T}_{n_1,n_2+N_2,n_3} \equiv \underset{\sim}{T}_{n_1,n_2,n_3+N_3} \qquad (2.3.11)$$

The numbers N_1, N_2 and N_3 are large but finite and $\mathcal{T}$ is the cyclical group of order $N_1 \times N_2 \times N_3$. Therefore each of the integers n_i cycle through a period of length N_i. A number of ranges may be chosen but the most convenient is:

$$n_i = 0, \pm 1, \ldots, + \frac{1}{2} N_i. \qquad (2.3.12)$$

The group $\mathcal{T}$ is Abelian and has three independent cycles based upon $\underset{\sim}{a}_1$, $\underset{\sim}{a}_2$ and $\underset{\sim}{a}_3$. The irreducible representations of a group such as this are all one dimensional and there are $N_1 \times N_2 \times N_3$ of them. These characters may be written as follows:

$$\chi^{(\underset{\sim}{y})}(\underset{\sim}{T}_n) = \exp\,[2\pi i \underset{\sim}{y}\cdot\underset{\sim}{T}_n] \qquad (2.3.13)$$

where the vector $\underset{\sim}{y}$ labels the representation and may be written in terms of the basis $\underset{\sim}{b}_i$, which is the set of vectors reciprocal to the set of vectors $\underset{\sim}{a}_i$. These are defined as follows:

$$\underset{\sim}{b}_i = \frac{1}{v} (\underset{\sim}{a}_j \times \underset{\sim}{a}_k) \qquad (2.3.14)$$

where i, j and k are in the cyclical order 1, 2, 3 and v is the volume of the parallelepiped bounded by the vectors $\underset{\sim}{a}_i$, ie the volume of the unit cell.

The vector $\underset{\sim}{y}$ is generally known as the wave-vector and is also often identified by $\underset{\sim}{k}$ instead. The space defined in terms of these reciprocal lattice vectors is often referred to as k-space. The full set of independent wave-vectors is found within the first Brillouin zone of the crystal. The vector $\underset{\sim}{y}$ has the components in the reciprocal basis y_i which are defined by:

$$y_i = K_i / N_i \qquad (2.3.15)$$

where $K_i = 0, \pm 1, \ldots, \frac{1}{2} N_i$.

For a molecular crystal each molecule i, within the crystal can be labelled by the coordinate u_α^i, where α labels the components of the externally fixed coordinate system. To take advantage of the translational symmetry of the crystal the index i labelling the molecule is replaced by a double index $u_\alpha\begin{pmatrix} l \\ k \end{pmatrix}$, where l labels the unit cell and k labels the molecule within the unit cell. Standard projection operator procedure yields the symmetry coordinates:

$$u_\alpha\begin{pmatrix} \underset{\sim}{y} \\ k \end{pmatrix} = N^{-1/2} \sum_l \exp\left[-2\pi i \underset{\sim}{y} \cdot \underset{\sim}{x}(l)\right] u_\alpha\begin{pmatrix} l \\ k \end{pmatrix} \qquad (2.3.16)$$

where $\underset{\sim}{x}(l)$ is the vector with components $\underset{\sim}{t}_i$ locating the unit cell l. This symmetry coordinate forms the basis for the irreducible representation $\underset{\sim}{y}$ of $\mathcal{T}$.

2.4: Theory for the Lattice Dynamics of Molecular Crystals

It has been shown in section (2.2) how the intermolecular pair potential can be expressed as a Taylor series up to second order. Each element of the Taylor series can be shown to represent a different lattice property. The leading term, ϕ_0 represents the total energy of the lattice at the reference configuration, the first order terms represent forces and torques acting on the molecules at the reference configuration while the second order terms represent the vibrations within the lattice.

Equilibrium Conditions

It has already been discussed that for the observed crystal structure to be at a stable equilibrium the reference configuration needs to be chosen such that the linear terms in the Taylor expansion of the intermolecular potential function disappear. For this condition to be satisfied the potential for each molecule within the lattice must be force-free in each direction. In the case of the infinite lattice model each unit cell is considered as being within an identical environment and therefore as long as each molecule within one unit cell is force-free then every unit cell and hence the whole crystal will be force-free. In terms of the notation given previously there will be 3n of these conditions. These may be expressed as follows:

$$\phi_\alpha\left(1k\right) = 0 \qquad (2.4.1)$$

Only one value of 1 (ie only one unit cell) need be considered.

One further consequence of the infinite lattice model is that the equilibrium conditions defined by (2.4.1) are incomplete. If the lattice is considered as being infinite then the forces acting on any single point due to the other molecules in any one direction will be

exactly balanced by the equivalent molecules in the opposite direction. Born and Huang[1] have shown that the additional equilibrium conditions required are that the crystal must be free from stress. If the crystal is considered as being a homogeneous macroscopic body then the stress is a measure of the forces due to a small change in the dimensions of the crystal itself (known as a strain). If the crystal is to be free from stress then the unit cells of the crystal must be free from stress and therefore their dimensions must be minimised with respect to the potential.

The symmetry of a given system may well lead to simplifications, for example any stress which is associated with a strain whose coordinate is not totally symmetric is automatically zero. Similarly any strain which automatically lowers the symmetry of the crystal under consideration will ensure that the associated stress is zero.

Lattice Vibrations

The second order terms in the Taylor expansion of the intermolecular potential function are non-vanishing and are of the form:

$$\sum_{\alpha,l,k} \sum_{\beta,l',k'} \phi_{\alpha\beta}\left(lk\ l'k'\right) u_\alpha\begin{pmatrix} l \\ k \end{pmatrix}\ u_\beta\begin{pmatrix} l' \\ k' \end{pmatrix} \qquad (2.4.2)$$

This may transformed so that it is expressed in terms of the symmetry adapted coordinates introduced in section (2.3) as follows:

$$\sum_{\underset{\sim}{y}} \sum_{k,k'} \sum_{\alpha,\beta} \phi_{\alpha\beta}\left(\underset{\sim}{y}\ k\ k'\right)\ u_\alpha\begin{pmatrix} \underset{\sim}{y} \\ k \end{pmatrix}\ u^*_\beta\begin{pmatrix} \underset{\sim}{y} \\ k' \end{pmatrix} \qquad (2.4.3)$$

The kinetic energy for this system in terms of these coordinates is given by:

$$T = \frac{1}{2} \sum_{\underset{\sim}{y}} \sum_{\alpha,k} K_\alpha(k)\ \dot{u}^*_\alpha\begin{pmatrix} \underset{\sim}{y} \\ k \end{pmatrix}\ \dot{u}_\alpha\begin{pmatrix} \underset{\sim}{y} \\ k \end{pmatrix} \qquad (2.4.4)$$

where $K_\alpha(k)$ is a general mass factor. For translational coordinates this factor is the molecular mass, for orientational coordinates this factor is the molecular moment of inertia as follows:

$$K_\alpha(k) = \begin{cases} M(k); & \alpha = 1,2,3 \\ I(k); & \alpha = 4,5 \end{cases} \qquad (2.4.5)$$

The following secular determinant may then be formed:

$$\left| \phi_{\alpha\beta}\left(\underset{\sim}{y}\ k\ k'\right) - \omega^2\ K_\alpha(k)\ \delta_{\alpha\beta}\ \delta_{kk'} \right| = 0 \qquad (2.4.5)$$

There are N of these secular determinants to be solved each of order 3n, where N is the number of distinct values that $\underset{\sim}{y}$ runs through according to the cyclical boundary conditions discussed in section (2.3). For a system in which the rigid molecule approximation is being used the solutions of the secular equations ω^2 are the lattice vibration frequencies. Those belonging to the zero wave-vector ($\underset{\sim}{y}$=0) are of particular significance for Raman and infra-red spectroscopy.

These lattice vibration frequencies provide further information about the lattice structure. If the lattice is to be stable then all of the frequencies must be real (ie the corresponding second derivatives must be positive). For coordinates which are not totally symmetric it has already been mentioned that the first derivatives are automatically zero and therefore provide no information about the stability of the lattice with respect to that particular coordinate. The requirement that the second derivatives of these coordinates must be positive provides a test for the stability of the lattice with respect to these non-symmetric coordinates.

3.1: Introduction

In the previous chapter a number of properties of molecular crystals were discussed whose values could be calculated for a given empirical potential and used as a test of the quality of that potential as a model for a given system. Another property of molecular crystals which can be examined as a test of an empirical potential is the elasticity of the crystal. In this chapter the basic measure of elasticity, the elastic constants of the crystal, will be introduced, the basic theory having been outlined in detail by Huntingdon[9] and a suitable method for their determination will be described for the particular case of rhombohedral crystals.

The elastic constants of rhombohedral crystals such as carbonyl sulphide are in principle quantities which may be experimentally determined by a variety of techniques, including ultrasonic transmission and Brillouin scattering. However experimental values of these constants do not, as yet, appear to have measured for the crystals considered within this thesis. Nevertheless the calculated elastic constants may be used to derive other properties, such as the isothermal compressibility, which have been experimentally determined and to determine whether the system satisfies elastic stability.

3.2: Elasticity Theory

For an unstrained medium the position of each element of volume can be described by a cartesian coordinate system with coordinates x_1, x_2 and x_3. When the material is homogeneously stressed each volume element is subject to a force, with components ΔF_i, at the bounding surface, ΔA_j (perpendicular to the j axis).

The tensor T_{ij} is introduced, defined as the limit as $\Delta A_j \to 0$ of the ratio of ΔF_i to ΔA_j,

$$T_{ij} = \lim_{\Delta A_j \to 0} \left(\frac{\Delta F_i}{\Delta A_j} \right) \qquad (3.2.1)$$

The symmetric part of T_{ij} is the stress tensor, the antisymmetric part is the density of the resultant torque and is generally neglected in elastic theory. The normal stresses, T_{ii} are tensions when positive. The T_{ij} $(i \neq j)$ are the shear stresses.

When the material is strained, each element of volume moves to a new position, the displacement being described by a cartesian coordinate system with coordinates u_1, u_2 and u_3. Using these coordinates the strains, labelled by e_{ij}, have been defined by Love[10] as follows:

$$e_{11} = \frac{\partial u_1}{\partial x_1} ; \qquad e_{22} = \frac{\partial u_2}{\partial x_2} ; \qquad e_{33} = \frac{\partial u_3}{\partial x_3} ;$$

$$e_{23} = \frac{\partial u_2}{\partial x_3} + \frac{\partial u_3}{\partial x_2} ; \quad e_{13} = \frac{\partial u_1}{\partial x_3} + \frac{\partial u_3}{\partial x_1} ; \quad e_{12} = \frac{\partial u_1}{\partial x_2} + \frac{\partial u_2}{\partial x_1} \qquad (3.2.2)$$

The e_{ii} are the normal strains and are positive when the medium is extended. The non-diagonal components of e_{ij} $(i \neq j)$ are the shear strains. Both the stresses and the strains are symmetric to interchange of the subscripts and later in this chapter it will prove to be convenient to replace the double subscript notation by a single subscript notation which is introduced as follows:

Double Subscript	11	22	33	23	13	12
Single Subscript	1	2	3	4	5	6

so that for example e_{12} may be rewritten as e_6.

A further quantity is introduced which relates the stresses and

strains, derived from Thermodynamic calculations, being the stored energy density function w defined as:

$$\delta w = \sum_{i \geq j}^{3} T_{ij} \, \delta e_{ij} \qquad (3.2.3)$$

and δw is a perfect differential so that:

$$T_{ij} = \frac{\partial w}{\partial e_{ij}} \qquad (3.2.4)$$

The usual starting point for elasticity theory is Hooke's law, which states that the stress is proportional to the strain for sufficiently small strains. This relationship may be expressed for an anisotropic medium as follows:

$$T_{ij} = \sum_{k \geq l}^{3} c_{ijkl} \, e_{kl} \qquad (3.2.5)$$

and the constants of proportionality introduced, c_{ijkl} are the elastic constants, otherwise known as the elastic moduli.

In the most general case the array of elastic constants would contain 36 (6×6) independent quantities. However, the requirement that the matrices should be symmetric to interchange of the pairs of double indices reduces this independent number to 21. This condition may be illustrated by considering the tensor T_{ij} expressed in terms of the strain energy density w as follows:

$$c_{ijkl} = \frac{\partial T_{ij}}{\partial e_{kl}} = \frac{\partial^2 w}{\partial e_{kl} \, \partial e_{ij}} = \frac{\partial^2 w}{\partial e_{ij} \, \partial e_{kl}} = \frac{\partial T_{kl}}{\partial e_{ij}} = c_{klij} \qquad (3.2.6)$$

The values of these elastic constants may be illustrated as a 6×6 matrix which is conveniently written in terms of the single subscript notation introduced previously (the indices running from 1 to 6) and illustrated in figure 3.1.

Figure 3.1: General Elastic Constant Matrix

$$\begin{pmatrix} c_{11} & c_{12} & c_{13} & c_{14} & c_{15} & c_{16} \\ c_{12} & c_{22} & c_{23} & c_{24} & c_{25} & c_{26} \\ c_{13} & c_{23} & c_{33} & c_{34} & c_{35} & c_{36} \\ c_{14} & c_{24} & c_{34} & c_{44} & c_{45} & c_{46} \\ c_{15} & c_{25} & c_{35} & c_{45} & c_{55} & c_{56} \\ c_{16} & c_{26} & c_{36} & c_{46} & c_{56} & c_{66} \end{pmatrix}$$

This matrix, which is necessarily symmetric about its leading diagonal is more usually expressed in upper triangular form.

The assumption of linearity between the stress and strain allows the expression for δw (3.2.3) to be integrated to give w, also known as the strain energy density:

$$w = \frac{1}{2} \sum_{i,j \geq 1} T_{ij}\, e_{ij} \qquad (3.2.7)$$

For an elastic medium, the forces on an element of volume are given by the divergence of the stress field as follows:

$$\rho \frac{\partial^2 u_i}{\partial t^2} = \sum_{j=x,y,z} \frac{\partial T_{ij}}{\partial x_j} \qquad (3.2.8)$$

which after substitution of (3.2.5) leads to:

$$\rho \frac{\partial^2 u_i}{\partial t^2} = \sum_{j,k,l=x,y,z} \frac{\partial}{\partial x_j} \left\{ c_{ijkl}\, \frac{1}{2} \left(\frac{\partial u_k}{\partial x_l} + \frac{\partial u_l}{\partial x_k} \right) \right\} \qquad (3.2.9)$$

For the particular case of an elastic plane wave one solution of this equation is given by:

$$u_k = A_k\, e^{i(\omega t - \underset{\sim}{k} . \underset{\sim}{x})} \qquad (3.2.10)$$

where A_k is the amplitude of the vibration component, ω is the angular

frequency related to the wave velocity v by $v = \omega/|\underset{\sim}{k}|$, $\underset{\sim}{k}$ is the wavenumber vector with wavelength $\lambda = 2\pi/|\underset{\sim}{k}|$ and $\underset{\sim}{x}$ is the vector describing the position of the element of the volume with components x_1, x_2 and x_3.

The equations of motion which follow, are known as the Christoffel equations:

$$\rho v^2 A_i = \sum_{j=x,y,z} \sum_{m=x,y,z} \sum_{n=x,y,z} c_{imjn} A_j \hat{k}_m \hat{k}_n \qquad (3.2.11)$$

where $\hat{k}_m$ is the component of the unit wave vector along the cartesian axis m. Solutions for the amplitudes, A exist providing that:

$$\left| \Gamma_{ij} - \rho v^2 \delta_{ij} \right| = 0 \qquad (3.2.12)$$

where Γ_{ij} is defined as:

$$\Gamma_{ij} = \sum_{m=x,y,z} \sum_{n=x,y,z} c_{imjn} \hat{k}_m \hat{k}_n \qquad (3.2.13)$$

The 3×3 matrix formed by these components will be referred to here as the Gamma matrix and is symmetric about its leading diagonal. The individual components are written as follows, where the single suffix notation for the elastic constants is now adopted:

$$\Gamma_{xx} = c_{11}\hat{k}_x^2 + c_{66}\hat{k}_y^2 + c_{55}\hat{k}_z^2 + 2c_{16}\hat{k}_x\hat{k}_y + 2c_{15}\hat{k}_x\hat{k}_z + 2c_{56}\hat{k}_y\hat{k}_z \qquad (3.2.14)$$

$$\Gamma_{yy} = c_{66}\hat{k}_x^2 + c_{22}\hat{k}_y^2 + c_{44}\hat{k}_z^2 + 2c_{26}\hat{k}_x\hat{k}_y + 2c_{46}\hat{k}_x\hat{k}_z + 2c_{24}\hat{k}_y\hat{k}_z \qquad (3.2.15)$$

$$\Gamma_{zz} = c_{55}\hat{k}_x^2 + c_{44}\hat{k}_y^2 + c_{33}\hat{k}_z^2 + 2c_{45}\hat{k}_x\hat{k}_y + 2c_{35}\hat{k}_x\hat{k}_z + 2c_{34}\hat{k}_y\hat{k}_z \qquad (3.2.16)$$

$$\Gamma_{xy} = c_{16}\hat{k}_x^2 + c_{26}\hat{k}_y^2 + c_{45}\hat{k}_z^2 + (c_{12} + c_{66})\hat{k}_x\hat{k}_y + (c_{14} + c_{56})\hat{k}_x\hat{k}_y + (c_{25} + c_{46})\hat{k}_y\hat{k}_z \qquad (3.2.17)$$

$$\Gamma_{xz} = c_{15}\hat{k}_x^2 + c_{46}\hat{k}_y^2 + c_{35}\hat{k}_z^2 + (c_{14} + c_{56})\,\hat{k}_x\hat{k}_y + (c_{13} + c_{55})\,\hat{k}_x\hat{k}_z + (c_{36} + c_{45})\,\hat{k}_y\hat{k}_z \qquad (3.2.18)$$

$$\Gamma_{yz} = c_{56}\hat{k}_x^2 + c_{24}\hat{k}_y^2 + c_{34}\hat{k}_z^2 + (c_{25} + c_{46})\,\hat{k}_x\hat{k}_y + (c_{36} + c_{45})\,\hat{k}_x\hat{k}_z + (c_{23} + c_{44})\,\hat{k}_y\hat{k}_z \qquad (3.2.19)$$

3.3: Elastic Constants and Acoustic Velocities

The relationship between the elastic constants of a crystal and the wave-vectors which correspond to the acoustic waves propagating within a crystal have been illustrated in the previous section by the Christoffel equations (3.2.11) and the relations which follow from it (3.2.12 - 3.2.19). For a rhombohedral crystal, with C_{3v} (3m) space group the effects of symmetry simplify the coefficients of the elastic constant matrix and these simplifications have been extensively described by Bhagavantam[11]. Using these and choosing the cartesian axis system such that the z axis represents the three-fold axis, the x axis lies in the symmetry plane and the y axis is perpendicular to the x and z axes, the full elastic matrix is simplified (and expressed in upper triangular form) as follows:

Figure 3.2: Elastic Constant Matrix for a Rhombohedral Crystal

$$\begin{matrix} c_{11} & c_{12} & c_{13} & 0 & c_{15} & 0 \\ & c_{11} & c_{13} & 0 & -c_{15} & 0 \\ & & c_{33} & 0 & 0 & 0 \\ & & & c_{55} & 0 & -c_{15} \\ & & & & c_{55} & 0 \\ & & & & & \frac{1}{2}(c_{11} - c_{12}) \end{matrix}$$

and it may be seen that for a rhombohedral crystal there are only six independent elastic constants.

As a result of these symmetry simplifications the components of the Gamma matrix given by (3.2.14 - 3.2.19) reduce as follows:

$$\Gamma_{xx} = c_{11}\hat{k}_x^2 + \frac{1}{2}(c_{11} - c_{12})\,\hat{k}_y^2 + c_{55}\hat{k}_z^2 + 2c_{15}\hat{k}_x\hat{k}_z \qquad (3.3.1)$$

$$\Gamma_{yy} = \frac{1}{2}(c_{11} - c_{12})\,\hat{k}_x^2 + c_{11}\hat{k}_y^2 + c_{55}\hat{k}_z^2 - 2c_{15}\hat{k}_x\hat{k}_z \qquad (3.3.2)$$

$$\Gamma_{zz} = c_{55}\hat{k}_x^2 + c_{55}\hat{k}_y^2 + c_{33}\hat{k}_z^2 \qquad (3.3.3)$$

$$\Gamma_{xy} = -2c_{15}\hat{k}_y\hat{k}_z + \frac{1}{2}(c_{11} + c_{12})\,\hat{k}_x\hat{k}_y \qquad (3.3.4)$$

$$\Gamma_{xz} = c_{15}\left(\hat{k}_x^2 - \hat{k}_y^2\right) + (c_{13} + c_{55})\,\hat{k}_x\hat{k}_z \qquad (3.3.5)$$

$$\Gamma_{yz} = (c_{13} + c_{55})\,\hat{k}_y\hat{k}_z - 2c_{15}\hat{k}_x\hat{k}_y \qquad (3.3.6)$$

These are the equations describing the components of the Gamma matrix for a rhombohedral crystal in the direction whose wave-vector has components $\hat{k}_x$, $\hat{k}_y$ and $\hat{k}_z$. For each such direction calculation of the initial slopes of the acoustic branches of the dispersion curves gives three velocities v_1, v_2 and v_3, each of which leads to a separate solution of (3.2.12). For each of these solutions the Christoffel equation may be rewritten such that:

$$\rho v_i^2 A_{i\alpha} = \Gamma_{\alpha\beta} A_{i\beta} \quad ; \quad i=1,2,3 \qquad (3.3.7)$$

and if the values of the amplitudes are normalised these three equations can be rearranged such that they are expressed in terms of the components of the Gamma Matrix, $\Gamma_{\alpha\beta}$ as follows:

$$\Gamma_{\alpha\beta} = \sum_{n=1}^{3} \rho v_n^2 A_{n\alpha} A_{n\beta} \qquad (3.3.8)$$

Consequently by choosing a particular wave-vector direction defined by $\hat{k}_x$, $\hat{k}_y$ and $\hat{k}_z$ the non-zero components of the relevant Gamma matrix can be calculated in terms of the elastic constants using (3.3.1 - 3.3.6). Calculation of the wave velocities and their corresponding amplitudes leads to the numerical values of these components of the Gamma matrix and hence the values of the elastic constants. Three directions are conveniently chosen for this purpose and with the respective Gamma matrices are as follows:

$$\hat{k}_x = 0,\ \hat{k}_y = 0,\ \hat{k}_z = 1 \qquad \begin{pmatrix} c_{55} & 0 & 0 \\ 0 & c_{55} & 0 \\ 0 & 0 & c_{33} \end{pmatrix}$$

$$\hat{k}_x = 0,\ \hat{k}_y = 1,\ \hat{k}_z = 0 \qquad \begin{pmatrix} \frac{1}{2}(c_{11}-c_{12}) & 0 & -c_{15} \\ 0 & c_{11} & 0 \\ -c_{15} & 0 & c_{55} \end{pmatrix}$$

$$\hat{k}_x = 0,\ \hat{k}_y = \sqrt{\tfrac{1}{2}},\ \hat{k}_z = \sqrt{\tfrac{1}{2}} \qquad \begin{pmatrix} \frac{1}{4}(c_{11}-c_{12})+\frac{1}{2}c_{55} & -c_{15} & -\frac{1}{2}c_{15} \\ -c_{15} & \frac{1}{2}(c_{11}+c_{55}) & \frac{1}{2}(c_{13}+c_{55}) \\ -\frac{1}{2}c_{15} & \frac{1}{2}(c_{13}+c_{55}) & \frac{1}{2}(c_{33}+c_{55}) \end{pmatrix}$$

Consideration of these three directions within the Brillouin Zone will yield all six independent elastic constants, the first direction (which elsewhere within this thesis is illustrated by dispersion curves parallel to the molecular C_3 axis for the calculations on the OCS crystal) yields the values for c_{33} and c_{55} (for example in the direction defined by $\hat{k}_x = 0$, $\hat{k}_y = 0$, $\hat{k}_z = 1$; $c_{55} = \Gamma_{xx}$ and $c_{33} = \Gamma_{zz}$). The second direction (elsewhere illustrated by dispersion curves perpendicular to the molecular C_3 axis) yields the values for c_{11}, c_{12} and c_{15}. With the values of these five already determined the the third direction yields the value for the final elastic constant, c_{13}.

3.4: Elastic Properties

It has previously been discussed that the calculated values for the elastic constants cannot be directly compared with experimental values but two other quantities, the compressibility and elastic stability may be derived from these elastic constants and then compared with experimental values as a further test of an empirical potential.

Compressibility

The compressibility of a crystal represents the extent to which a crystal is susceptible to deformation under an external force. The lattice dynamical theory outlined within this work assumes zero temperature and pressure. At high temperatures elastic properties vary rapidly and are approximately proportional to the change in temperature. At lower temperatures variation is slower and at very low temperature variation is effectively temperature independent. This behaviour has been approximately represented by Bondi[12], relating κ_0, the compressibility at zero temperature and pressure and κ_T, the compressibility at temperature T (a quantity which can be measured experimentally) as follows:

$$\kappa_T^{-1} = \kappa_0^{-1} - d\ T \exp\left(-\theta_D^\circ / 2T\right) \qquad (3.4.1)$$

The reciprocal compressibilities are often known as bulk moduli, θ_D° is the Debye temperature at 0 K and d is a constant. The compressibility of a crystal can be expressed in terms of the elastic constants and for a rhombohedral crystal the relationship between the compressibility and the elastic constants is given by:

$$\kappa_T = \frac{c_{11} + c_{12} + 2c_{33} - 4c_{13}}{c_{33}(c_{11} + c_{12}) - 2c_{13}^2} \qquad (3.4.2)$$

Elastic Stability

For a crystal to be stable the strain energy given by (3.2.7) must be positive. This may be rewritten in terms of the elastic constants such that:

$$w = \frac{1}{2} \sum_{i=1}^{3} \sum_{j=1}^{3} \sum_{k=1}^{3} \sum_{l=1}^{3} c_{ijkl}\, e_{ij}\, e_{kl} \qquad (3.4.3)$$

For the strain energy to be positive the determinant of the matrix of elastic moduli must be positive definite for all values. This is the condition for elastic stability:

$$|c| \geq 0 \qquad (3.4.4)$$

where c is the symmetric 6×6 matrix of elastic constants. For a rhombohedral crystal it was shown in section 3.3 how the elastic constant matrix can be simplified and the full expression for elastic stability of a rhombohedral crystal is written as follows:

$$\begin{vmatrix} c_{11} & c_{12} & c_{13} & 0 & c_{15} & 0 \\ c_{12} & c_{11} & c_{13} & 0 & -c_{15} & 0 \\ c_{13} & c_{13} & c_{33} & 0 & 0 & 0 \\ 0 & 0 & 0 & c_{55} & 0 & -c_{15} \\ c_{15} & -c_{15} & 0 & 0 & c_{55} & 0 \\ 0 & 0 & 0 & -c_{15} & 0 & \frac{1}{2}(c_{11} - c_{12}) \end{vmatrix} > 0 \qquad (3.4.5)$$

This determinant may be factorised and leads to four independent conditions for elastic stability which are as follows:

$$S_1 = c_{33} > 0 \qquad (3.4.6)$$

$$S_2 = c_{55} > 0 \qquad (3.4.7)$$

$$S_3 = c_{33}(c_{11} + c_{12}) - 2c_{13}^2 > 0 \qquad (3.4.8)$$

$$S_4 = c_{55}(c_{11} - c_{12}) - 2c_{15}^2 > 0 \qquad (3.4.9)$$

where the quantities S_1, S_2, S_3 and S_4 have been introduced and are referred to as stability constants elsewhere in this thesis.

4.1: Introduction

Any empirical potential function which is used to model the interactions within a molecular crystal needs to be able to account for both long and short range interactions, the theories of which have been discussed by Buckingham[13].

Long range interactions are considered as being those interactions for which the electron overlap between the two molecules is negligible. Using standard quantum mechanical perturbation theory the ground-state energy of a pair of molecules may be developed as a perturbation series. The first order perturbation energy is known as the electrostatic energy and represents the Coulomb interaction between the two ground-state molecular charge distributions. This contribution may be positive or negative dependent upon the form of the molecular charge distributions concerned.

The second order terms can be divided into two components, the induction energy and the dispersion energy. The induction energy represents the distortion of one molecules ground-state charge distribution due to its interaction with a second molecules unperturbed charge distribution and is necessarily always negative. The dispersion energy represents the interaction of two perturbed charge distributions and is also always negative. Each of these energies has a radial dependence and for the interactions between two neutral ground-state molecules the leading term in the electrostatic energy varies as R^{-3} while the leading terms for the (second order) induction and dispersion energies vary as R^{-6}. Within this thesis the induction energy, which is generally small, is initially neglected.

Short-range interactions are generally considered as being those for

which there is a significant degree of electron overlap. These interactions do not lend themselves to a convenient perturbation treatment. It is well known that at short-range the dominant interactions are repulsive and they increase rapidly as the intermolecular distance R decreases. Empirical observations suggest that such behaviour may be well represented by a radial function of the form e^{-R} or R^{-n} (where n is usually chosen to be not less than 9).

Within this thesis the potential function is represented by a combination of two basic potentials. The first is the atom-atom model, which has been used to construct empirical potentials for a wide range of molecular crystals[2,3,4,14] and models both the short-range repulsion and the long-range dispersion energies, both being functions of the intermolecular distance R. Two variants of this type of potential are used, the well known Lennard-Jones potential and an anisotropic molecule-molecule potential derived by Berne and Pechukas[15]. In addition the electrostatic energy is represented by one of two expansions of the molecular charge distribution. The first is an expansion in terms of the molecular multipole moments while the second is an expansion in terms of charges and multipole moments located on the individual atoms.

Generally the values of the exponents employed within atom-atom potentials are considered as being fairly restricted. It is unusual for the repulsive power to be considered as anything other than six and it is similarly unusual for the dispersive power to be considered outside the range nine to thirteen. Within this thesis the values of the atom-atom exponents employed will exhibit wider flexibility and the exponents themselves will be considered as empirical parameters.

The basic theory of lattice dynamics has been introduced in Chapter 2. For a crystal to be in stable equilibrium the forces and torques

(the first derivatives of the potential) acting upon the molecules must vanish, the crystal must be free from stress and the force constants corresponding to the normal coordinates (the second derivatives) must be positive. The forces, torques and force constants are represented by the appropriate Taylor expansion coefficients.

Each of the potentials utilised within this thesis is considered in detail in this chapter and expressions for the first and second derivatives of the potentials with respect to the vibrational coordinates are given, these being required to determine the values of the various lattice properties described in Chapter 2.

4.2: Lennard-Jones Atom-Atom Potential

The molecule pair approximation given by (2.2.3) may be more conveniently rewritten as:

$$V = \frac{1}{2} \sum_{A} \sum_{B \neq A} V^{AB} \qquad (4.2.1)$$

where V is the total potential and V^{AB} is the potential between molecules A and B. The intermolecular interaction is expressed as a sum of these molecule-pair interactions. In the case of the Lennard-Jones potential the molecule-pair potential is further partitioned into atom-pair potentials between the constituent atoms of the two molecules. The full potential is given by:

$$V = \frac{1}{2} \sum_{A} \sum_{i} \sum_{B \neq A} \sum_{j} V^{AiBj} \qquad (4.2.2)$$

where i labels the atom within molecule A and j labels the atom within molecule B. The Lennard-Jones potential has the general form:

$$V^{AiBj} = \frac{\varepsilon}{n-m} \left[m \left(\frac{r^{AiBj}}{r_0^{AiBj}} \right)^{-n} - n \left(\frac{r^{AiBj}}{r_0^{AiBj}} \right)^{-m} \right] \qquad (4.2.3)$$

where r^{AiBj} is the interatomic distance. The potential tends towards zero as r^{AiBj} tends to infinity. The potential has a minimum at the configuration for which $r^{AiBj} = r_0^{AiBj}$ and the value of the potential at that configuration is given by ϵ, otherwise known as the well depth. The magnitude of n is a measure of the steepness of the repulsive part of the potential and the magnitude of m is a measure of the steepness of the attractive part of the potential. The potential is a central interaction potential and its two components can be easily seen to model the repulsion and dispersion components of the intermolecular potential.

The Lennard-Jones potential is a function of the interatomic coordinate r^{AiBj}, whereas the Taylor expansion coefficients required are those with respect to the vibrational coordinates t_α^A and λ_α^A. To relate the two sets of coordinates a set of intermediate coordinates, r_α^{Ai}, are introduced such that:

$$r^{AiBj} = \left[\sum_\alpha \left(r_\alpha^{Bj} - r_\alpha^{Ai}\right)^2\right]^{1/2} \qquad (4.2.4)$$

where the coordinate r_α^{Ai} is defined by:

$$r_\alpha^{Ai} = R_\alpha^A + \sum_\beta \Lambda_{\alpha\beta}^A \rho_\beta^{Ai} \qquad (4.2.5)$$

where R_α^A is the α'th component of the coordinate of the centre of mass of molecule A relative to the crystal fixed origin and ρ_β^{Ai} is the β'th component of the coordinate of atom i in molecule A relative to the molecule fixed origin of molecule A. For convenience the molecule fixed axis system is chosen to be a cartesian system such that the molecular axis is the z axis and (4.2.5) may be simplified:

$$r_\alpha^{Ai} = R_\alpha^A + \Lambda_\alpha^A \rho_z^{Ai} \qquad (4.2.6)$$

where Λ^A_α are the direction cosines discussed in section 2.3. The coordinates above are related to the vibrational coordinates, R^A_α are dependent only upon the translational coordinates t^A_β, while Λ^A_α are dependent only upon the orientational coordinates λ^A_β.

The first derivatives of the interatomic potential with respect to the vibrational coordinates may now be formed using the chain rule:

$$\left(\frac{\partial V^{AiBj}}{\partial u^A_\gamma}\right)_0 = \sum_\alpha \left(\frac{\partial V^{AiBj}}{\partial r^{AiBj}}\right)_0 \left(\frac{\partial r^{AiBj}}{\partial r^{Ai}_\alpha}\right)_0 \left(\frac{\partial r^{Ai}_\alpha}{\partial u^A_\gamma}\right)_0 \tag{4.2.7}$$

and the second derivatives may similarly be formed:

$$\begin{aligned}\left(\frac{\partial^2 V^{AiBj}}{\partial u^A_\gamma\, \partial u^A_\delta}\right)_0 = &\sum_{\alpha,\beta} \left(\frac{\partial^2 V^{AiBj}}{\partial r^{(AiBj)2}}\right)_0 \left(\frac{\partial r^{AiBj}}{\partial r^{Ai}_\alpha}\right)_0 \left(\frac{\partial r^{AiBj}}{\partial r^{Ai}_\beta}\right)_0 \left(\frac{\partial r^{Ai}_\alpha}{\partial u^A_\gamma}\right)_0 \left(\frac{\partial r^{Ai}_\beta}{\partial u^A_\delta}\right)_0 \\ &+ \sum_{\alpha,\beta} \left(\frac{\partial V^{AiBj}}{\partial r^{AiBj}}\right)_0 \left(\frac{\partial^2 r^{AiBj}}{\partial r^{Ai}_\alpha\, \partial r^{Ai}_\beta}\right)_0 \left(\frac{\partial r^{Ai}_\alpha}{\partial u^A_\gamma}\right)_0 \left(\frac{\partial r^{Ai}_\beta}{\partial u^A_\delta}\right)_0 \\ &+ \sum_{\alpha} \left(\frac{\partial V^{AiBj}}{\partial r^{AiBj}}\right)_0 \left(\frac{\partial r^{AiBj}}{\partial r^{Ai}_\alpha}\right)_0 \left(\frac{\partial^2 r^{Ai}_\alpha}{\partial u^A_\gamma\, \partial u^A_\delta}\right)_0 \end{aligned} \tag{4.2.8}$$

$$\begin{aligned}\left(\frac{\partial^2 V^{AiBj}}{\partial u^A_\gamma\, \partial u^B_\delta}\right)_0 = &\sum_{\alpha,\beta} \left(\frac{\partial^2 V^{AiBj}}{\partial r^{(AiBj)2}}\right)_0 \left(\frac{\partial r^{AiBj}}{\partial r^{Ai}_\alpha}\right)_0 \left(\frac{\partial r^{AiBj}}{\partial r^{Bj}_\beta}\right)_0 \left(\frac{\partial r^{Ai}_\alpha}{\partial u^A_\gamma}\right)_0 \left(\frac{\partial r^{Bj}_\beta}{\partial u^B_\delta}\right)_0 \\ &+ \sum_{\alpha,\beta} \left(\frac{\partial V^{AiBj}}{\partial r^{AiBj}}\right)_0 \left(\frac{\partial^2 r^{AiBj}}{\partial r^{Ai}_\alpha\, \partial r^{Bj}_\beta}\right)_0 \left(\frac{\partial r^{Ai}_\alpha}{\partial u^A_\gamma}\right)_0 \left(\frac{\partial r^{Bj}_\beta}{\partial u^B_\delta}\right)_0 \\ &+ \sum_{\alpha} \left(\frac{\partial V^{AiBj}}{\partial r^{AiBj}}\right)_0 \left(\frac{\partial r^{AiBj}}{\partial r^{Ai}_\alpha}\right)_0 \left(\frac{\partial^2 r^{Ai}_\alpha}{\partial u^A_\gamma\, \partial u^B_\delta}\right)_0 \end{aligned} \tag{4.2.9}$$

The derivatives of r^{AiBj} with respect to r_α^{Ai} and r_β^{Bj} at the equilibrium configuration are given by:

$$\left(\frac{\partial r^{AiBj}}{\partial r_\alpha^{Ai}}\right)_0 = - \frac{r_\alpha^{AiBj}}{r^{AiBj}} \; ; \tag{4.2.10}$$

$$\left(\frac{\partial r^{AiBj}}{\partial r_\beta^{Bj}}\right)_0 = \frac{r_\beta^{AiBj}}{r^{AiBj}} \tag{4.2.11}$$

$$\left(\frac{\partial^2 r^{AiBj}}{\partial r_\alpha^{Ai}\, \partial r_\beta^{Ai}}\right)_0 = \frac{\delta_{\alpha\beta}}{r^{AiBj}} - \frac{r_\alpha^{AiBj}\, r_\beta^{AiBj}}{r^{AiBj\,3}} \tag{4.2.12}$$

$$\left(\frac{\partial^2 r^{AiBj}}{\partial r_\alpha^{Ai}\, \partial r_\beta^{Bj}}\right)_0 = \frac{r_\alpha^{AiBj}\, r_\beta^{AiBj}}{r^{AiBj\,3}} - \frac{\delta_{\alpha\beta}}{r^{AiBj}} \tag{4.2.13}$$

The derivatives of r_α^{Ai} with respect to the vibrational coordinates are given by consideration of (2.3.5), (2.3.6) and (4.2.6):

$$\left(\frac{\partial r_\alpha^{Ai}}{\partial t_\gamma^{A}}\right)_0 = \left(\frac{\partial r_\alpha^{Bj}}{\partial t_\gamma^{B}}\right)_0 = \delta_{\alpha\gamma} \tag{4.2.14}$$

$$\left(\frac{\partial^2 r_\alpha^{Ai}}{\partial t_\gamma^{A}\, \partial t_\delta^{A}}\right)_0 = \left(\frac{\partial^2 r_\alpha^{Ai}}{\partial t_\gamma^{A}\, \partial t_\delta^{B}}\right)_0 = 0 \tag{4.2.15}$$

$$\left(\frac{\partial r_\alpha^{Ai}}{\partial \lambda_\gamma^{A}}\right)_0 = \left(\frac{\partial r_\alpha^{Ai}}{\partial \Lambda_\beta^{A}}\right)_0 \left(\frac{\partial \Lambda_\beta^{A}}{\partial \lambda_\gamma^{A}}\right)_0 = \rho_z^{Ai}\; \Lambda_{\alpha\gamma}^{A0} \tag{4.2.16}$$

$$\left(\frac{\partial^2 r_\alpha^{Ai}}{\partial \lambda_\gamma^{A}\, \partial \lambda_\delta^{A}}\right)_0 = - \delta_{\gamma\delta}\; \Lambda_{\alpha z}^{A0} \tag{4.2.17}$$

$$\left(\frac{\partial^2 r_\alpha^{Ai}}{\partial\lambda_\gamma^A\ \partial\lambda_\delta^B}\right)_0 = 0 \tag{4.2.18}$$

$$\left(\frac{\partial^2 r_\alpha^{Ai}}{\partial t_\gamma^A\ \partial\lambda_\delta^A}\right)_0 = \left(\frac{\partial^2 r_\alpha^{Ai}}{\partial t_\gamma^A\ \partial\lambda_\delta^B}\right)_0 = 0 \tag{4.2.19}$$

Using these relationships the non-zero first and second derivatives of the Lennard-Jones potential with respect to the vibrational coordinates may be written:

$$\left(\frac{\partial V^{AiBj}}{\partial t_\gamma^A}\right)_0 = -\frac{r_\gamma^{AiBj}}{r^{AiBj}}\left(\frac{\partial V^{AiBj}}{\partial r^{AiBj}}\right)_0 \tag{4.2.20}$$

$$\left(\frac{\partial V^{AiBj}}{\partial\lambda_\gamma^A}\right)_0 = -\sum_\alpha \rho_z^{Ai}\ \Lambda_{\alpha\gamma}^{A0}\ \frac{r_\alpha^{AiBj}}{r^{AiBj}}\left(\frac{\partial V^{AiBj}}{\partial r^{AiBj}}\right)_0 \tag{4.2.21}$$

$$\left(\frac{\partial^2 V^{AiBj}}{\partial t_\gamma^A\ \partial t_\delta^A}\right)_0 = \frac{r_\gamma^{AiBj}\ r_\delta^{AiBj}}{r^{AiBj^2}}\left(\frac{\partial^2 V^{AiBj}}{\partial r^{(AiBj)2}}\right)_0 + \left(\frac{\delta_{\gamma\delta}}{r^{AiBj}} - \frac{r_\gamma^{AiBj}\ r_\delta^{AiBj}}{r^{AiBj^3}}\right)\left(\frac{\partial V^{AiBj}}{\partial r^{AiBj}}\right)_0 \tag{4.2.22}$$

$$\left(\frac{\partial^2 V^{AiBj}}{\partial t_\gamma^A\ \partial\lambda_\delta^A}\right)_0 = \sum_\beta \rho_z^{Ai}\ \Lambda_{\beta\delta}^{A0}\left\{\frac{r_\gamma^{AiBj}\ r_\beta^{AiBj}}{r^{AiBj^2}}\left(\frac{\partial^2 V^{AiBj}}{\partial r^{(AiBj)2}}\right)_0 + \left(\frac{\delta_{\gamma\beta}}{r^{AiBj}} - \frac{r_\gamma^{AiBj}\ r_\beta^{AiBj}}{r^{AiBj^3}}\right)\left(\frac{\partial V^{AiBj}}{\partial r^{AiBj}}\right)_0\right\} \tag{4.2.23}$$

$$\left(\frac{\partial^2 V^{AiBj}}{\partial\lambda_\gamma^A\ \partial\lambda_\delta^A}\right)_0 = \sum_{\alpha,\beta} \rho_z^{Ai\,2}\ \Lambda_{\alpha\gamma}^{A0}\ \Lambda_{\beta\delta}^{A0} \left\{\frac{r_\alpha^{AiBj}\ r_\beta^{AiBj}}{r^{AiBj\,2}} \left(\frac{\partial^2 V^{AiBj}}{\partial r^{(AiBj)2}}\right)_0 + \left(\frac{\delta_{\alpha\beta}}{r^{AiBj}} - \frac{r_\alpha^{AiBj}\ r_\beta^{AiBj}}{r^{AiBj\,3}}\right) \left(\frac{\partial V^{AiBj}}{\partial r^{AiBj}}\right)_0\right\}$$

$$+ \sum_{\alpha} \delta_{\gamma\delta}\ \Lambda_{\alpha z}^{A0}\ \frac{r_\alpha^{AiBj}}{r^{AiBj}} \left(\frac{\partial V^{AiBj}}{\partial r^{AiBj}}\right)_0 \qquad (4.2.24)$$

$$\left(\frac{\partial^2 V^{AiBj}}{\partial t_\gamma^A\ \partial t_\delta^B}\right)_0 = -\frac{r_\gamma^{AiBj}\ r_\delta^{AiBj}}{r^{AiBj\,2}} \left(\frac{\partial^2 V^{AiBj}}{\partial r^{(AiBj)2}}\right)_0 + \left\{\frac{r_\gamma^{AiBj}\ r_\delta^{AiBj}}{r^{AiBj\,3}} - \frac{\delta_{\gamma\delta}}{r^{AiBj}}\right\} \left(\frac{\partial V^{AiBj}}{\partial r^{AiBj}}\right)_0 \qquad (4.2.25)$$

$$\left(\frac{\partial^2 V^{AiBj}}{\partial t_\gamma^A\ \partial\lambda_\delta^B}\right)_0 = -\sum_{\beta} \frac{r_\gamma^{AiBj}\ r_\beta^{AiBj}}{r^{AiBj\,2}}\ \rho_z^{Bj}\ \Lambda_{\beta\delta}^{B0} \left(\frac{\partial^2 V^{AiBj}}{\partial r^{(AiBj)2}}\right)_0 + \sum_{\beta} \left\{\frac{r_\gamma^{AiBj}\ r_\beta^{AiBj}}{r^{AiBj\,3}} - \frac{\delta_{\gamma\beta}}{r^{AiBj}}\right\} \rho_z^{Bj}\ \Lambda_{\beta\delta}^{B0} \left(\frac{\partial V^{AiBj}}{\partial r^{AiBj}}\right)_0 \qquad (4.2.26)$$

$$\left(\frac{\partial^2 V^{AiBj}}{\partial\lambda_\gamma^A\ \partial\lambda_\delta^B}\right)_0 = -\sum_{\alpha,\beta} \frac{r_\alpha^{AiBj}\ r_\beta^{AiBj}}{r^{AiBj\,2}}\ \rho_z^{Ai}\ \rho_z^{Bj}\ \Lambda_{\alpha\gamma}^{A0}\ \Lambda_{\beta\delta}^{B0} \left(\frac{\partial^2 V^{AiBj}}{\partial r^{(AiBj)2}}\right)_0$$

$$+ \sum_{\alpha,\beta} \left\{\frac{r_\alpha^{AiBj}\ r_\beta^{AiBj}}{r^{AiBj\,3}} - \frac{\delta_{\alpha\beta}}{r^{AiBj}}\right\} \rho_z^{Ai}\ \rho_z^{Bj}\ \Lambda_{\alpha\gamma}^{A0}\ \Lambda_{\beta\delta}^{B0} \left(\frac{\partial V^{AiBj}}{\partial r^{AiBj}}\right)_0 \qquad (4.2.27)$$

4.3: Anisotropic Berne-Pechukas Molecule-Molecule Potential

The atom-atom Lennard-Jones potential described in the previous section is isotropic in the sense that there is no direct accounting for the molecular surroundings. An alternative approach to considering the short-range repulsive part of the potential would be to consider a moment expansion about the centre and allocate the terms within this expansion to the atomic centres as interactions which are locally anisotropic.

There is no unique form for the functions representing the terms within the expansion and one particularly compact form has been suggested by Berne and Pechukas[15]. Within their treatment the interaction between two molecules is represented by a function which is directly related to the overlap of two ellipsoidal Gaussian charge distributions. The charge distributions are of the form:

$$G(x,y,z) = \exp\left[-(x^2+y^2)\sigma_{\perp}^{-2} - z^2\sigma_{\parallel}^{-2}\right] \qquad (4.3.1)$$

where x, y and z are Cartesian coordinates, z being the principal axis of the molecule. The quantities $\sigma_{\perp}$ and $\sigma_{\parallel}$ quantify the spatial extent of the distribution perpendicular and parallel to the principal axis. The total potential interaction is given by the sum of the interactions of these ellipsoids and this interaction is considered as being proportional to the mathematical overlap between the ellipsoids. Thus an alternative model for the short-range repulsion term has been proposed which is dependent upon the shape of the molecules concerned.

A suitable set of coordinates for describing the relative orientation of the two Gaussians have been introduced by Walmsley[16] and consist of the direction cosine coordinates introduced in Chapter 2 plus R, the distance between the origins of the two Gaussians. Λ_{α}^{A} relates the principal (z) axis of molecule A and the α'th crystal

fixed axis. The relative orientation of the two Gaussians is given by $\Lambda^A_\gamma \Lambda^B_\gamma$ where the summation convention is assumed. This quantity is represented by t_{AB}:

$$t_{AB} = \Lambda^A_\gamma \Lambda^B_\gamma \tag{4.3.2}$$

Berne and Pechukas detail the derivation of the overlap integral and point out a number of simplifications for the treatment of overlap integrals of axially symmetric functions such as the Gaussians under consideration here. Furthermore the formulae which they detail may be simplified if the two functions are the same, ie the values of $\sigma_\perp$ and $\sigma_\parallel$ are the same for both molecules. Under these circumstances, the overlap, S, is given by:

$$S = \xi \exp(-R^2 \lambda^{-2}) \tag{4.3.3}$$

where ξ and λ are angular functions whose definitions are as follows:

$$\xi(t_{AB}) = \xi\, t^{1/2} \tag{4.3.4}$$

$$\lambda^2(\Lambda^A_\gamma, \Lambda^B_\gamma, t_{AB}) = \lambda^2\, t\, (s/R^2)^{-1} \tag{4.3.5}$$

where the quantities t and s are defined by:

$$t = 1 - \chi^2 t^2_{AB} \tag{4.3.6}$$

$$s = R_\alpha R_\beta \left[\delta_{\alpha\beta} t - \chi(\Lambda^A_\alpha \Lambda^A_\beta + \Lambda^B_\alpha \Lambda^B_\beta) + 2\chi^2\, \Lambda^A_\alpha \Lambda^B_\beta \Lambda^A_\gamma \Lambda^B_\gamma\right] \tag{4.3.7}$$

The parameters, ξ, λ and χ represent the strength, the range and the degree of anisotropy of the Gaussian function and the latter two may be expressed purely in terms of $\sigma_\perp$ and $\sigma_\parallel$ as follows:

$$\lambda = \sqrt{2}\, \sigma_\perp \tag{4.3.8}$$

$$\chi = \frac{(\sigma_{\parallel}^2 - \sigma_{\perp}^2)}{(\sigma_{\parallel}^2 + \sigma_{\perp}^2)} \qquad (4.3.9)$$

Corner[17] has suggested that such a potential should be developed such that the interaction is through a Lennard-Jones potential. Berne and Pechukas have further developed this idea by proposing that the strength of the Gaussian function parameter, ξ should be identical with ϵ, the value of the energy at the minimum of a standard atom-atom pair potential (for example the Lennard-Jones potential discussed in the previous section) and λ should be identical to R_0, the value of the interatomic distance, R at the minimum. Explicitly the expressions for these functions are as follows:

$$\epsilon(t_{AB}) = \epsilon/t^{1/2} \qquad (4.3.10)$$

$$R_0(\Lambda_{\alpha}^{A}, \Lambda_{\beta}^{B}, t_{AB}) = \frac{t^{1/2}}{s^{1/2}} R_0 \qquad (4.3.11)$$

These two expressions represent systematic anisotropic replacements for the quantities ϵ and R_0 and may be substituted directly into any suitable potential. In the case of the standard Lennard-Jones 12-6 potential the anisotropic treatment may be applied to both the repulsion and dispersion terms to give:

$$V^{AiBj} = \epsilon\left[t^{11/2}s^{-6}R_0^{12} - 2t^{5/2}s^{-3}R_0^{6}\right] \qquad (4.3.12)$$

It should be noted that for a molecule whose degree of anisotropy, χ is zero then from (4.3.6) and (4.3.7), $t = 1$ and $s = R^2$ so that the above expression becomes:

$$V^{AiBj} = \epsilon\left[\left(\frac{R_0}{R}\right)^{12} - 2\left(\frac{R_0}{R}\right)^{6}\right] \qquad (4.3.13)$$

which is the standard isotropic Lennard-Jones 12-6 potential.

The anisotropic Berne Pechukas potential is therefore a function of three variables; ϵ, R_0 and χ. It should be noted that the theory introduced here is appropriate only to the interaction of linear molecules as it accounts only for the direction of the symmetry axis of the ellipsoidal function. It is also adapted to functions which are located at the molecular centre of mass. The potential may be extended so that it may be used as an atom-atom potential but within this thesis it is only employed as a molecule-molecule potential.

The Taylor expansion coefficients may be obtained in a similar manner to the procedure described in the previous section, applying the chain rule and using s and t as intermediate variables.

4.4: Molecular Multipole Potential

It has already been discussed that in addition to the short-range potentials described in the previous sections any suitable model will also require a contribution from the molecular charge distributions. The simplest method of describing this distribution is to express it in terms of a set of charges located on the atoms. The simple form of the interatomic potential described in section 4.2 is retained and a term which is a function of $(r^{AiBj})^{-1}$ is added.

Alternatively the charge distribution may be represented by a series of molecular multipole moments, each referred to the molecular centre of mass as the origin. For a pair of neutral linear molecules Neto, Righini, Califano and Walmsley[18] have provided a convenient form for expressing this multipolar series:

$$V^{AB} = \sum_{m=1}^{\infty} \sum_{n=1}^{\infty} \frac{(-1)^m}{m!n!} V_{mn}^{AB} \qquad (4.4.1)$$

Each term represents the interaction between two multipole moments,

the moment of order m on molecule A and the moment of order n on molecule B. The component of the potential, V_{mn}^{AB} is given by:

$$V_{mn}^{AB} = M^{A}(m)\, M^{B}(n) \times [\underset{\sim}{L}^{A}(m) \cdot \underset{\sim}{T}^{AB}(m+n) \cdot \underset{\sim}{L}^{B}(n)] \qquad (4.4.2)$$

where $M^{A}(m)$ is the m'th multipole moment of molecule A defined by:

$$M^{A}(m) = \sum_{i} e_i (r_i)^m \, P_m(r_{iz}/r_i) \qquad (4.4.3)$$

where the sum is over all charges, e_i within molecule A which are a distance r_i from the molecular centre of mass and have the Cartesian coordinate r_{iz} along the molecular axis. $P_m(r_{iz}/r_i)$ is the Legendre function of degree m. The first four multipole moments are more commonly known as the dipole (μ), quadrupole (Θ), octupole (Ω) and hexadecapole (Φ) moments. The term $\underset{\sim}{L}^{A}(m) \cdot \underset{\sim}{T}^{AB}(m+n) \cdot \underset{\sim}{L}^{B}(n)$ is the inner product of three tensors. $\underset{\sim}{L}^{A}(m)$ is a tensor of rank m and its components are the direction cosines introduced in Chapter 2, relating the crystal fixed Cartesian axes and the linear axis of the molecule such that its components may be written:

$$L^{A}_{\alpha\beta\ldots\mu}(m) = \Lambda^{A}_{\alpha}\Lambda^{A}_{\beta}\underbrace{\ldots\ldots}_{(m)}\Lambda^{A}_{\mu} \qquad (4.4.4)$$

The subscript (m) indicates the number of terms Λ^{A}_{α}. The tensor, $\underset{\sim}{T}^{AB}(m+n)$ is of rank (m+n) and its Cartesian components are given by:

$$T^{(m+n)}_{\alpha..\mu\alpha'..\mu'}(R^{AB}) = \frac{\partial}{\partial R^{AB}_{\alpha}} \underbrace{\ldots\ldots}_{(m)} \frac{\partial}{\partial R^{AB}_{\mu}} \frac{\partial}{\partial R^{AB}_{\alpha'}} \underbrace{\ldots\ldots}_{(n)} \frac{\partial}{\partial R^{AB}_{\mu'}} \left(\frac{1}{R^{AB}}\right) \qquad (4.4.5)$$

where R^{AB} is the intermolecular coordinate and locates the centre of mass of molecule a from molecule b and is defined by:

$$R^{AB} = \left[\sum_{\alpha} \left(R^{B}_{\alpha} - R^{A}_{\alpha}\right)^2\right]^{1/2} \qquad (4.4.6)$$

where R_α^A is the intermediate coordinate introduced in (4.2.5) and is related to the translational coordinate t_α^A by the relation:

$$t_\alpha^A = R_\alpha^A - R_\alpha^{AO} \qquad (4.4.7)$$

where R_α^{AO} is the value of R_α^A at the reference configuration.

The expression for the components of the multipolar potential given by (4.4.2) can now be written such that:

$$V_{mn}^{AB} = \Lambda_{\alpha\ldots\ldots}^{A}{}_{(m)} \Lambda_{\mu}^{A}\Lambda_{\alpha'}^{B}{}_{\ldots\ldots(n)} \Lambda_{\mu'}^{B}\ T_{\alpha\ldots\mu\alpha'\ldots\mu'}^{(m+n)}(R^{AB})\ M^A(m)\ M^B(n) \qquad (4.4.8)$$

The connection between this expression and the vibrational coordinates used in the Taylor expansion of the potential can now be easily seen. The expression for the multipolar potential has been split up into the components of the orientation of molecule A (the direction cosines Λ_α^A), the components of the orientation of molecule B (the direction cosines $\Lambda_{\alpha'}^B$) and $T_{\alpha\ldots\mu\alpha'\ldots\mu'}^{(m+n)}(R^{AB})$, the only term which is a function of the positions of the centres of mass. Thus the derivatives of the potential with respect to the translational coordinates will be simply given by differentiation of the tensor component, $T_{\alpha\ldots\mu\alpha'\ldots\mu'}^{(m+n)}(R^{AB})$ while the derivatives of the potential with respect to the orientational coordinates will be given by differentiation of the appropriate direction cosines Λ_α^A. This may be illustrated by forming the first derivatives of the potential using the chain rule:

$$\left(\frac{\partial V^{AB}}{\partial t_\gamma^A}\right)_0 = \sum_{\alpha,\rho} \left(\frac{\partial V^{AB}}{\partial R_\alpha^{AB}}\right)_0 \left(\frac{\partial R_\alpha^{AB}}{\partial R_\rho^A}\right)_0 \left(\frac{\partial R_\rho^A}{\partial t_\gamma^A}\right)_0 \qquad (4.4.9)$$

$$\left(\frac{\partial V^{AB}}{\partial \lambda_\gamma^A}\right)_0 = \sum_{\alpha} \left(\frac{\partial V^{AB}}{\partial \Lambda_\alpha^A}\right)_0 \left(\frac{\partial \Lambda_\alpha^A}{\partial \lambda_\gamma^A}\right)_0 \qquad (4.4.10)$$

The first and second order Taylor expansion coefficients may now be written in full:

$$\left(\frac{\partial V^{AB}_{mn}}{\partial t^{A}_{\sigma}}\right)_0 = - \Lambda^{A0}_{\alpha z}\underbrace{\ldots\ldots}_{(m)}\Lambda^{A0}_{\mu z}\Lambda^{B0}_{\alpha' z}\underbrace{\ldots\ldots}_{(n)}\Lambda^{B0}_{\mu' z}\, T^{(m+n+1)}_{\sigma\alpha.\mu\alpha'.\mu'}(R^{AB})\; M^{A}(m)\; M^{B}(n) \tag{4.4.11}$$

$$\left(\frac{\partial V^{AB}_{mn}}{\partial \lambda^{A}_{\sigma}}\right)_0 = m\,\Lambda^{A0}_{\alpha\sigma}\Lambda^{A0}_{\beta z}\underbrace{\ldots\ldots}_{(m-1)}\Lambda^{A0}_{\mu z}\Lambda^{B0}_{\alpha' z}\underbrace{\ldots\ldots}_{(n)}\Lambda^{B0}_{\mu' z}\, T^{(m+n)}_{\alpha.\mu\alpha'.\mu'}(R^{AB})\; M^{A}(m)\; M^{B}(n) \tag{4.4.12}$$

$$\left(\frac{\partial^2 V^{AB}_{mn}}{\partial t^{A}_{\sigma}\,\partial t^{A}_{\tau}}\right)_0 = \Lambda^{A0}_{\alpha z}\underbrace{\ldots\ldots}_{(m)}\Lambda^{A0}_{\mu z}\Lambda^{B0}_{\alpha' z}\underbrace{\ldots\ldots}_{(n)}\Lambda^{B0}_{\mu' z}\, T^{(m+n+2)}_{\sigma\tau\alpha.\mu\alpha'.\mu'}(R^{AB})\; M^{A}(m)\; M^{B}(n) \tag{4.4.13}$$

$$\left(\frac{\partial^2 V^{AB}_{mn}}{\partial t^{A}_{\sigma}\,\partial t^{B}_{\tau}}\right)_0 = - \Lambda^{A0}_{\alpha z}\underbrace{\ldots\ldots}_{(m)}\Lambda^{A0}_{\mu z}\Lambda^{B0}_{\alpha' z}\underbrace{\ldots\ldots}_{(n)}\Lambda^{B0}_{\mu' z}\, T^{(m+n+2)}_{\sigma\alpha.\mu\tau\alpha'.\mu'}(R^{AB})\; M^{A}(m)\; M^{B}(n) \tag{4.4.14}$$

$$\left(\frac{\partial^2 V^{AB}_{mn}}{\partial \lambda^{A}_{\sigma}\,\partial \lambda^{A}_{\tau}}\right)_0 = m\left((m-1)\,\Lambda^{A0}_{\alpha\sigma}\Lambda^{A0}_{\beta\tau} - \delta_{\sigma\tau}\Lambda^{A0}_{\alpha z}\Lambda^{A0}_{\beta z}\right)\Lambda^{A0}_{\gamma z}\underbrace{\ldots\ldots}_{(m-2)}\Lambda^{A0}_{\mu z}\Lambda^{B0}_{\alpha' z}\underbrace{\ldots\ldots}_{(n)}\Lambda^{B0}_{\mu' z}$$

$$T^{(n+m)}_{\alpha.\mu\alpha'.\mu'}(R^{AB})\; M^{A}(m)\; M^{B}(n) \tag{4.4.15}$$

$$\left(\frac{\partial^2 V^{AB}_{mn}}{\partial \lambda^{A}_{\sigma}\,\partial \lambda^{B}_{\tau}}\right)_0 = mn\Lambda^{A0}_{\alpha\sigma}\Lambda^{A0}_{\beta z}\underbrace{\ldots\ldots}_{(m-1)}\Lambda^{A0}_{\mu z}\Lambda^{B0}_{\alpha'\tau}\Lambda^{B0}_{\beta' z}\underbrace{\ldots\ldots}_{(n-1)}\Lambda^{B0}_{\mu' z}\, T^{(n+m)}_{\alpha.\mu\alpha'.\mu'}(R^{AB})$$

$$M^{A}(m)\; M^{B}(n) \tag{4.4.16}$$

$$\left(\frac{\partial^2 V^{AB}_{mn}}{\partial t^{A}_{\sigma}\,\partial \lambda^{A}_{\tau}}\right)_0 = - m\Lambda^{A0}_{\alpha\tau}\Lambda^{A0}_{\beta z}\underbrace{\ldots\ldots}_{(m-1)}\Lambda^{A0}_{\mu z}\Lambda^{B0}_{\alpha' z}\underbrace{\ldots\ldots}_{(n)}\Lambda^{B0}_{\mu' z}\, T^{(m+n+1)}_{\sigma\alpha.\mu\alpha'.\mu'}(R^{AB})$$

$$M^{A}(m)\; M^{B}(n) \tag{4.4.17}$$

$$\left(\frac{\partial^2 V^{AB}_{mn}}{\partial t^A_\sigma \, \partial \lambda^B_\tau}\right)_0 = - n\Lambda^{AO}_{\alpha\tau}\Lambda^{AO}_{\beta z}{}_{(m-1)}\ldots\ldots\Lambda^{AO}_{\mu z}\Lambda^{BO}_{\alpha' z}{}_{(n)}\ldots\ldots\Lambda^{BO}_{\mu' z} T^{(m+n+1)}_{\alpha.\mu\sigma\alpha'.\mu'}(R^{AB})$$

$$M^A(m)\; M^B(n) \qquad (4.4.18)$$

4.5: Atomic Multipole Potential

The multipolar model detailed in the previous section may be further developed by considering multipoles located on the individual atoms rather than at the molecular centres of mass. The treatment which was employed for the molecular multipole potential is followed and for a pair of linear molecules the atomic multipole series is given by:

$$V^{AiBj} = \sum_{m=0}^{\infty}\sum_{n=0}^{\infty} \frac{(-1)^m}{m!n!} V^{AiBj}_{mn} \qquad (4.5.1)$$

in which it should be noted that unlike the molecular multipole expansion the terms m,n = 0 are included within the expansion, for while the molecules are restricted to being neutral the individual atoms will commonly have charges associated with them. The components of the multipolar expansion are given by:

$$V^{AiBj}_{mn} = \Lambda^A_{\alpha}{}_{(m)}\ldots\ldots\Lambda^A_{\mu}\Lambda^B_{\alpha'}{}_{(n)}\ldots\ldots\Lambda^B_{\mu'}\; T^{(m+n)}_{\alpha.\mu\alpha'.\mu'}(r^{AiBj})\; M^{Ai}(m)\; M^{Bj}(n) \qquad (4.5.2)$$

The Taylor expansion coefficients for the atomic multipole potential are not as simple to obtain as for the molecular multipole potential because the tensor is no longer independent of the orientational coordinates. Recalling (4.2.6) the first derivatives of the potential with respect to vibrational coordinates may be formed using the chain rule:

$$\left(\frac{\partial V^{AiBj}}{\partial t^{A}_{\gamma}}\right)_0 = \sum_{\alpha,\rho} \left(\frac{\partial V^{AiBj}}{\partial r^{AiBj}_{\alpha}}\right)_0 \left(\frac{\partial r^{AiBj}_{\alpha}}{\partial r^{Ai}_{\rho}}\right)_0 \left(\frac{\partial r^{Ai}_{\rho}}{\partial t^{A}_{\gamma}}\right)_0 \qquad (4.5.3)$$

$$\left(\frac{\partial V^{AiBj}}{\partial \lambda^{A}_{\gamma}}\right)_0 = \sum_{\alpha} \left(\frac{\partial V^{AiBj}}{\partial \Lambda^{A}_{\alpha}}\right)_0 \left(\frac{\partial \Lambda^{A}_{\alpha}}{\partial \lambda^{A}_{\gamma}}\right)_0 + \sum_{\alpha,\rho} \left(\frac{\partial V^{AiBj}}{\partial r^{AiBj}_{\alpha}}\right)_0 \left(\frac{\partial r^{AiBj}_{\alpha}}{\partial r^{Ai}_{\rho}}\right)_0 \left(\frac{\partial r^{Ai}_{\rho}}{\partial \lambda^{A}_{\gamma}}\right)_0 \qquad (4.5.4)$$

and the final term, the derivative of the intermediate coordinate with respect to the orientational coordinates is non-zero in the case of the atomic multipole potential. Its value is given by differentiation of (4.2.6):

$$\left(\frac{\partial r^{Ai}_{\rho}}{\partial \lambda^{A}_{\gamma}}\right)_0 = \delta_{\rho\gamma}\, \rho^{Ai}_{z} \qquad (4.5.5)$$

The Taylor expansion coefficients may now be formed as follows:

$$\left(\frac{\partial V^{AiBj}_{mn}}{\partial t^{A}_{\sigma}}\right)_0 = -\Lambda^{AO}_{\alpha z}\underset{(m)}{\ldots\ldots}\Lambda^{AO}_{\mu z}\Lambda^{BO}_{\alpha' z}\underset{(n)}{\ldots\ldots}\Lambda^{BO}_{\mu' z} T^{(m+n+1)}_{\sigma\alpha.\mu\alpha'.\mu'}(r^{AiBj}) \; M^{Ai}(m)\; M^{Bj}(n) \qquad (4.5.6)$$

$$\left(\frac{\partial V^{AiBj}_{mn}}{\partial \lambda^{A}_{\sigma}}\right)_0 = \Lambda^{AO}_{\beta z}\underset{(m-1)}{\ldots\ldots}\Lambda^{AO}_{\mu z}\Lambda^{BO}_{\alpha' z}\underset{(n)}{\ldots\ldots}\Lambda^{BO}_{\mu' z} \Big\{ m\Lambda^{AO}_{\alpha\sigma} T^{(n+m)}_{\alpha.\mu\alpha'.\mu'}(r^{AiBj}) - \Lambda^{AO}_{\rho\sigma}\Lambda^{AO}_{\alpha z}\rho^{Ai}_{z}\, T^{(n+m+1)}_{\rho\alpha.\mu\alpha'.\mu'}(r^{AiBj}) \Big\} M^{Ai}(m)\; M^{Bj}(n) \qquad (4.5.7)$$

$$\left(\frac{\partial^2 V^{AiBj}_{mn}}{\partial t^{A}_{\sigma}\, \partial t^{A}_{\tau}}\right)_0 = \Lambda^{AO}_{\alpha z}\underset{(m)}{\ldots\ldots}\Lambda^{AO}_{\mu z}\Lambda^{BO}_{\alpha' z}\underset{(n)}{\ldots\ldots}\Lambda^{BO}_{\mu' z} T^{(n+m+2)}_{\sigma\tau\alpha.\mu\alpha'.\mu'}(r^{AiBj}) \; M^{Ai}(m)\; M^{Bj}(n) \qquad (4.5.8)$$

$$\left(\frac{\partial^2 V_{mn}^{AiBj}}{\partial t_\sigma^A \, \partial t_\tau^B}\right)_0 = - \Lambda^{AO}_{\alpha z} \underset{(m)}{\ldots\ldots} \Lambda^{AO}_{\mu z} \Lambda^{BO}_{\alpha' z} \underset{(n)}{\ldots\ldots} \Lambda^{BO}_{\mu' z} T^{(n+m+2)}_{\sigma\alpha.\mu\tau\alpha'.\mu'}(r^{AiBj})$$

$$M^{Ai}(m)\ M^{Bj}(n) \qquad (4.5.9)$$

$$\left(\frac{\partial^2 V_{mn}^{AiBj}}{\partial \lambda_\sigma^A \, \partial \lambda_\tau^A}\right)_0 = \Lambda^{AO}_{\gamma z} \underset{(m-2)}{\ldots\ldots} \Lambda^{AO}_{\mu z} \Lambda^{BO}_{\alpha' z} \underset{(n)}{\ldots\ldots} \Lambda^{BO}_{\mu' z} \Big\{ m\Big[(m-1)\Lambda^{AO}_{\alpha\sigma}\Lambda^{AO}_{\beta\tau} - \delta_{\sigma\tau}\Lambda^{AO}_{\alpha z}\Lambda^{AO}_{\beta z}\Big]$$

$$T^{(n+m)}_{\alpha.\mu\alpha'.\mu'}(r^{AiBj}) - \rho_z^{Ai}\Lambda^{AO}_{\beta z}\Big[2m\Lambda^{AO}_{\rho\tau}\Lambda^{AO}_{\alpha\sigma} + \Lambda^{AO}_{\rho z}\Lambda^{AO}_{\alpha z}\delta_{\sigma\tau}\Big] T^{(n+m+1)}_{\rho\alpha.\mu\alpha'.\mu'}(r^{AiBj})$$

$$+ \Lambda^{AO}_{\rho\sigma}\Lambda^{AO}_{\nu\tau}\Lambda^{AO}_{\alpha z}\Lambda^{AO}_{\beta z}\rho_z^{Ai\,2} T^{(n+m+2)}_{\rho\nu\alpha.\mu\alpha'.\mu'}(r^{AiBj})\Big\}\ M^{Ai}(m)\ M^{Bj}(n) \qquad (4.5.10)$$

$$\left(\frac{\partial^2 V_{mn}^{AiBj}}{\partial \lambda_\sigma^A \, \partial \lambda_\tau^B}\right)_0 = \Lambda^{AO}_{\beta z} \underset{(m-1)}{\ldots\ldots} \Lambda^{AO}_{\mu z} \Lambda^{BO}_{\beta' z} \underset{(n-1)}{\ldots\ldots} \Lambda^{BO}_{\mu' z} \Big\{ mn\Lambda^{AO}_{\alpha\sigma}\Lambda^{BO}_{\alpha'\tau} T^{(n+m)}_{\alpha.\mu\alpha'.\mu'}(r^{AiBj})$$

$$- \Big(n\Lambda^{AO}_{\alpha' z}\rho_z^{Ai} - m\Lambda^{BO}_{\alpha' z}\rho_z^{Bj}\Big)\ \Lambda^{AO}_{\alpha\sigma}\Lambda^{BO}_{\nu\tau} T^{(n+m+1)}_{\alpha.\mu\alpha'.\mu'\nu}(r^{AiBj})$$

$$- \Lambda^{AO}_{\rho\sigma}\Lambda^{AO}_{\alpha z}\Lambda^{BO}_{\nu\tau}\Lambda^{BO}_{\alpha' z}\rho_z^{Ai}\rho_z^{Bj} T^{(n+m+2)}_{\rho\alpha.\mu\nu\alpha'.\mu'}(r^{AiBj})\Big\}\ M^{Ai}(m)\ M^{Bj}(n) \qquad (4.5.11)$$

$$\left(\frac{\partial^2 V_{mn}^{AiBj}}{\partial t_\sigma^A \, \partial \lambda_\tau^A}\right)_0 = - \Lambda^{AO}_{\beta z} \underset{(m-1)}{\ldots\ldots} \Lambda^{AO}_{\mu z} \Lambda^{BO}_{\alpha' z} \underset{(n)}{\ldots\ldots} \Lambda^{BO}_{\mu' z} \Big\{ m\Lambda^{AO}_{\alpha\tau} T^{(n+m+1)}_{\sigma\alpha.\mu\alpha'.\mu'}(r^{AiBj})$$

$$- \Lambda^{AO}_{\rho\tau}\Lambda^{AO}_{\alpha z}\rho_z^{Ai} T^{(n+m+2)}_{\sigma\rho\alpha.\mu\alpha'.\mu'}(r^{AiBj})\Big\}\ M^{Ai}(m)\ M^{Bj}(n) \qquad (4.5.12)$$

$$\left(\frac{\partial^2 V_{mn}^{AiBj}}{\partial t_\sigma^A \, \partial \lambda_\tau^B}\right)_0 = - \Lambda^{AO}_{\alpha z} \underset{(m)}{\ldots\ldots} \Lambda^{AO}_{\mu z} \Lambda^{BO}_{\beta' z} \underset{(n-1)}{\ldots\ldots} \Lambda^{BO}_{\mu' z} \Big\{ n\Lambda^{BO}_{\alpha'\tau} T^{(n+m+1)}_{\sigma\alpha.\mu\alpha'.\mu'}(r^{AiBj})$$

$$+ \Lambda^{BO}_{\rho\tau}\Lambda^{BO}_{\alpha' z}\rho_z^{Bj} T^{(n+m+2)}_{\sigma\alpha.\mu\rho\alpha'.\mu'}(r^{AiBj})\Big\}\ M^{Ai}(m)\ M^{Bj}(n) \qquad (4.5.13)$$

5.1: Introduction

The multipolar potentials introduced in Chapter 4 all contain derivatives with respect to the intermolecular (or interatomic) distance and these have been expressed in terms of the tensors defined by equation (4.4.5). In principle each tensor has 3^n components (where n is the order of the tensor) but as these tensors are symmetric to interchange of indices this number reduces to $\frac{1}{2}(n+1)(n+2)$. For low values of n the components may be determined explicitly without too much inconvenience. However for higher values this procedure becomes very time consuming it will be more efficient to find algorithms for the values of the components which may be included within the computer programs used to perform the lattice dynamical calculations. In this chapter the tensors involved will be discussed and it will be shown that they may be related to Legendre polynomials and their derivation from these polynomials will be illustrated.

5.2: Legendre Polynomials and Associated Legendre Polynomials

Legendre Polynomials

The series of Legendre Polynomials, represented by $P_n(z)$ may be defined as follows:

$$P_n(z) = \frac{1}{2^n n!} \frac{d^n}{dz^n}(z^2-1)^n \qquad (5.2.1)$$

where n is an integer and the series runs from n=0. The first two Legendre polynomials are as follows:

$$P_0(z) = 1 \qquad (5.2.2)$$

$$P_1(z) = z \qquad (5.2.3)$$

The series of Legendre Polynomials are related by the following recursion formula:

$$P_{n+1}(z) = \frac{(2n+1)}{(n+1)} zP_n(z) - \frac{n}{(n+1)} P_{n-1}(z) \qquad (5.2.4)$$

and it may be seen that once the zero and first order Legendre polynomials have been defined all other polynomials may be determined. The polynomial in z given in (5.2.1) may be expanded using the binomial theorem as follows:

$$(z^2-1)^n = z^{2n} - \frac{n!}{1!(n-1)!} z^{2n-2} + \frac{n!}{2!(n-2)!} z^{2n-4} - \ldots + (-1)^n \qquad (5.2.5)$$

and the general derivative of order n is given by:

$$\frac{\partial^n}{\partial z^n}(z^2-1)^n = 2n(2n-1)..(n+1)\ z^n - \frac{n!}{1!(n-1)!}(2n-2)(2n-3)..(n-1)\ z^{n-2}$$

$$+ \frac{n!}{2!(n-2)!}(2n-4)(2n-5)..(n-3)\ z^{n-4} - \ldots \qquad (5.2.6)$$

This expression will terminate with a term in z^1 if n is an odd integer and a term in z^0 if n is an even integer. Noting that:

$$2n(2n-1)\ldots(n+1) = \frac{2n!}{n!} \qquad (5.2.7)$$

equation (5.2.6) can be expressed as a series as follows:

$$\frac{\partial^n}{\partial z^n}(z^2-1)^n = \sum_{m=0}^{\lfloor n/2 \rfloor} (-1)^m \frac{n!}{m!(n-m)!} \frac{(2n-2m)!}{(n-2m)!} z^{n-2m} \qquad (5.2.8)$$

where the slightly clumsy summation denoted by $m=0,\lfloor n/2 \rfloor$ is used to indicate that m is an integer which runs from 0 to $\frac{(n-1)}{2}$ if n is an odd power and runs from 0 to $\frac{n}{2}$ if n is an even power.

The expression for the n'th Legendre Polynomial given by (5.2.1) can

now be written using this summation as follows:

$$P_n(z) = \sum_{m=0}^{\lfloor n/2 \rfloor} \frac{2^{-n}\,(-1)^m\,(2n-2m)!}{m!(n-m)!\,(n-2m)!}\, z^{n-2m} \qquad (5.2.9)$$

It is now noted that the factorial (2n-2m)! may be rewritten as:

$$(2n-2m)! = 2^{(n-m)}(n-m)!(2n-2m-1)!! \qquad (5.2.10)$$

where the double factorial (2n-2m-1)!! represents the number:

$$(2n-2m-1)!! = (2n-2m-1)\times(2n-2m-3)\times(2n-2m-5)\times\ldots\ldots\times 1 \qquad (5.2.11)$$

and using this (5.2.9) may be rewritten to give a series generating the n'th Legendre Polynomial:

$$P_n(z) = \sum_{m=0}^{\lfloor n/2 \rfloor} \frac{2^{-m}(-1)^m(2n-2m-1)!!}{m!(n-2m)!}\, z^{n-2m} \qquad (5.2.12)$$

Associated Legendre Polynomials

A second series of polynomials in z which are closely related to the Legendre Polynomials are the series of Associated Legendre Polynomials which are defined as follows:

$$P_n^t(z) = (1-z^2)^{t/2}\,\frac{\partial^t}{\partial z^t}\,P_n(z) \qquad (5.2.13)$$

These polynomials are also related by a recursion formula:

$$(2n+1)\,z\,P_n^t(z) = (n-t+1)\,P_{n+1}^t(z) + (n+t)\,P_{n-1}^t(z) \qquad (5.2.14)$$

The series given by (5.2.12) may now be differentiated with respect to z to give the explicit expressions for the first and second derivatives which form the first and second series of Associated Legendre polynomials:

$$\frac{\partial P_n(z)}{\partial z} = \sum_{m=0}^{\lfloor (n-1)/2 \rfloor} \frac{2^{-m}(-1)^m(2n-2m-1)!!}{m!(n-2m-1)!} z^{n-2m-1} \qquad (5.2.15)$$

$$\frac{\partial^2 P_n(z)}{\partial z^2} = \sum_{m=0}^{\lfloor (n-2)/2 \rfloor} \frac{2^{-m}(-1)^m(2n-2m-1)!!}{m!(n-2m-2)!} z^{n-2m-2} \qquad (5.2.16)$$

It should be noted that each successive differentiation reduces the power of z^{n-2m} by one and reduces the factorial (n-2m)! by one. The summation is effectively reduced by one term every other derivative as the z^1 term is successively reduced to z^0 and then disappears. The general derivative may be expressed as follows:

$$\frac{\partial^t P_n(z)}{\partial z^t} = \sum_{m=0}^{\lfloor (n-t)/2 \rfloor} \frac{2^{-m}(-1)^m(2n-2m-1)!!}{m!(n-2m-t)!} z^{n-2m-t} \qquad (5.2.17)$$

so that the a general Associated Legendre Polynomial can be expressed as a sum of terms as follows:

$$P_n^t(z) = (1-z^2)^{t/2} \sum_{m=0}^{\lfloor (n-t)/2 \rfloor} \frac{2^{-m}(-1)^m(2n-2m-1)!!}{m!(n-2m-t)!} z^{n-2m-t} \qquad (5.2.18)$$

It may be easily seen by inspection that by setting t = 0 the standard series of Legendre Polynomials are recovered.

5.3: Tensors

The set of tensor components which are under consideration may be defined as follows:

$$T_{\alpha\beta\gamma\delta..\nu}(R) = \frac{\partial}{\partial R_\alpha}\frac{\partial}{\partial R_\beta}\frac{\partial}{\partial R_\gamma}\frac{\partial}{\partial R_\delta}\cdots\left(R^{-1}\right) \qquad (5.3.1)$$

where $\alpha,\beta,\gamma,\delta$ label the cartesian axis system. The first few tensors are written explicitly (note that it is usually taken as implicit that

$T_{\alpha\beta..\nu}(R)$ may be written as $T_{\alpha\beta..\nu}$ instead).

$$T = R^{-1} \tag{5.3.2}$$

$$T_{\alpha} = -R_{\alpha} R^{-3} \tag{5.3.3}$$

$$T_{\alpha\beta} = 3R_{\alpha}R_{\beta}R^{-5} - \delta_{\alpha\beta}R^{-3} \tag{5.3.4}$$

$$T_{\alpha\beta\gamma} = -15R_{\alpha}R_{\beta}R_{\gamma}R^{-7} + 3\left(\delta_{\beta\gamma}R_{\alpha} + \delta_{\alpha\gamma}R_{\beta} + \delta_{\alpha\beta}R_{\gamma}\right)R^{-5} \tag{5.3.5}$$

$$T_{\alpha\beta\gamma\delta} = 105R_{\alpha}R_{\beta}R_{\gamma}R_{\delta}R^{-9} - 15\left(R_{\alpha}R_{\beta}\delta_{\gamma\delta} + R_{\alpha}R_{\gamma}\delta_{\beta\delta} + R_{\alpha}R_{\delta}\delta_{\beta\gamma} + R_{\beta}R_{\gamma}\delta_{\alpha\delta}\right.$$
$$\left. + R_{\beta}R_{\delta}\delta_{\alpha\gamma} + R_{\gamma}R_{\delta}\delta_{\alpha\beta}\right)R^{-7} + 3\left(\delta_{\alpha\beta}\delta_{\gamma\delta} + \delta_{\alpha\gamma}\delta_{\beta\delta} + \delta_{\alpha\delta}\delta_{\beta\gamma}\right)R^{-5} \tag{5.3.6}$$

It can be seen that the expressions for the tensors rapidly become clumsy, especially for terms such as the second in (5.3.6) which is simply the six different ways that the suffices α, β, γ and δ can be arranged in the form of $R_a R_b \delta_{cd}$. To simplify this an expression is introduced which is of the form:

$$\sum_{(6)} R_{\alpha}R_{\beta}\delta_{\gamma\delta}$$

which represents the sum of the six different terms obtained by rearrangement of the suffices. For example (5.3.6) would be more conveniently rewritten as:

$$T_{\alpha\beta\gamma\delta} = 105R_{\alpha}R_{\beta}R_{\gamma}R_{\delta}R^{-9} - 15\sum_{(6)} R_{\alpha}R_{\beta}\delta_{\gamma\delta}R^{-7} + 3\sum_{(3)} \delta_{\alpha\beta}\delta_{\gamma\delta}R^{-5} \tag{5.3.7}$$

The next two tensors in the series are as follows:

$$T_{\alpha\beta\gamma\delta\epsilon} = -945R_{\alpha}R_{\beta}R_{\gamma}R_{\delta}R_{\epsilon}R^{-11} + 105\sum_{(10)} R_{\alpha}R_{\beta}R_{\gamma}\delta_{\delta\epsilon}R^{-9} - 15\sum_{(15)} R_{\alpha}\delta_{\beta\gamma}\delta_{\delta\epsilon}R^{-7} \tag{5.3.8}$$

$$T_{\alpha\beta\gamma\delta\varepsilon\eta} = 10395R_\alpha R_\beta R_\gamma R_\delta R_\varepsilon R_\eta R^{-13} - 945\sum_{(15)} R_\alpha R_\beta R_\gamma R_\delta \delta_{\varepsilon\eta} R^{-11}$$

$$+ 105\sum_{(45)} R_\alpha R_\beta \delta_{\gamma\delta} \delta_{\varepsilon\eta} R^{-9} - 15\sum_{(15)} \delta_{\alpha\beta} \delta_{\gamma\delta} \delta_{\varepsilon\eta} R^{-7} \qquad (5.3.9)$$

The tensors are now partitioned and the first four terms for a general tensor may be written as follows:

$$T^{(n)1}_{\alpha\ldots\nu} = (-1)^n (2n-1)!! R_{\alpha\,(n)\ldots\ldots} R_\nu R^{-(2n+1)} \qquad (5.3.10)$$

$$T^{(n)2}_{\alpha\ldots\nu} = (-1)^{n+1} (2n-3)!! \sum_{(\chi_n)} \delta_{\alpha\beta} R_{\gamma\,(n-2)\ldots\ldots} R_\nu R^{-(2n-1)} \qquad (5.3.11)$$

$$T^{(n)3}_{\alpha\ldots\nu} = (-1)^{n+2} (2n-5)!! \sum_{(\phi_n)} \delta_{\alpha\beta} \delta_{\gamma\delta} R_{\varepsilon\,(n-4)\ldots\ldots} R_\nu R^{-(2n-3)} \qquad (5.3.12)$$

$$T^{(n)4}_{\alpha\ldots\nu} = (-1)^{n+3} (2n-7)!! \sum_{(\varphi_n)} \delta_{\alpha\beta} \delta_{\gamma\delta} \delta_{\varepsilon\lambda} R_{\tau\,(n-6)\ldots\ldots} R_\nu R^{-(2n-5)} \qquad (5.3.13)$$

The numbers χ_n, ϕ_n and φ_n represent the number of terms which contribute to each summation. These numbers are related and each may be expressed as an arithmetic progression:

$$\chi_n = \sum_{i=1}^{n-1} i = \frac{1}{2}(n-1)n \qquad (5.3.14)$$

$$\phi_n = \sum_{j=3}^{n-1} (j-2)\chi_j = \sum_{j=1}^{n-3} \frac{1}{2} j(j+1)(j+2) \qquad (5.3.15)$$

$$\varphi_n = \sum_{k=5}^{n-1} (k-4)\phi_k = \sum_{k=1}^{n-5} \frac{1}{8} k(k+1)(k+2)(k+3)(k+4) \qquad (5.3.16)$$

These arithmetic progressions may now be evaluated and compared:

$$\chi_n = \frac{1}{2}(n-1)n \qquad (5.3.17)$$

$$\phi_n = \frac{1}{8}(n-3)(n-2)(n-1)n \qquad (5.3.18)$$

$$\varphi_n = \frac{1}{48}(n-5)(n-4)(n-3)(n-2)(n-1)n \qquad (5.3.19)$$

Each one of the numbers can be recognised as having the value:

$$\Sigma_n^m = \frac{1}{2.4.6....2m}\,(n-2m+1)(n-2m+2)...n = \frac{2^{-m}n!}{m!(n-2m)!} \qquad (5.3.20)$$

where the number m corresponds to the number of Kronecker delta functions which appear in each component of the tensor given by equations (5.3.10 - 5.3.13). The numbers χ_n, ϕ_n and φ_n can be recognised as Σ_n^1, Σ_n^2 and Σ_n^3.

The table of values from Σ_0^0 to Σ_{12}^6 is presented as follows:

Table 5.1: Values of Σ_n^m for n = 0 to 12

Σ_n^m	m=0	m=1	m=2	m=3	m=4	m=5	m=6
n=0	1	-	-	-	-	-	-
n=1	1	-	-	-	-	-	-
n=2	1	1	-	-	-	-	-
n=3	1	3	-	-	-	-	-
n=4	1	6	3	-	-	-	-
n=5	1	10	15	-	-	-	-
n=6	1	15	45	15	-	-	-
n=7	1	21	105	105	-	-	-
n=8	1	28	210	420	105	-	-
n=9	1	36	378	1260	945	-	-
n=10	1	45	630	3150	4725	945	-
n=11	1	55	990	6930	17325	10395	-
n=12	1	66	1485	13860	51975	62370	10395

The general expression for a tensor of order n may be written as a summation of terms as follows:

$$T^{(n)}_{\alpha..\nu}(R) = \sum_{m=0}^{\lfloor n/2 \rfloor} (-1)^{n+m}(2n-2m-1)!! \sum_{(n,m)} \delta_{\alpha\beta}\ldots\delta_{\varepsilon\lambda}R_{\tau}\ldots\ldots R_{\nu}R^{-(2n-2m+1)} \qquad (5.3.21)$$

where the summation over (n,m) indicates that there are Σ^m_n terms of the form $\delta_{\alpha\beta}\ldots\delta_{\varepsilon\lambda}R_{\tau}\ldots\ldots R_{\nu}$ to be considered.

Each of these components is expressed in a cartesian axis system and consequently each subscript can take one of only three values; x, y or z. The subscripts can therefore be logically "grouped" together and the above expression can be greatly simplified dependent upon which tensors are being considered.

The most simple subset of tensors will be those of the form $T^{(n)}_{\alpha..\alpha}$ (for example $T^{(6)}_{zzzzzz}$) representing the n'th derivative of 1/R with respect to the component R_α. For tensors such as this the product of terms of the form $\delta_{\alpha\beta}\ldots\delta_{\varepsilon\lambda}$ is replaced by $\delta_{\alpha\alpha}\ldots\delta_{\alpha\alpha}$ and consequently all terms in the general expression contribute to $T^{(n)}_{\alpha..\alpha}$. The summation is over Σ^m_n terms, all of which are identical, so that the summation may be simply replaced by the number Σ^m_n:

$$\sum_{(n,m)} \delta_{\alpha\beta}\ldots\delta_{\varepsilon\lambda}R_{\tau}\ldots\ldots R_{\nu} \ (\alpha=\beta=\ldots\ldots=\nu) \equiv \Sigma^m_n \, R_\alpha^{(n-2m)} \qquad (5.3.22)$$

The general expression for n'th order tensor given by (5.3.21) may be written:

$$T^{(n)}_{\alpha..\alpha}(R) = (-1)^n n! \, R^{-(n+1)} \sum_{m=0}^{\lfloor n/2 \rfloor} \frac{2^{-m}(-1)^m(2n-2m-1)!!}{m!(n-2m)!} \, (R_\alpha/R)^{(n-2m)} \qquad (5.3.23)$$

and recalling equation (5.2.12) the summation component can be

recognised as being the Legendre Polynomial of order n. Hence the expression for the tensor $T^{(n)}_{\alpha..\alpha}(R)$ may be simply written as:

$$T^{(n)}_{\alpha..\alpha}(R) = (-1)^n n!\ R^{-(n+1)}\ P_n(R_\alpha/R) \qquad (5.3.24)$$

It may be seen that by evaluating just four Legendre polynomials, namely P_0, $P_1(R_x/R)$, $P_1(R_y/R)$ and $P_1(R_z/R)$, application of the recursion formula given by (5.2.4) will yield all higher Legendre polynomials and hence all tensors of the form $T^{(n)}_{\alpha..\alpha}$ may be generated using (5.3.24).

The next set of tensors to be considered are those which represent differentiation with respect to two different cartesian components, ie those tensors of the form $T^{(n)}_{\alpha.\alpha\beta.\beta}(R)$, where $\alpha\neq\beta$.

If n is the order of the tensor, a is introduced as the number of occurrences of the cartesian subscript α and b is introduced as the number of occurrences of the cartesian subscript β (and hence n=a+b). Of the Σ^m_n terms which are of the form $\delta_{\alpha\beta}\ldots\delta_{\varepsilon\lambda}R_\tau\ldots\ldots R_\nu$ in the general expression for the tensor, (5.3.21) the only non-zero components will be those of the form:

$$\underbrace{\delta_{\alpha\alpha}\ldots\delta_{\alpha\alpha}}_{(i)}\underbrace{\delta_{\beta\beta}\ldots\delta_{\beta\beta}}_{(j)}\underbrace{R_\alpha\ldots\ldots R_\alpha}_{(a-2i)}R_\beta\underbrace{\ldots\ldots R_\beta}_{(b-2j)}.$$

where two further indices have been introduced, i is the number of Kronecker delta functions of the form $\delta_{\alpha\alpha}$ and j is the number of Kronecker delta functions of the form $\delta_{\beta\beta}$ (and hence m=i+j). Noting (5.3.22) the number of the terms which will be of the above form may be written in a number of ways:

$$\frac{2^{-i}a!}{i!(a-2i)!}\ \frac{2^{-j}b!}{j!(b-2j)!} = \frac{2^{-i}a!}{i!(a-2i)!}\ \Sigma^j_b = \Sigma^i_a\ \Sigma^j_b \qquad (5.3.25)$$

The general expression for the tensor given by (5.3.21) may now be

rewritten for this specific case:

$$T^{(a+b)}_{\alpha.\alpha\beta.\beta}(R) = \sum_{i=0}^{\lfloor a/2 \rfloor} \sum_{j=0}^{\lfloor b/2 \rfloor} (-1)^{n+i+j} (2n-2i-2j-1)!! \frac{2^{-i} a!}{i!(a-2i)!} R^{-(n+1)}$$

$$(R_\alpha/R)^{(a-2i)} \Sigma^j_b (R_\beta/R)^{(b-2j)} \qquad (5.3.26)$$

Recalling the expression for the Associated Legendre Polynomial given by (5.2.17) then the component of (5.3.26) which is given by:

$$\sum_{i=0}^{\lfloor a/2 \rfloor} \frac{2^{-i}(-1)^i (2n-2i-2j-1)!!}{i!(a-2i)!} (R_\alpha/R)^{(a-2i)}$$

can be recognized as being closely related to the Associated Legendre Polynomial $P^{b-j}_{n-j}(R_\alpha/R)$, recalling that b=n-a. The general expression for the tensor simplifies to give:

$$T^{(a+b)}_{\alpha.\alpha\beta.\beta}(R) = (-1)^n \, a! \, R^{-(n+1)} \sum_{j=0}^{\lfloor b/2 \rfloor} \frac{\partial^{b-j} P_{n-j}(R_\alpha/R)}{\partial (R_\alpha/R)^{b-j}}$$

$$(-1)^j \Sigma^j_b (R_\beta/R)^{b-2j} \qquad (5.3.27)$$

The final set of tensors to be considered are those which represent differentiation with respect to three different cartesian components, ie those tensors of the form $T^{(n)}_{\alpha.\alpha\beta.\beta\gamma.\gamma}(R)$, where $\alpha \neq \beta \neq \gamma$. Two further indices are introduced, c is the number of occurrences of the cartesian subscript γ (so that now n=a+b+c) and k is the number of Kronecker delta functions of the form $\delta_{\gamma\gamma}$ (and m=i+j+k).

The only non-zero components of the Σ^m_n terms which are of the form $\delta_{\alpha\beta}\ldots\delta_{\varepsilon\lambda}R_\tau\ldots\ldots R_\nu$ in the general expression for the tensor (5.3.21) will be those which are of the form:

$$\delta_{\alpha\alpha}\ldots\delta_{\alpha\alpha}\delta_{\beta\beta}\ldots\delta_{\beta\beta}\delta_{\gamma\gamma}\ldots\delta_{\gamma\gamma}R_{\alpha}\ldots\ldots R_{\alpha}R_{\beta}\ldots\ldots R_{\beta}R_{\gamma}\ldots\ldots R_{\gamma}$$
$$\underbrace{\qquad}_{(i)}\qquad\underbrace{\qquad}_{(j)}\qquad\underbrace{\qquad}_{(k)}\qquad\underbrace{\qquad}_{(a-2i)}\qquad\underbrace{\qquad}_{(b-2j)}\qquad\underbrace{\qquad}_{(c-2k)}$$

and the analogue of (5.3.26) may be written:

$$T^{(a+b+c)}_{\alpha.\alpha\beta.\beta\gamma.\gamma}(R) = \sum_{i=0}^{|a/2|}\sum_{j=0}^{|b/2|}\sum_{k=0}^{|c/2|}(-1)^{n}\,(2n-2i-2j-2k-1)!!\,\frac{2^{-i}a!}{i!(a-2i)!}$$
$$(-1)^{i+j+k}\,(R_{\alpha}/R)^{(a-2i)}\,\Sigma^{j}_{b}(R_{\beta}/R)^{(b-2j)}$$
$$\Sigma^{k}_{c}(R_{\gamma}/R)^{(c-2k)}\,R^{-(n+1)} \qquad (5.3.28)$$

After recognition of the derivative related to the Associated Legendre Polynomial, $P^{b+c-j-k}_{n-j-k}(R_{\alpha}/R)$ the analogue of (5.3.27) may be written:

$$T^{(a+b+c)}_{\alpha.\alpha\beta.\beta\gamma.\gamma}(R) = (-1)^{n}\,a!\,R^{-(n+1)}\sum_{j=0}^{|b/2|}\sum_{k=0}^{|c/2|}\frac{\partial^{b+c-j-k}P_{n-j-k}(R_{\alpha}/R)}{\partial(R_{\alpha}/R)^{b+c-j-k}}$$
$$(-1)^{j+k}\,\Sigma^{j}_{b}(R_{\beta}/R)^{b-2j}\,\Sigma^{k}_{c}(R_{\gamma}/R)^{c-2k} \qquad (5.3.29)$$

This is the general expression required and permits any general tensor of the form $T^{(a+b+c)}_{\alpha.\alpha\beta.\beta\gamma.\gamma}(R)$ to be evaluated. It may be seen by inspection that by setting c=0 (and by implication k=0) the expression (5.3.27) for tensors of the form $T^{(a+b)}_{\alpha.\alpha\beta.\beta}(R)$ is generated and that by setting b=c=0 (and by implication j=k=0) the expression (5.3.24) for tensors of the form $T^{(a)}_{\alpha.\alpha}(R)$ is generated.

An alternative derivation of (5.3.28) may be obtained by treating all three subscripts in identical fashion and not using the Legendre Polynomials at all. In this case either the number Σ^{i}_{a} may be identified within (5.3.28) or the derivative in (5.3.29) may be recognised as being given by:

$$a!\ \frac{\partial^{b+c-j-k} P_{n-j-k}(R_\alpha/R)}{\partial(R_\alpha/R)^{b+c-j-k}} = \sum_{i=0}^{\lfloor a/2 \rfloor} \Sigma_a^i\ (-1)^i (2n-2m-1)!!\ (R_\alpha/R)^{a-2i} \qquad (5.3.30)$$

Hence the general expression for a tensor given by (5.3.29) may be alternatively written without any reference to Legendre polynomials:

$$T^{(a+b+c)}_{\alpha.\alpha\beta.\beta\gamma.\gamma}(R) = \sum_{i=0}^{\lfloor a/2 \rfloor} \sum_{j=0}^{\lfloor b/2 \rfloor} \sum_{k=0}^{\lfloor c/2 \rfloor} (-1)^{n+m}\ (2n-2m-1)!!\ R^{-(n+1)}$$

$$\Sigma_a^i (R_\alpha/R)^{a-2i}\ \Sigma_b^j (R_\beta/R)^{b-2j}\ \Sigma_c^k (R_\gamma/R)^{c-2k} \qquad (5.3.31)$$

It may be seen that when c=0 (and k=0) the term $\Sigma_c^k (R_\gamma/R)^{c-2k}$ reduces to one and the analogue of (5.3.27) is generated. Similarly with b=c=0 (and j=k=0) the analogue of (5.3.24) is generated.

5.4: Discussion

Two forms for obtaining the values of tensors have been detailed above, the general expressions (5.3.29) and (5.3.31) enabling the tensors to be evaluated with and without the Legendre Polynomials. The second general expression illustrates the symmetry inherent to these tensors, a symmetry which is not apparent within the first general expression. The primary objective for the derivation of these relationships is for the purpose of calculating tensors within a computer program. For this purpose both expressions will have their uses.

In general the second expression is likely to prove to be the most convenient to use, for it is basically a triple summation with a function of two numbers (Σ_n^m). As an illustration the tensor $T^{(8)}_{xxyyzzzz}(R)$ is considered. If the expression (4.3.28) is used to

calculate the tensors, to minimise the summation required over the indices j and k the cartesian component within the Legendre Polynomials, α is chosen to be z, the most common subscript. The indices b and c are both equal to two and it can be seen that three derivatives of Legendre Polynomials would be required, the fourth derivative of $P_8(R_z/R)$, the third derivative of $P_7(R_z/R)$ and the second derivative of $P_6(R_z/R)$. As each is generated by a different recursion series six initial values for the derivatives of Legendre Polynomials are required to generate the single tensor. Unless a number of other tensors are required in the calculations whose components include second, third and fourth derivatives of Legendre Polynomials of (R_z/R) it is likely to be more efficient to program the second expression (4.3.30).

However under certain circumstances the tensors required are much simpler than that given above. For the crystal of carbonyl sulphide, discussed later, symmetry reduces the tensors required to those of the form $T^{(n)}_{z..z}$, $T^{(n)}_{xz..z}$ and $T^{(n)}_{xxz..z}$ only. In the case of the first it is clearly more efficient to use the Legendre Polynomial algorithm (it is actually the simplified expression, (5.3.24) which would be utilised), the zero and first order polynomials given by (5.2.2) and (5.2.3) are simple to determine and these generate all of the other polynomials required. For the latter two tensors the expression (5.3.29) will be less efficient, the function Σ^m_n is required with or without the Legendre Polynomials and its usage should therefore be maximised. It should be stressed that in all cases either form may be used and that no qualitative analysis of computational processing time has been described here.

6.1: Introduction

The empirical potentials which have been discussed previously are to be used for modelling real systems. The technique followed here is to vary a number of the potential parameters to fit a set of known lattice properties. The basic theory concerning the lattice properties of a general system has been described in Chapter 2. In this chapter a specific crystal will be considered and the general properties discussed previously will be detailed.

To be suitable for such an investigation the crystal concerned needs to be one for which the values of appropriate lattice properties are known. The number of lattice properties cannot be too low or it will be too easy to fit the empirical potential and the fitted potential obtained would be unlikely to prove satisfactory if it were required to satisfy further conditions. Similarly the number of lattice properties cannot be too high or it would be virtually impossible to ever fit any potential and be in a position to make any critical evaluation of a given empirical potential.

Commonly this fitting procedure has been applied only to zero and first order properties. Where attempts have been made to fit second order properties as well, the process has been of least-squares type and not exact. The inherent disadvantage of this particular procedure is that it is not clear how much deviation from an exact fit should be expected by the least-squares procedure. When a calculated property deviates from the experimental value there will always be some doubt as to whether the deviation is due to an intrinsic shortcoming in the empirical potential used for the modelling or due to the inefficiency of the iteration procedure in the fitting.

Within this thesis an intermediate procedure is adopted. The empirical potential is fitted exactly to a limited number of properties (which include zero, first and second order) of a crystal with relatively low symmetry. The solution will be unique and the parameter values obtained by the fitting may be examined to determine whether they are physically reasonable. A number of additional lattice properties, not used within the fitting procedure, are also calculated to enable a critical evaluation of the potential. An ideal crystal for this purpose is carbonyl sulphide, OCS.

6.2: Lattice Properties of Carbonyl Sulphide

Lattice Energy

Kemp and Giauque[19] have investigated the thermodynamic properties of solid and liquid carbonyl sulphide from 15 K to its boiling point. Their data has been analysed by Aung and Strauss[20] who have given a value of -6.485 kcal mol^{-1} for the enthalpy of sublimation at zero temperature and pressure. An estimate of the lattice energy of the crystal may be obtained by the addition of a small correction for the zero-point energy. The value of this energy is not known exactly but it may be estimated from the Debye temperature at 0 K which Aung and Strauss have estimated at 104.9 K and leads to a zero-point energy of -0.2345 kcal mol^{-1} and thence an estimate of the lattice energy at -6.72 kcal mol^{-1}. The lattice energy is the first property to which an empirical potential is fitted for carbonyl sulphide.

Lattice Structure

The crystal structure of carbonyl sulphide has been investigated by Vegard[21] using X-ray diffraction at liquid air temperature and subsequently by Overell, Pawley and Powell[22] using neutron powder diffraction at 90 K. Both experiments agree that the crystal structure

is rhombohedral, with space group R3m (C_{3v}^5) and only one molecule per unit cell. Their results for the values of the unit cell dimensions differ slightly and within this thesis the values obtained by Overell et al are used, namely a = 4.063 Å and $\alpha = 98.81^\circ$. The results for the bond lengths differ greatly and the values obtained by Overell et al are, unlike the Vegard values, in good agreement with gas phase measurements. These are the values which are used within this thesis, r(C-O) = 1.21 Å and r(C-S) = 1.51 Å.

The lattice structure of carbonyl sulphide is illustrated in figure 6.1. It may seen that the single molecule within each unit cell lies along the crystal fixed three-fold axis and has the full C_{3v} symmetry at the crystal site. With there being only one molecule per unit cell the position of the molecular centre of mass is fixed and with the molecule lying along the three fold fold axis the orientation is also fixed. Consequently the equilibrium conditions described by (2.4.1), representing the first derivatives of the potential with respect to the five vibrational coordinates, are all automatically satisfied by the symmetry of the system.

This only leaves the requirement that the crystal should be stress free (or equivalently that the dimensions of the unit cell should correspond to a minimum in the potential energy). Chandrasekharan and Walmsley[23] have shown that some components of the stress vanish by symmetry. In the case of carbonyl sulphide all off-diagonal components of the stress are zero and there are only two independent diagonal stresses, the components along the three-fold axis and perpendicular to the three fold axis. It is these last two conditions, referred to within this thesis as the z-stress and the x-stress which constitute the second and third properties to which an empirical potential for carbonyl sulphide is fitted.

Figure 6.1: Lattice Structure of Carbonyl Sulphide Crystal

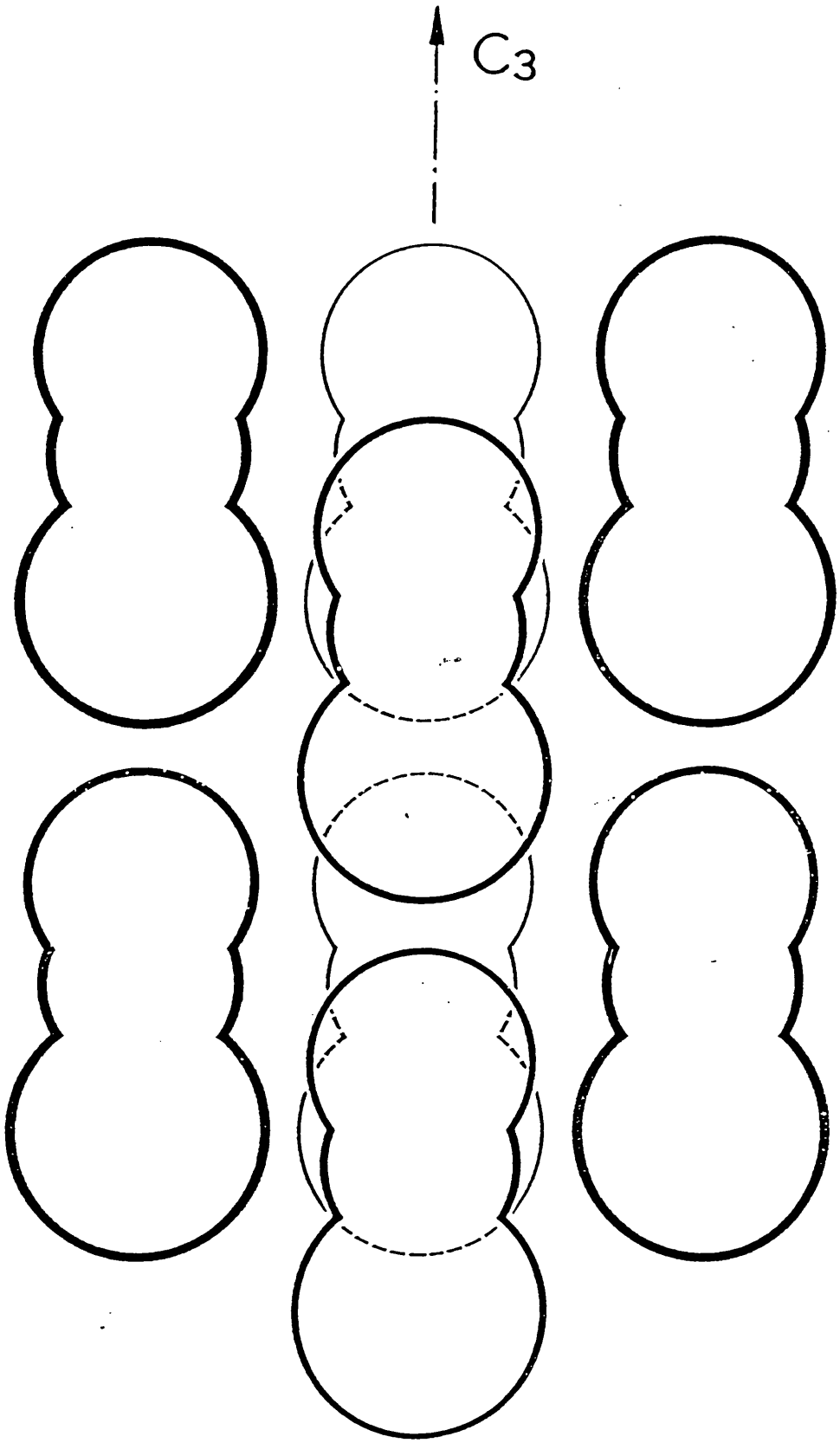

Lattice Vibrations

The far-infrared spectrum of solid carbonyl sulphide has been measured at 77 K by Anderson and Walmsley[24] and yields a single fundamental frequency of 92 cm^{-1}. Cahill, Treuil, Miller and Leroi[25] have also investigated the Raman spectrum at 90K and obtained a single peak at 89 cm^{-1}. Theory predicts that there should be only one fundamental vibration and that it should appear in both the infrared and Raman spectra and these results are reasonably consistent with this prediction. The vibration concerned is a torsional vibration (libration) in which all of the molecules tilt away from the three-fold axis in phase. The vibration is doubly degenerate. The torsional frequency of vibration (whose value is taken as 92 cm^{-1}) is chosen to be the fourth property to which an empirical potential will be fitted. Thus the four properties chosen, the lattice energy, the x-stress, the z-stress and the torsional frequency of vibration, which will be those to which an empirical potential is fitted, cover zero, first and second order terms in the Taylor expansion.

As has been mentioned in Chapter 2 the lattice vibration frequencies obtained from infrared and Raman spectroscopy are associated with the zero wave-vector. In general each normal vibration of the crystal may be classified in terms of a wave-vector which determines the relative phase of the motion from one unit cell to another. The complete set of wave-vectors may be found within the first Brillouin zone of the crystal. The corresponding frequencies of vibration are in principle accessible using neutron scattering but no such results have been published. However, there is an additional requirement, namely that for the crystal to be stable the normal modes must all be real. These frequencies may also be obtained from an empirical potential and although the values cannot be used for direct comparison with

experimental values the requirement that they must all be real provides a further test of an empirical potential. The lattice vibration frequencies are calculated along specific wave-vector directions in the first Brillouin zone of the crystal. The corresponding ranges of values for the frequencies constitute "branches" of the "dispersion curves". For carbonyl sulphide, a linear molecule with one molecule per unit cell, there are five of these branches in any given direction. As the magnitude of the wave-vector tends toward zero, the frequencies of three of the branches also tend toward zero and are known as acoustic branches, being associated with the propagation of sound within the crystal. The frequencies of the remaining two branches tend towards a finite limit and are known as optical branches. For carbonyl sulphide the two finite frequencies have the same value, being the fundamental frequency 92 cm^{-1} discussed previously.

Within this thesis the results quoted are for the wave-vectors in two directions, the first along the three-fold axis (referred to as the parallel direction) and the second perpendicular to the three-fold axis in one of the σ_v planes of symmetry (referred to as the perpendicular direction). The symmetry of carbonyl sulphide reduces the number of independent branches in the parallel direction to three, the two optical branches being degenerate and two of the three acoustic branches also being degenerate. No such degeneracy occurs in the perpendicular direction and all five branches persist.

It should also be noted that these two directions are also the first two directions conveniently chosen for the formation of the Gamma matrices used for the determination of elastic constants from wave velocities described in Chapter 3.

Compressibility

As discussed in Chapter 3 the elastic constants of carbonyl sulphide are, in principle, quantities which may be determined experimentally but as yet they have not been measured. However the calculated values for the elastic constants may be used indirectly as a further test of an empirical potential. The compressibility of carbonyl sulphide may be derived from the elastic constants using (3.4.2) and the value for the compressibility at zero temperature has been estimated by Deakin[26] at $\varkappa_0 = 0.22\ GPa^{-1}$ from pressure-volume measurements by Stevenson[27]. Additionally the conditions for elastic stability detailed in section 3.4 also permit the calculated elastic constants to be used as a further test of an empirical potential.

6.3: Potentials for Carbonyl Sulphide

Lennard-Jones Atom-Atom Potential

Carbonyl sulphide is comprised of three different atoms and for an atom-atom Lennard-Jones potential there would generally be six different interaction types; O-O, O-C, O-S, C-C, C-S and S-S. All of the four crystal properties to which the function is to fitted are linear in the ϵ parameters (strictly it is the square of the frequency which is linear). Furthermore all four properties depend equivalently upon the different homonuclear interactions and consequently the O-O, C-C and S-S interactions are not independent. The three are combined so that there are only four independent interaction types, like-like (L-L), O-C, O-S and C-S.

The fitting procedure involves supplying suitable values for the four parameters r_0^{LL}, r_0^{OC}, r_0^{OS} and r_0^{CS} in the Lennard-Jones potentials which model each interaction type and then solving the four equations (the values for the lattice energy, the x-stress, the z-stress and the

torsional frequency) in the four unknowns (ϵ_{LL}, ϵ_{OC}, ϵ_{OS} and ϵ_{CS}). This procedure will yield a unique solution. The requirement that the ϵ parameters obtained should be physically realistic provides a further test of the parameters obtained.

The choice of the r_0 parameters is generally governed by packing considerations within the crystal. Each atom pair can contribute a maximum of $-\epsilon$ to the lattice energy if the pair separation is exactly r_0 and a favourable structure is likely to result when a number of atom pairs have a separation close to the appropriate value of r_0. The near-neighbour contact distances for carbonyl sulphide are presented in table 6.1:

Table 6.1: Atom-Atom Contact Distances for OCS

Atom Pair	Distance (Å)	Molecule	No.Contacts
like-like	4.063	(100)	18
	5.288	(110)	18
	5.861	(111)	6
O-C	3.639	(100)	6
	4.469	(110)	6
	4.651	(111)	2
	4.765	(100)	6
O-S	3.141	(111)	2
	3.644	(100)	6
	3.755	(110)	6
	5.877	(100)	6
C-S	3.590	(100)	6
	4.294	(110)	6
	4.351	(111)	2
	4.969	(100)	6

It may be seen that there is generally a clustering effect for the various interactions and the values of r_0 may be chosen such that the equilibrium distances do fall reasonably within these "cluster ranges". However there are exceptions, in particular the O-S interaction at 3.141 Å, which is the interaction between the oxygen and sulphur atoms along the three-fold axis. This "anomalous" short contact has been considered by Deakin and Walmsley[28] as being one of the primary contributors to the failure of a purely atom-atom model for modelling carbonyl sulphide. Instead the atom-atom potential is combined with some sort of multipolar potential to include the electrostatic interaction discussed in Chapter 4. The procedure adopted to include these multipolar interactions is to calculate the contribution of the multipolar potential to the specimen lattice properties and fit the atom-atom potential to the adjusted values.

Multipolar Potentials

The molecular multipole and atomic multipole potentials have been discussed in Chapter 4. For carbonyl sulphide both the molecular dipole and molecular quadrupole moments have been determined experimentally. Both of these moments have been measured using molecular-beam electric-resonance spectroscopy by de Leeuw and Dymanus[29,30] and their values are 0.71512 Debye and -0.79 Debye Å respectively. Both moments are relatively small and correspond to a molecule with relatively little dipolar or quadrupolar character. Inclusion of the molecular dipole and molecular quadrupole moments into the overall potential do not lead to any significant improvements on the atom-atom model. The molecular octupole moment has not been determined experimentally but calculations discussed in the next chapter suggest that the octupole is the first molecular moment which contributes significantly to the specimen lattice properties for

carbonyl sulphide.

The lattice structure of carbonyl sulphide also leads to simplifications in the Taylor expansion coefficients for the multipolar potentials (both molecular and atomic). With all the molecules lying in the same direction the crystal fixed axes are conveniently defined such that they are coincident with all of the molecule fixed axes. Consequently the values of the direction cosines at the reference configuration may be written:

$$\Lambda^{AO}_{\alpha\beta} = \delta_{\alpha\beta} \qquad (6.3.1)$$

and the Taylor expansion coefficients detailed in sections 4.4 and 4.5 may be rewritten without the multiple (implied) summations over the cartesian subscripts in the direction cosines and tensors. For example the derivative given by (4.4.15):

$$\left(\frac{\partial^2 V^{AB}_{mn}}{\partial\lambda^A_\sigma\,\partial\lambda^A_\tau}\right)_0 = m\Big[(m-1)\;\Lambda^{AO}_{\alpha\sigma}\Lambda^{AO}_{\beta\tau}\Lambda^{AO}_{\gamma z\,(m-2)}\ldots\ldots\Lambda^{AO}_{\mu z}\Lambda^{BO}_{\alpha' z\,(n)}\ldots\ldots\Lambda^{BO}_{\mu' z}\;T^{(n+m)}_{\alpha.\mu\alpha'.\mu'}(R^{AB})$$

$$-\;\delta_{\sigma\tau}\Lambda^{AO}_{\alpha z}\Lambda^{AO}_{\beta z}\Lambda^{AO}_{\gamma z\,(m-2)}\ldots\ldots\Lambda^{AO}_{\mu z}\Lambda^{BO}_{\alpha' z\,(n)}\ldots\ldots\Lambda^{BO}_{\mu' z}\;T^{(n+m)}_{\alpha.\mu\alpha'.\mu'}(R^{AB})\Big]\;M^A(m)\;M^B(n)$$

is simplified and rewritten:

$$\left(\frac{\partial^2 V^{AB}_{mn}}{\partial\lambda^A_\sigma\,\partial\lambda^A_\tau}\right)_0 = m\Big[(m-1)\;T^{(n+m)}_{\sigma\tau z..z}(R^{AB}) - \delta_{\sigma\tau}\;T^{(n+m)}_{z..z}(R^{AB})\Big]\;M^A(m)\;M^B(n) \qquad (6.3.2)$$

It may be seen that for carbonyl sulphide the only tensors required for the multipolar potentials will be those of the form $T^{(n+m)}_{z..z}(R^{AB})$, $T^{(n+m)}_{\sigma z..z}(R^{AB})$ and $T^{(n+m)}_{\sigma\tau z..z}(R^{AB})$ and as discussed in Chapter 5 the values of these tensors may be determined relatively easily.

Anisotropic Berne-Pechukas Molecule-Molecule Potential

The procedure adopted for fitting the atom-atom Lennard-Jones potential cannot be directly applied to the Berne-Pechukas potential, the four atom-atom ϵ parameters having been replaced by a single molecule-molecule parameter. As discussed in Chapter 4 the Berne-Pechukas potential is a function of three parameters; ϵ (the energy minimum), R_0 (the intermolecular distance at the reference configuration) and χ (the degree of anisotropy). Two of the parameters may be conveniently rearranged:

$$A = \epsilon R_0^{12} \tag{6.3.3}$$

$$B = 2\epsilon R_0^{6} \tag{6.3.4}$$

so that the potential given by (4.3.12) may be rewritten:

$$V^{AiBj} = At^{11/2}s^{-6} - Bt^{5/2}s^{-3} \tag{6.3.5}$$

and it may be seen that the potential is linear in both A and B. The Berne-Pechukas potential is then combined with a molecular octupole potential so that the total potential is a function of four parameters; A, B, χ and C (where C is the square of the molecular octupole moment; $C = \Omega^2$). The crystal properties are also linear in C but not in χ. The procedure adopted is to fit the three linear parameters to the zero and first order lattice properties; the lattice energy and the two components of the stress. Then, the non-linear parameter, χ is adjusted so that the empirical potential yields the correct value for the torsional frequency of vibration.

7.1: Introduction

A wide range of potentials have been used to attempt to model the lattice properties of carbonyl sulphide. In this chapter a number of potentials will be considered, each of which is composed of a 12-6 Lennard-Jones atom-atom potential combined with some form of multipolar potential. The atom-atom potential is kept in a standard form so that the different representations of the multipolar interaction may be compared, the objective to gain an insight into the nature of the multipolar interactions in carbonyl sulphide.

Also the anisotropic Berne-Pechukas molecule-molecule potential is considered as an alternative to the atom-atom potential and is combined with a suitable form for the multipolar interaction, the molecular octupole. This potential utilises the multipolar potential in a slightly different manner, with the molecular octupole moment being employed as an empirical parameter. This provides an indication as to the direction of further development of these potentials.

7.2: Atom-Atom Potential

An empirical potential comprised of only an atom-atom potential with no multipolar component to model carbonyl sulphide has been investigated by Deakin and Walmsley[28] and they have found that although the 12-6 Lennard-Jones potential can be fitted to the four specimen lattice properties there are no solutions which also yield reasonable ϵ parameters. For all fittings of the four lattice properties at least one of the four ϵ parameters is negative and frequently the magnitude of one of the parameters in unreasonably large. Furthermore at least two of the acoustic branches are imaginary

throughout all directions within the first Brillouin zone. Further investigation of the atom-atom components shows that for each of the components at least one acoustic branch is imaginary in all directions and in certain regions at least two branches are imaginary for all components. Consequently no combination of the four components could be able to yield a full set of acoustic branches which are real throughout the first Brillouin zone. The atom-atom model is clearly an inadequate model for carbonyl sulphide and the "close" contact between adjacent sulphur and oxygen atoms along the three-fold axis discussed in the previous chapter has been considered as contributing to the failure of the pure atom-atom model.

7.3: Atom-Atom + Molecular Octupole Potential

The simplest model of the electrostatic interaction for carbonyl sulphide is to use molecular multipoles. As discussed in the previous chapter the molecular dipole and quadrupole moments of carbonyl sulphide are available from experimental measurements but the values suggest that carbonyl sulphide is a molecule with low dipolar and quadrupolar character. Calculation confirms this, the contributions of the molecular dipole and quadrupole moments to the lattice properties are small and in no way do either of the multipoles significantly improve the inadequate atom-atom potential.

The molecular octupole of carbonyl sulphide is not available experimentally but it is expected to be relatively large. The quadrupole moments of carbon dioxide and carbon disulphide have been measured by Battaglia, Buckingham, Neumark, Pierens and Williams[31] at -4.491 Debye Å and 3.60 Debye Å respectively. Carbonyl sulphide can be considered as being comprised of two halves, both strongly quadrupolar but of opposite sign. The quadrupole moment of carbonyl

sulphide would therefore be expected to be low, a result which is consistent with experiment, while the octupole moment would be expected to be large. Ab initio calculations (see Appendix A) indicate that the octupole moment will be in the range 12-15 Debye $Å^2$.

The first potential used is an atom-atom + molecular octupole potential, taking the value for the octupole moment as 10.0 Debye $Å^2$. It is found that this potential can be fitted to the specimen lattice properties and that the resultant potential, given in table 7.1 has realistic values for the ϵ parameters.

Table 7.1: Atom-Atom Lennard-Jones 12-6 + Molecular Octupole Potential for OCS: Parameters

Atom Pair	ϵ/kcal mol^{-1}	R_0/Å
like-like	0.06256	3.7
O-C	0.33476	3.9
O-S	0.04929	3.9
C-S	0.20619	3.9

Ω = 10.0 Debye $Å^2$

As discussed in the previous chapter a further test of this potential is that all of the lattice vibration frequencies should be real. The frequencies within the first Brillouin zone may be illustrated by plotting the relevant dispersion curves in the two directions detailed in the previous chapter. These are given by figures 7.1 and 7.2. It may be seen that the frequencies are real for all branches, though it should be noted that the lowest acoustic branch in the direction perpendicular to the three-fold axis is small in magnitude.

A further test of the potential is to calculate the elastic constants and thence to determine the compressibility and the

Figure 7.1: Atom-Atom Lennard-Jones 12-6 + Molecular Octupole Potential for OCS: Dispersion Curves Parallel to C_3

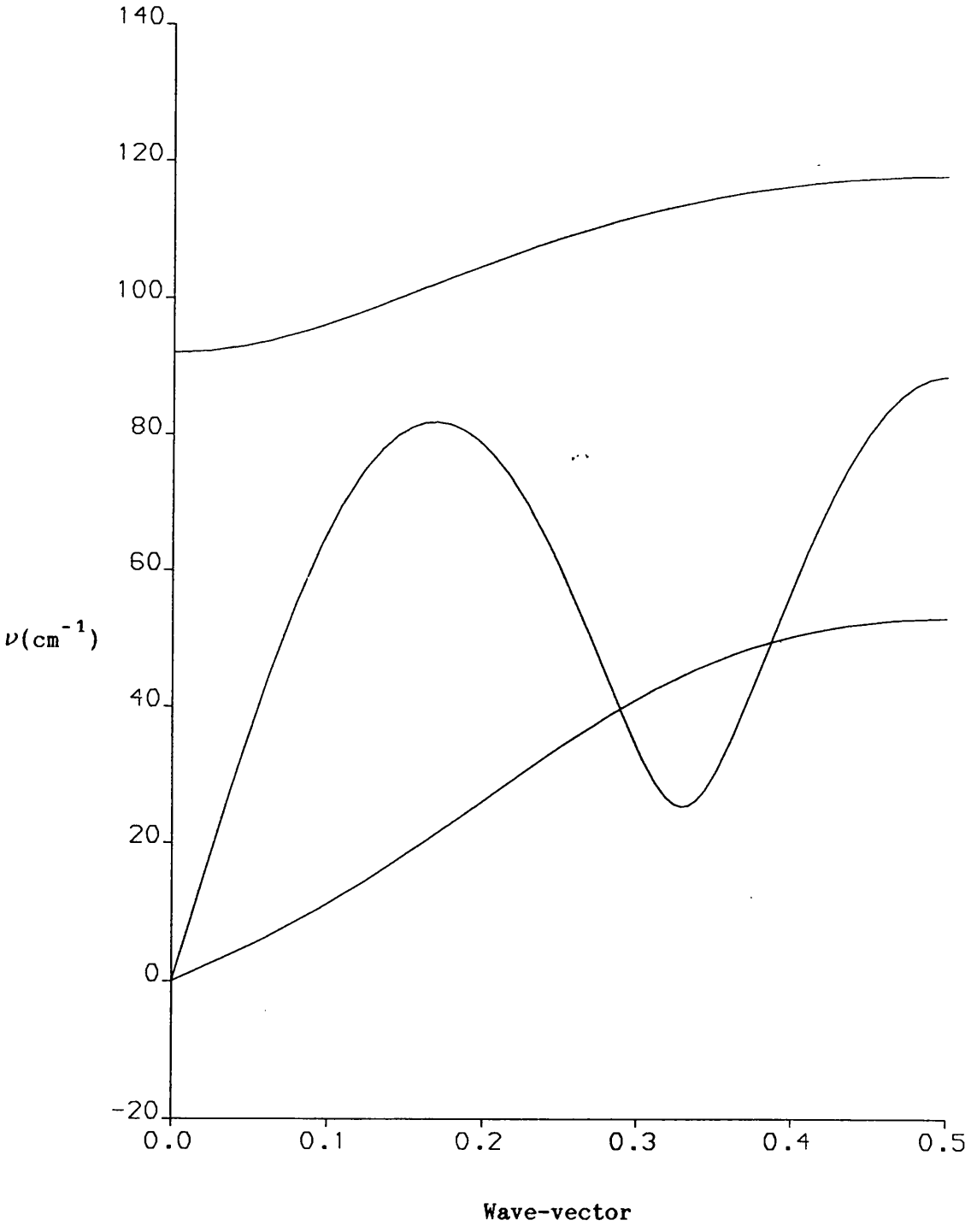

Figure 7.2: Atom-Atom Lennard-Jones 12-6 + Molecular Octupole Potential for OCS: Dispersion Curves Perpendicular to C_3

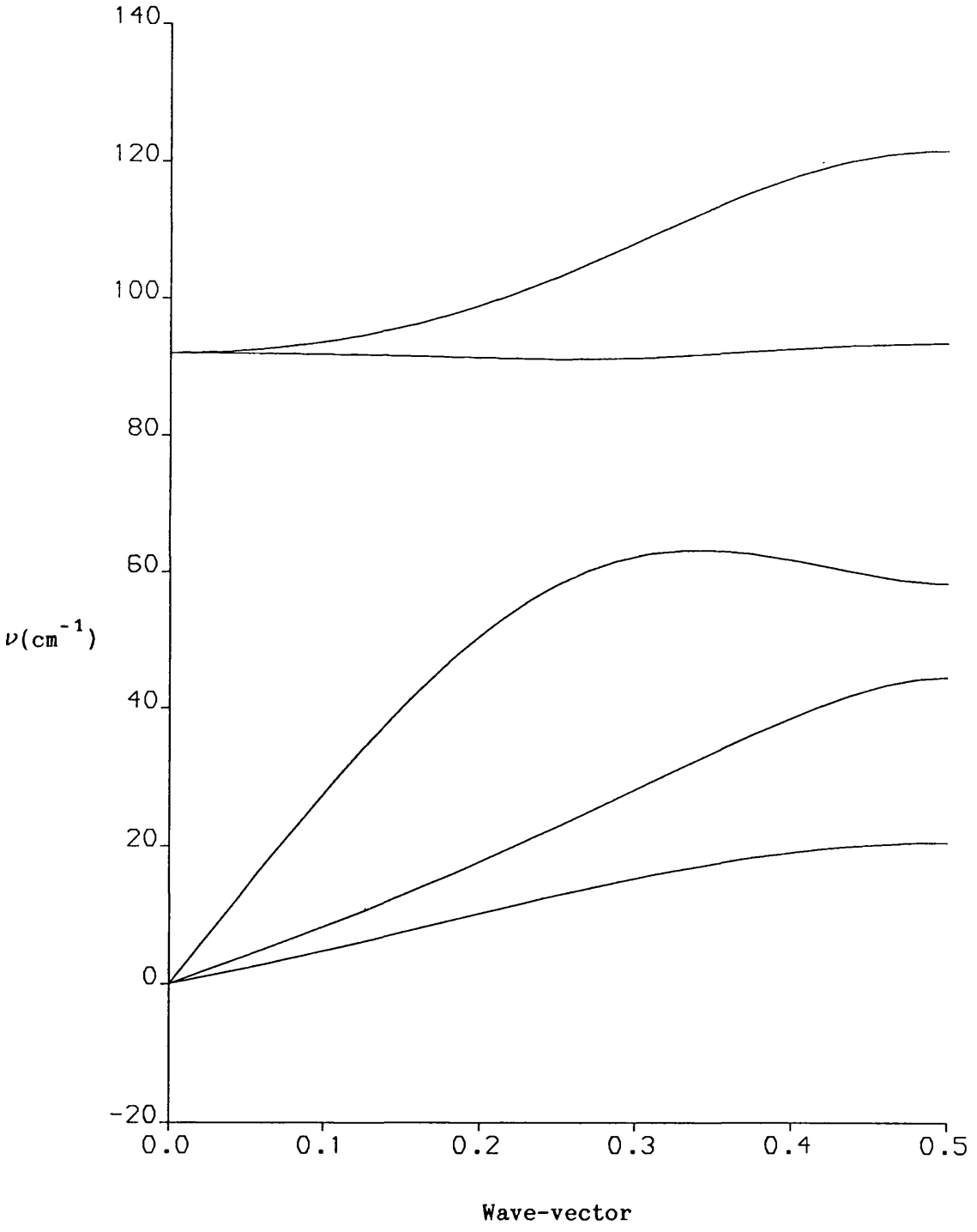

"stability constants". The values of the elastic constants, the compressibility and the stability constants are given in table 7.2.

Table 7.2: Atom-Atom Lennard-Jones 12-6 + Molecular Octupole Potential for OCS: Elastic Properties

c_{11} = 10.5967 GPa	c_{12} = 9.3948 GPa
c_{13} = -0.0111 GPa	c_{15} = 0.3052 GPa
c_{33} = 30.8875 GPa	c_{55} = 0.5352 GPa
S_3 = 687.4872 GPa^2	S_4 = 0.4570 GPa^2
$\varkappa_0$ = 0.1325 GPa^{-1}	

It can be seen that the four stability constants are positive (it should be recalled that $S_1 \equiv c_{33}$ and $S_2 \equiv c_{44}$) so that the requirement that the potential should be elastically stable is satisfied. The compressibility, at $\varkappa_0 = 0.1325\ GPa^{-1}$ is significantly lower than the experimental value ($0.22\ GPa^{-1}$) and this is identified as being the most serious failing of the atom-atom + molecular octupole potential.

Fittings have also been attempted with higher values for the molecular octupole of carbonyl sulphide. However increasing the value of this moment above 10.0 Debye $Å^2$ leads to unsatisfactory results. The fitted parameters ε_{LL} and ε_{CS} are found to be negative and therefore unrealistic. It is also worth noting that for octupolar values below 9.0 Debye $Å^2$ the parameter ε_{OC} is found to be negative. Consequently while a relatively successful fitting of this particular potential can be performed for carbonyl sulphide the value for the molecular octupole is very restricted and does lie below the range suggested by Ab Initio calculations. Nevertheless the model should not be discounted and it is notable that such a relatively simplistic potential is successful in modelling so many properties.

7.4: Atom-Atom + Atomic Charge + Molecular Octupole Potential

It has already been discussed that the molecular dipole and quadrupole moments are small in magnitude and that their contributions to its lattice properties are small. The next potential used to model carbonyl sulphide is an extension of the molecular octupole potential with the addition of a set of three charges located on the atoms, modelling these lower moments in a different form.

Bentley[32] has recently discussed the idea of fitting atomic multipole moments so that they reproduce known molecular moments and this has led to the "atomic multipole expansion" (AME) method. The number of atomic moments which may be fitted is equal to the number of available molecular moments (including the zeroth order moment, the molecular charge). The procedure adopted to form this particular potential is to fit the three atomic charges to the molecular charge (zero), the molecular dipole moment and the molecular quadrupole moment. The contribution of these calculated charges to the molecular octupole is then determined and a separate molecular octupole term is added so that an overall value for the effective molecular octupole moment of 11.0 Debye $Å^2$ is obtained.

The fitting procedure yields a set of physically realistic ϵ parameters and these are given in table 7.3. The dispersion curves for this potential are given in figures 7.3 and 7.4 and are of the same general form as those of the molecular octupole potential. The curves are generally poorer than their equivalents for the molecular octupole potential. In the parallel direction the curves are real throughout but the lower acoustic branch is smaller in magnitude and the frequency minimum which generally occurs in the upper acoustic branch at around $\underset{\sim}{k} = 0.3$ is much lower for this new potential. In the perpendicular direction the lowest acoustic branch, which for the

Table 7.3: Atom-Atom Lennard-Jones 12-6 + Atomic Charge + Molecular Octupole Potential for OCS: Parameters

Atom Pair	ε/kcal mol^{-1}	R_0/Å
like-like	0.16700	3.7
O-C	0.09869	3.9
O-S	0.05495	3.9
C-S	0.36025	3.9

Atomic Charges: q(O) = -0.0745 a.u.

q(C) = 0.0356 a.u.

q(S) = 0.0389 a.u.

Molecular Octupole: Ω = 9.0764 Debye Å^2

molecular octupole potential was small but real, is imaginary between $\underset{\sim}{k}$ = 0.0 and $\underset{\sim}{k}$ = 0.2 so that the requirement that the frequencies should be real throughout the first Brillouin zone is not fulfilled. The quality of the potential may be further tested by calculating its elastic properties and these are given in table 7.4.

Table 7.4: Atom-Atom Lennard-Jones 12-6 + Atomic Charge + Molecular Octupole Potential for OCS: Elastic Properties

c_{11} = 9.9054 GPa $\quad$ c_{12} = 9.7373 GPa

c_{13} = -0.1578 GPa $\quad$ c_{15} = -0.3026 GPa

c_{33} = 34.0082 GPa $\quad$ c_{55} = 0.1576 GPa

S_3 = 667.9631 GPa^2 $\quad$ S_4 = -0.1566 GPa^2

$\varkappa_0$ = 0.1322 GPa^{-1}

It can be seen that the potential does not satisfy the condition for elastic stability, the fourth stability constant being negative. Neither does the potential offer any improvement in the calculated

Figure 7.3: Atom-Atom Lennard-Jones 12-6 + Atomic Charge + Molecular Octupole Potential for OCS: Dispersion Curves Parallel to C_3

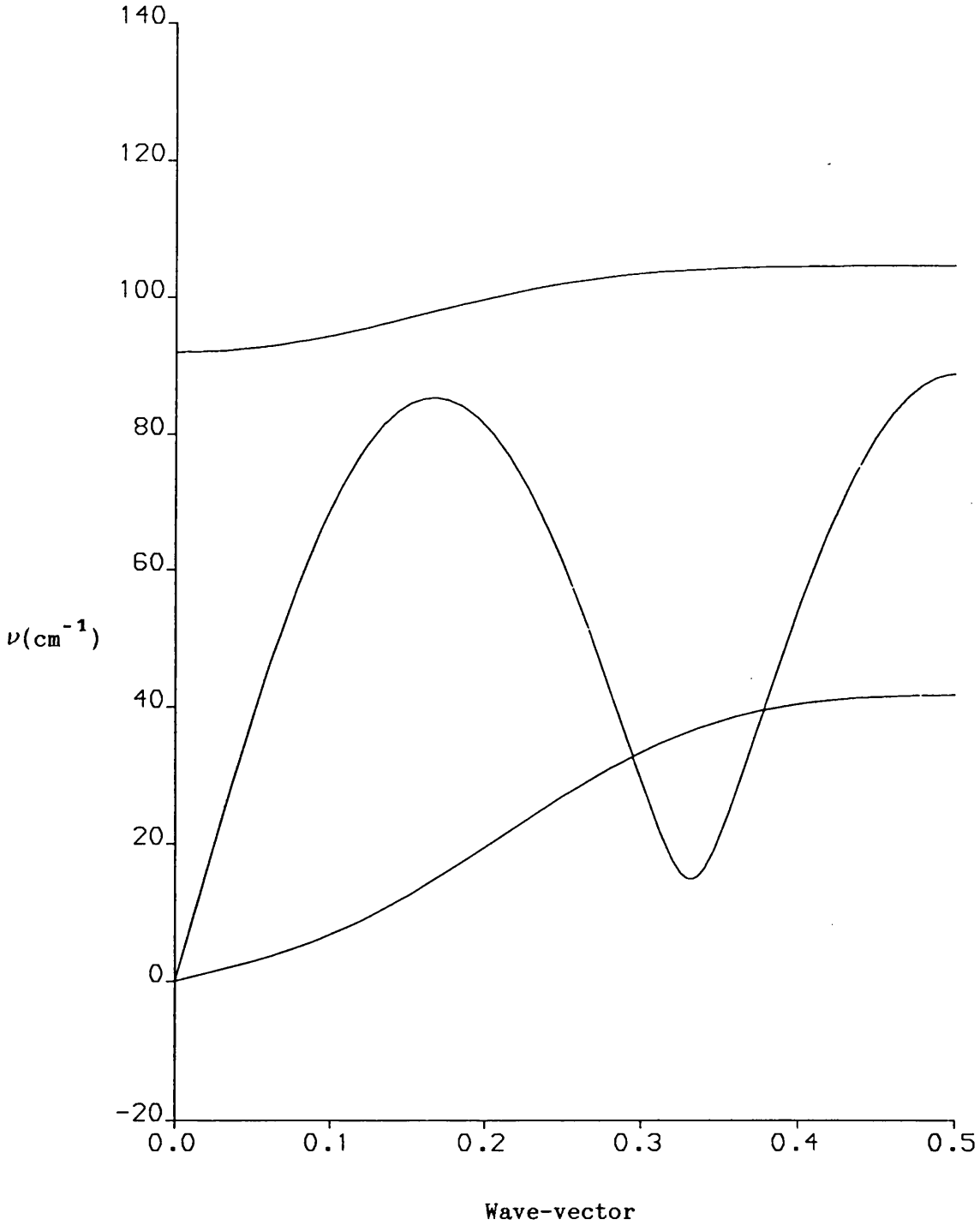

Figure 7.4: Atom-Atom Lennard-Jones 12-6 + Atomic Charge + Molecular Octupole Potential for OCS: Dispersion Curves Perpendicular to C_3

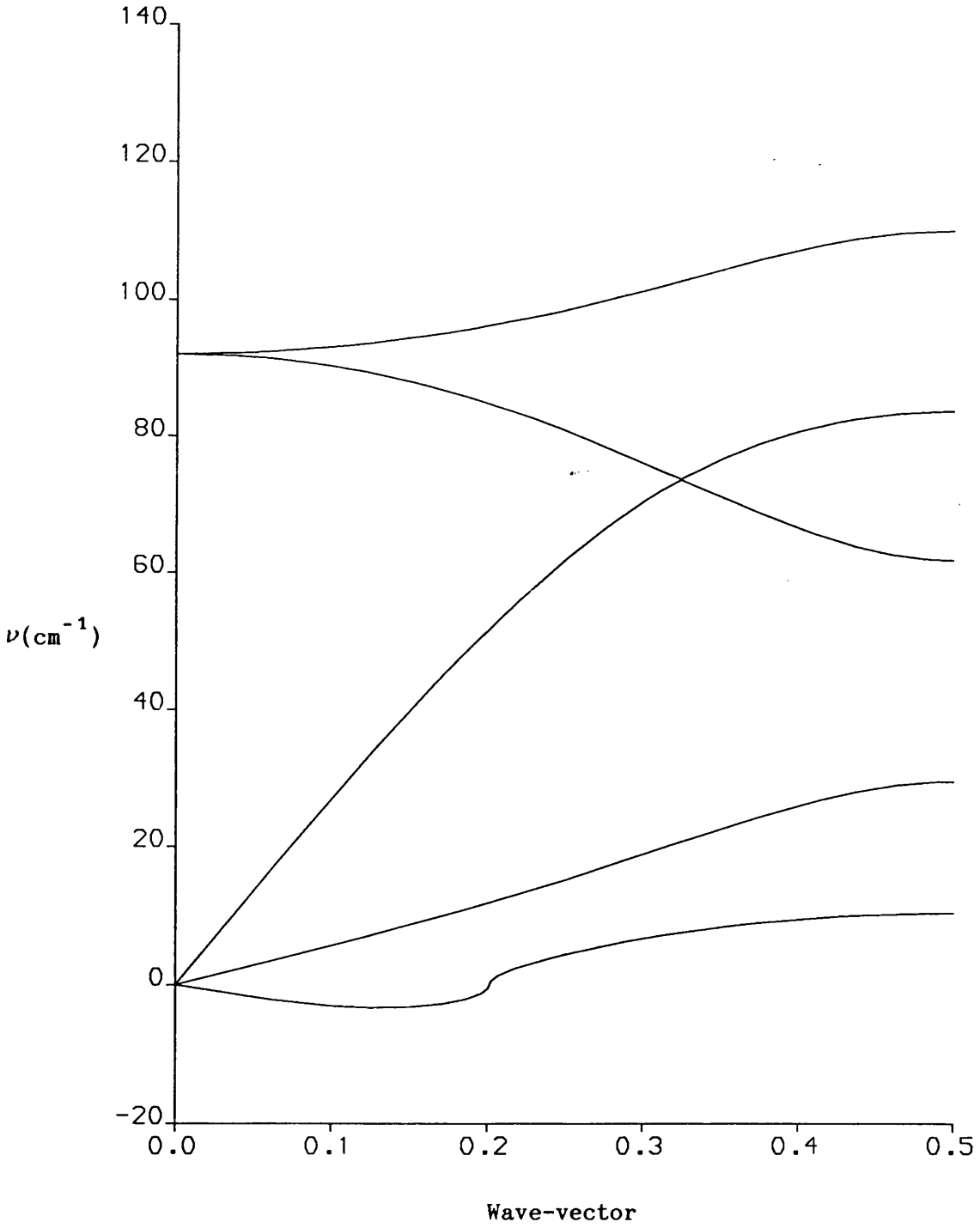

compressibility, its value being is virtually identical to that obtained from the molecular octupole potential.

Overall this potential compares unfavourably with the molecular octupole potential, a slightly surprising result. Unlike the molecular octupole potential it does not satisfy the basic criteria for an empirical potential. It exhibits imaginary dispersion curves and is not elastically stable. Even if the potential did not fail these criteria it offers no improvement to the property which is the major deficiency of the molecular octupole potential, the compressibility.

7.5: Atom Atom + Atomic Quadrupole Potential

The previous two potentials considered are a purely molecular multipole model and a model comprising both atomic and molecular terms. It has been shown that the addition of atomic charges to the molecular octupole does not improve the quality of the potential fitting and that in fact the "improved" potential is actually less satisfactory. The next multipolar potential which is considered is a potential comprised purely of atomic quadrupoles.

It has been discussed in section 7.3 that the multipolar character of carbonyl sulphide can be approximated to two quadrupoles of differing signs. This simple approximation leads to the next model used for the multipolar interaction, using quadrupoles located on the atoms. A first approximation to these moments would be simply to halve the molecular quadrupole moments of carbon dioxide (-4.491 Debye Å) and carbon disulphide (3.60 Debye Å) to obtain atomic quadrupoles for the oxygen and sulphur atoms. Further sets of quadrupoles may be obtained by varying these approximate values.

It is found that this potential can be fitted to the specimen lattice properties but to obtain a full set of realistic ϵ parameters

the atomic quadrupoles are generally smaller than the values suggested above. The full set of parameters is given in table 7.5.

Table 7.5: Atom-Atom Lennard-Jones 12-6 + Atomic Quadrupole Potential for OCS: Parameters

Atom Pair	ϵ/kcal mol^{-1}	R_0/Å
like-like	0.16926	3.7
O-C	0.20237	3.9
O-S	0.06258	3.9
C-S	0.22677	3.9

Atomic Quadrupoles: $\Theta(O)$ = -1.4869 a.u. = -2.0 Debye Å

$\Theta(C)$ = 0.0000 a.u.

$\Theta(S)$ = 0.8178 a.u. = 1.1 Debye Å

The dispersion curves for this potential have also been determined and are given in figures 7.5 and 7.6. Again the curves are poor in comparison to those obtained with the molecular octupole potential and imaginary frequencies are apparent. The lowest acoustic branch in the perpendicular direction, small but real for the two previous potentials, is small and imaginary for values of the wave-vector below $\underset{\sim}{k}$ = 0.07. The lowest branch in the parallel direction is also imaginary throughout the first Brillouin zone. This particular potential clearly does not satisfy the condition that the frequencies should be real throughout and this alone is a major failing of the atomic quadrupole potential. Additionally, the elastic properties have also been calculated for this particular potential and these are presented in table 7.6.

Figure 7.5: Atom-Atom Lennard-Jones 12-6 + Atomic Quadrupole Potential for OCS: Dispersion Curves Parallel to C_3

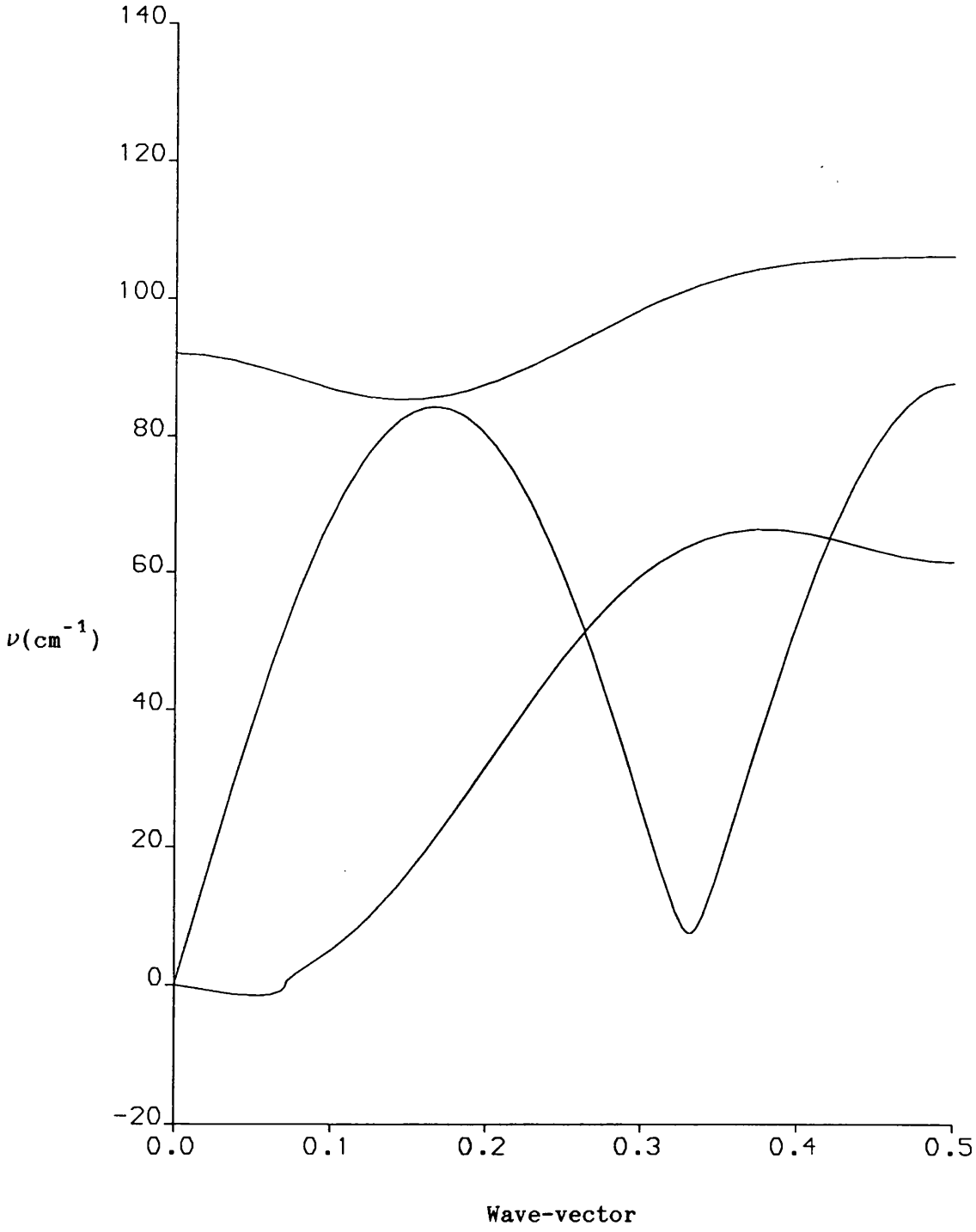

Figure 7.6: Atom-Atom Lennard-Jones 12-6 + Atomic Quadrupole Potential for OCS: Dispersion Curves Perpendicular to C_3

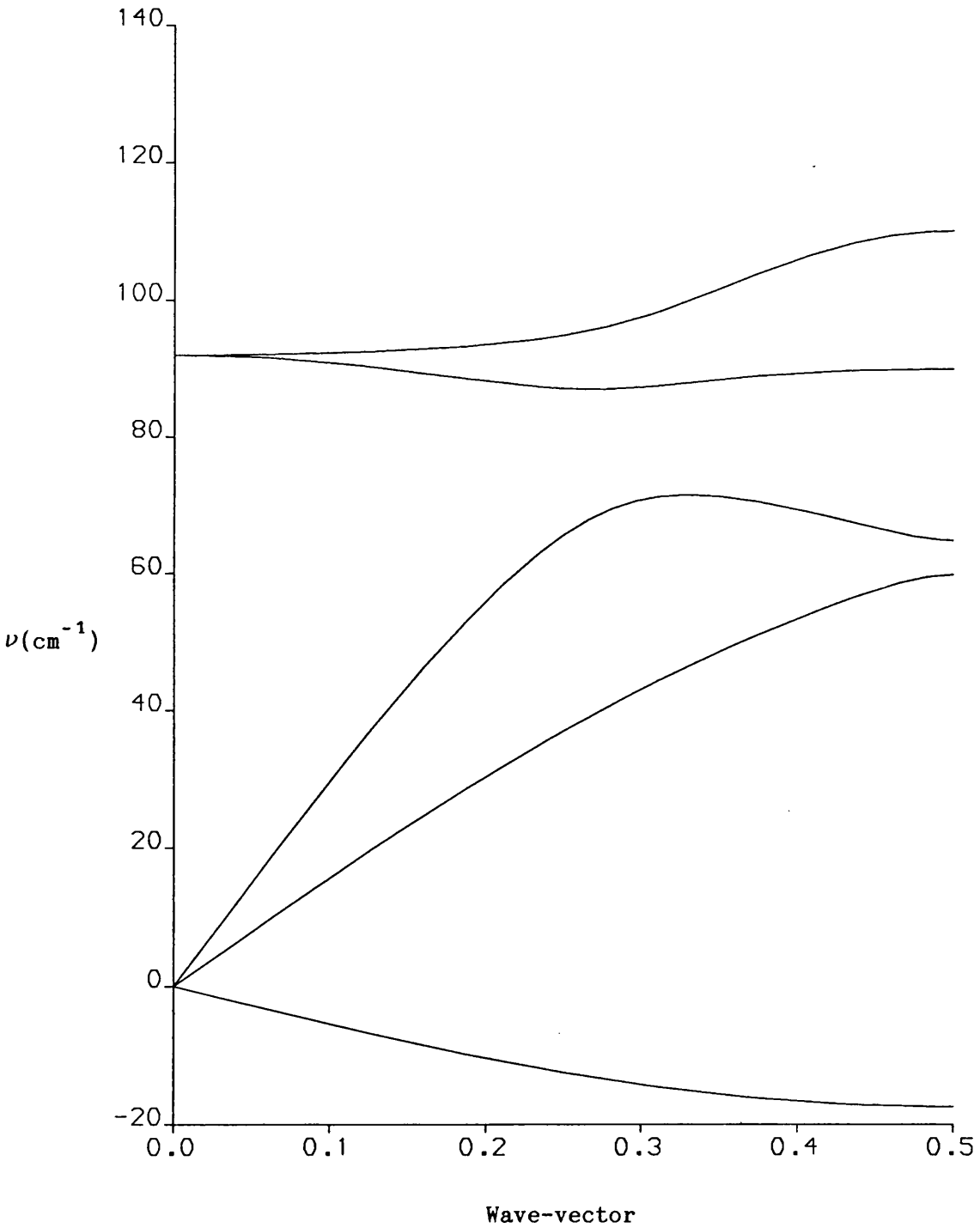

Table 7.6: Atom-Atom Lennard-Jones 12-6 + Atomic Quadrupole Potential for OCS: Elastic Properties

c_{11} = 12.0278 GPa	c_{12} = 6.0289 GPa
c_{13} = 0.7129 GPa	c_{15} = 1.0511 GPa
c_{33} = 33.4059 GPa	c_{55} = -0.0806 GPa
S_3 = 602.1839 GPa^2	S_4 = -2.6931 GPa^2
$\varkappa_0$ = 0.1362 GPa^{-1}	

These results illustrate further the failings of the potential, two of the four stability constants are negative and the compressibility obtained is not significantly higher than for the molecular octupole potential.

Overall the atomic quadrupole potential has little to offer for the modelling of carbonyl sulphide. To obtain realistic ε parameters a set of atomic quadrupoles has to be used which represent an effective molecular octupole of only 4.5 Debye $Å^2$, significantly lower than the value suggested by calculation. It does not offer any significant improvement to the calculation of the compressibility and it fails to produce a full set of real dispersion curves or to satisfy the conditions of elastic stability.

7.6: Atom Atom + Atomic Multipole Potential

The atomic quadrupole potential has been clearly shown to be an unsatisfactory model for carbonyl sulphide and it would appear that any atomic multipole potential would have to be more sophisticated than the simplistic quadrupole model proposed. Stone[33,34] has proposed a method, known as distributed multipole analysis (DMA), which generates atomic multipole moments from the charge density in an ab initio calculation. This method has been used for carbonyl sulphide

using CADPAC, the Cambridge Analytic Derivatives Package developed by Amos and others[35]. Details are given in Appendix A and the moments obtained are very dependent upon the quality of the basis set used. A typical set of moments, obtained from the TZP (triple-zeta plus a single polarisation function) basis set are given in table 7.7.

Table 7.7: Atomic Multipole Model for OCS - Distributed Multipole Analysis - TZP Basis Set

atom type	q(e)	μ(Debye)	Θ(Debye Å)
O	-0.4736	-0.1621	-0.0228
C	0.6189	-0.9654	-0.2888
S	-0.1453	0.3930	1.9108

This set of atomic moments may be combined with the atom-atom model in the standard manner and fitted to the four specimen lattice properties. The parameters obtained are given in table 7.8.

Table 7.8: Atom-Atom Lennard-Jones 12-6 + Atomic Multipole Potential for OCS: Atom-Atom Parameters

Atom Pair	ϵ/kcal mol^{-1}	R_0/Å
like-like	0.04504	3.7
O-C	0.44398	3.9
O-S	0.05696	3.9
C-S	0.09371	3.9

The four ϵ parameters are seen to be physically realistic. The dispersion curves have been calculated and are given in figures 7.7 and 7.8. There are no imaginary frequencies, although the lowest

Figure 7.7: Atom-Atom Lennard-Jones 12-6 + Atomic Multipole Potential for OCS: Dispersion Curves Parallel to C_3

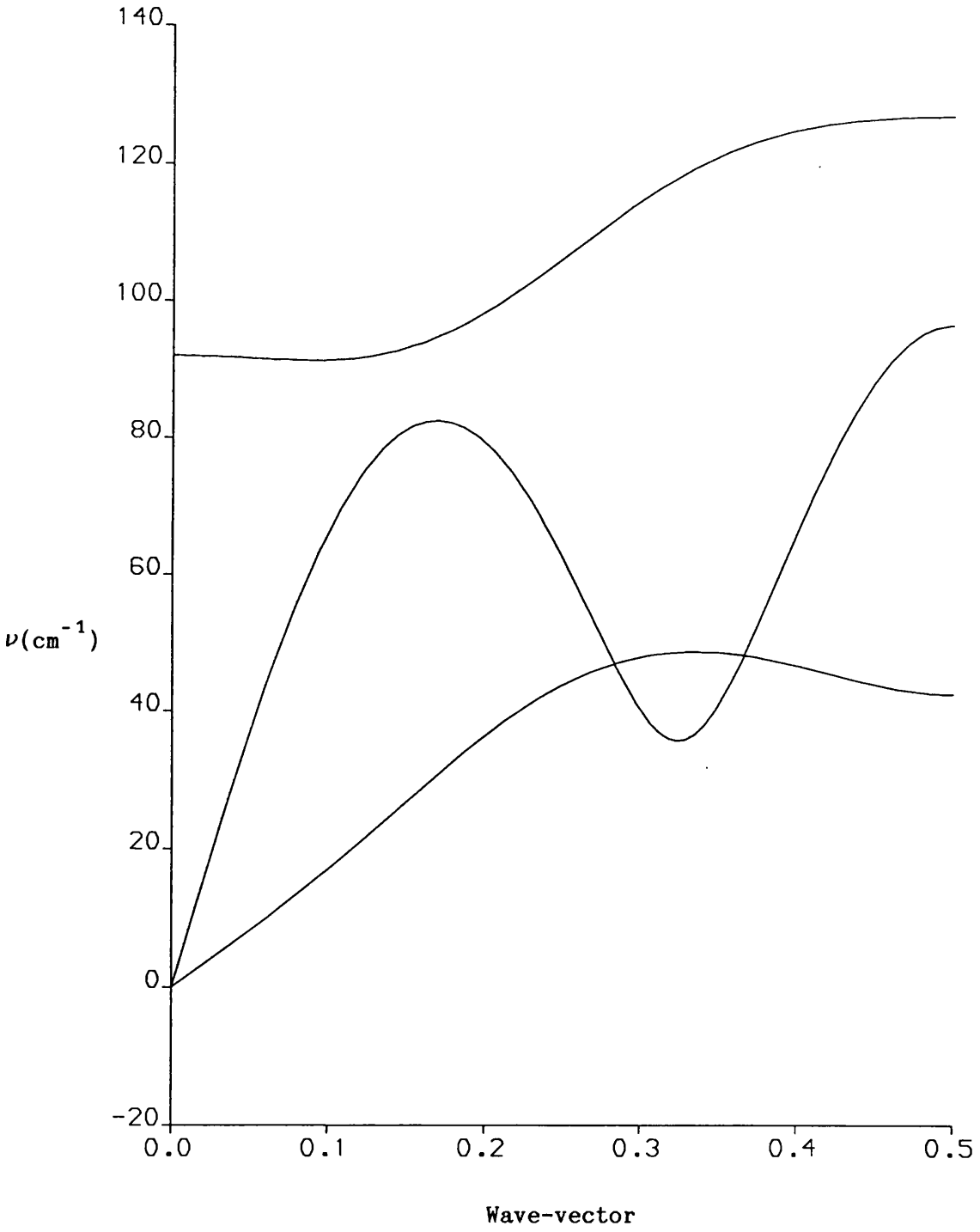

Figure 7.8: Atom-Atom Lennard-Jones 12-6 + Atomic Multipole Potential for OCS: Dispersion Curves Perpendicular to C_3

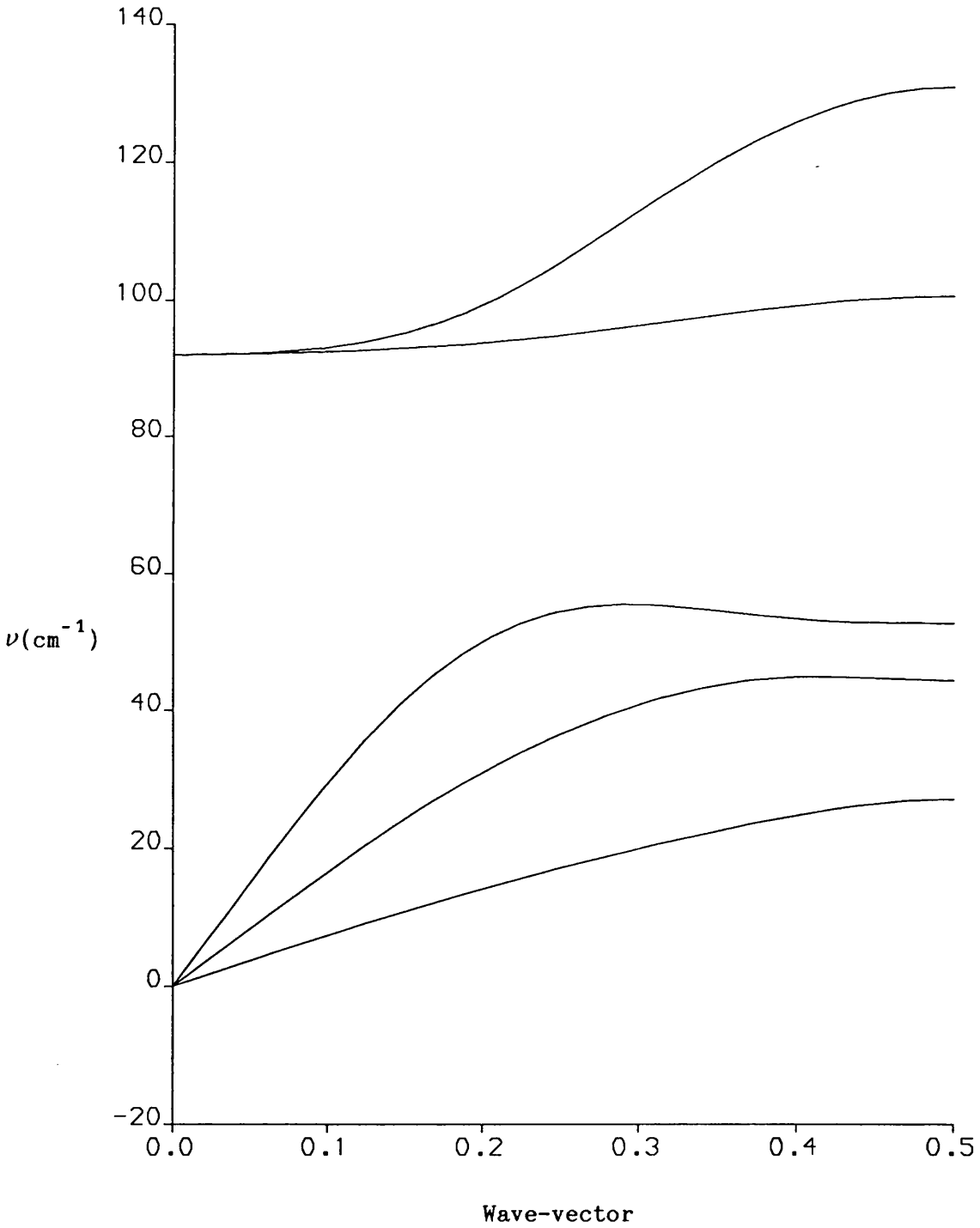

acoustic branches in each direction are small in magnitude. The elastic properties of the potential have also been determined and these are given in table 7.9.

Table 7.9: Atom-Atom Lennard-Jones 12-6 + Atomic Multipole Potential for OCS: Elastic Properties

c_{11} = 12.4537 GPa	c_{12} = 6.0105 GPa
c_{13} = 1.2654 GPa	c_{15} = 1.2193 GPa
c_{33} = 31.2502 GPa	c_{55} = 1.3532 GPa
S_3 = 573.8075 GPa^2	S_4 = 5.7456 GPa^2
$\varkappa_0$ = 0.1323 GPa^{-1}	

All four stability constants are real and the potential satisfies the conditions for elastic stability. The calculated compressibility does not differ significantly from the values calculated for previous models. However unlike the previous two models the atomic multipole model does fit the specimen lattice properties and satisfies the other conditions required of a model to the extent of being as successful as the molecular octupole model.

The success of the atomic multipole model also offers an indication as to the reasons for the failure of the atomic quadrupole model. The values of the quadrupoles within the atomic multipole model indicate that the oxygen atom has a very small quadrupole moment while the sulphur atom has a large positive quadrupole moment. This would suggest that the atomic quadrupole model does not provide a successful representation of the charge distribution for carbonyl sulphide.

The effective molecular multipole moments due to the atomic multipole model are given by; μ^{eff} = 0.964 Debye, Θ^{eff} = -3.82 Debye Å and Ω^{eff} = 11.82 Debye $Å^2$. The effective dipole moment is reasonably

close to the experimental value but the effective quadrupole moment is significantly higher than the experimental value. The evidence of this calculation and the consideration of carbon disulphide and carbon dioxide which led to the atomic quadrupole model suggests that carbonyl sulphide exhibits far less quadrupolar character than would be generally expected.

Furthermore the effective octupole moment for the atomic multipole potential is significantly higher than that inherent to the atomic quadrupole potential. In common with the molecular octupole potential it would appear that it is critical to the success of any model for carbonyl sulphide that the value of the molecular octupole moment, in the range 10-15 Å, is reproduced by the multipolar potential.

7.7: Anisotropic Berne-Pechukas Molecule-Molecule + Molecular Octupole Potential

The final potential considered in this chapter is the anisotropic Berne-Pechukas molecule-molecule + molecular octupole potential. It is of a similar form to the potentials previously considered, with the Lennard-Jones 12-6 potential being retained. However instead of being used as an atom-atom interaction it is utilised in the form of an anisotropic molecule-molecule potential. The multipolar component is modelled by a molecular octupole potential. The molecular octupole moment is now considered as being one of the four parameters fitted to the specimen lattice properties (the details of this procedure are given in Chapter 6).

As with the other potentials considered it is required that the value of the single ϵ parameter obtained by the fitting procedure should be positive. The value obtained for the molecular octupole moment may also be used as a further test of the quality of the

potential, with estimates for the magnitude of the octupole moment for carbonyl sulphide having been discussed earlier. Finally the usual properties which provide tests for an empirical potential, the dispersion curves and elastic properties, may be determined for this potential.

The molecule-molecule + molecular octupole potential is only one possibility for a potential of this form. In principle an anisotropic atom-atom potential could be used instead of the molecule-molecule potential and the multipolar interaction could be modelled by a more complex system such as the atomic multipole system. However the former is by far the simplest representation and the considerations of the previous models do not suggest that the more complicated multipolar potentials prove to be any better than the molecular octupole model. Consequently the attention here is confined to the molecule-molecule + molecular octupole potential.

The fitting procedure yields a large number of solutions with physically realistic parameters (recalling that three parameters; ϵ, R_0 and Ω^2 are fitted to the lattice energy and the two stress components) for differing values of the anisotropy parameter, χ. It is found that in general a particular value of χ may be chosen such that the torsional frequency of vibration is obtained to within ± 0.1 cm^{-1} of the required value of 92 cm^{-1}. The potential parameters obtained by this method are given in table 7.10.

Table 7.10: Anisotropic Berne-Pechukas Molecule-Molecule + Molecular Octupole Potential for OCS: Parameters

ϵ/kcal mol^{-1}	R_0/Å	Ω/Debye Å^2	χ
0.58325	4.0654	12.296	0.41440

The parameters obtained are excellent. ϵ is positive and relatively large while R_0 is found to be in the range expected by clustering considerations (recalling that the separation of the molecular centres of mass of nearest neighbours is the unit cell length, 4.063 Å). The value obtained for the molecular octupole moment is consistent with the value suggested by ab initio calculation. The dispersion curves for the potential have also been calculated and are illustrated in figures 7.9 and 7.10. The most important characteristic of the dispersion curves is the absence of any imaginary frequencies though the magnitudes of the frequencies for the lowest acoustic branches in each direction are relatively small. Nevertheless the requirement that the curves should be real is satisfied. The elastic properties for this potential are given in table 7.11.

Table 7.11: Anisotropic Berne-Pechukas Molecule-Molecule + Molecular Octupole Potential for OCS: Elastic Properties

c_{11} = 9.9026 GPa	c_{12} = 7.4252 GPa
c_{13} = 0.4195 GPa	c_{15} = 1.0007 GPa
c_{33} = 17.0027 GPa	c_{55} = 1.7342 GPa
S_3 = 294.2672 GPa^2	S_4 = 2.2935 GPa^2
$\varkappa_0$ = 0.1687 GPa^{-1}	

The four stability constants are seen to be positive, satisfying the conditions for elastic stability. However, the most notable result for this potential is the value for the calculated compressibility. Whilst it is still lower than the experimental value it is significantly higher than the values obtained from the other potentials detailed and as such this potential offers the first improvement on the calculation of this particular property which has been previously identified as

Figure 7.9: Anisotropic Berne-Pechukas Molecule-Molecule + Molecular Octupole Potential for OCS: Dispersion Curves Parallel to C_3

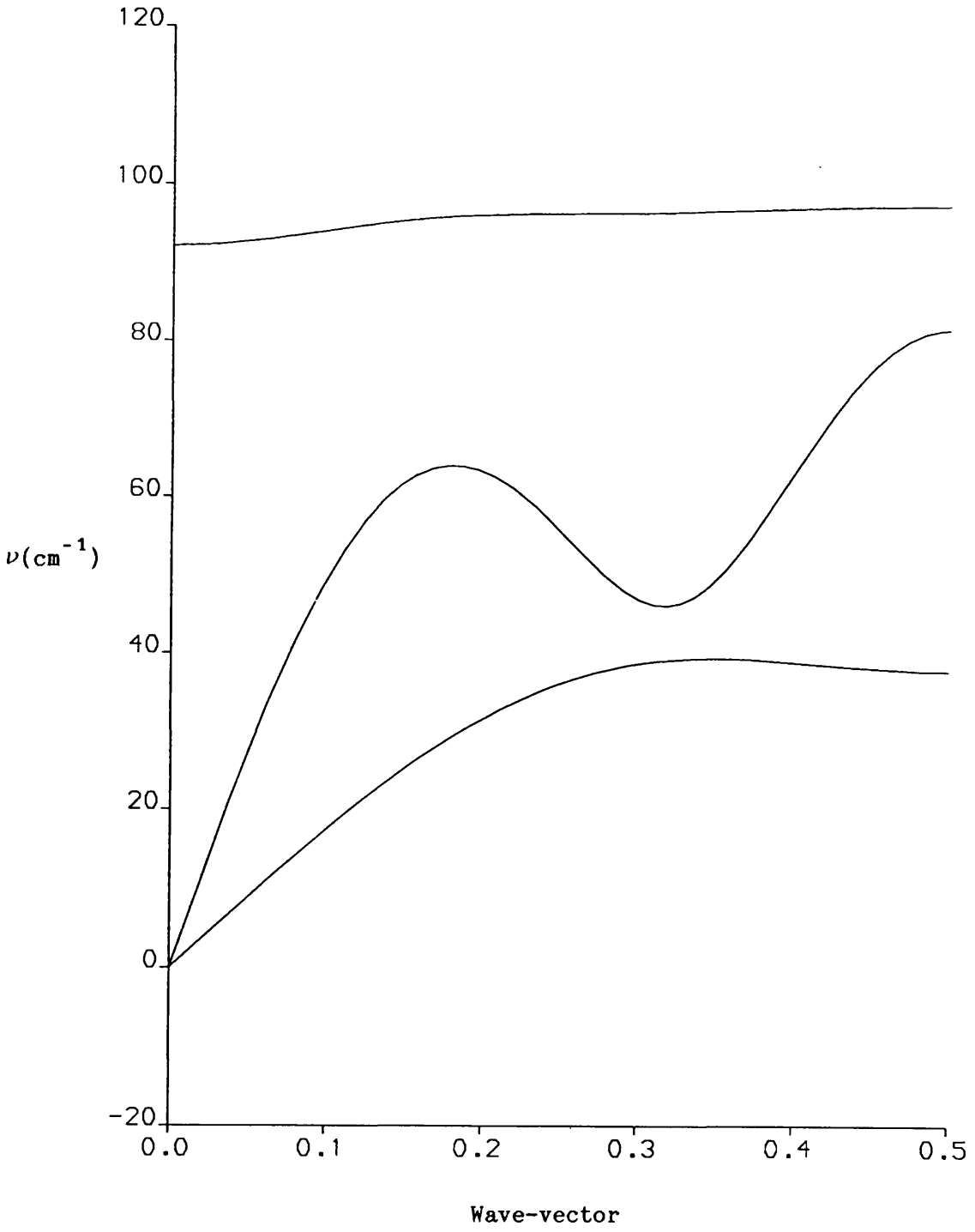

Figure 7.10: Anisotropic Berne-Pechukas Molecule-Molecule + Molecular Octupole Potential for OCS: Dispersion Curves Perpendicular to C_3

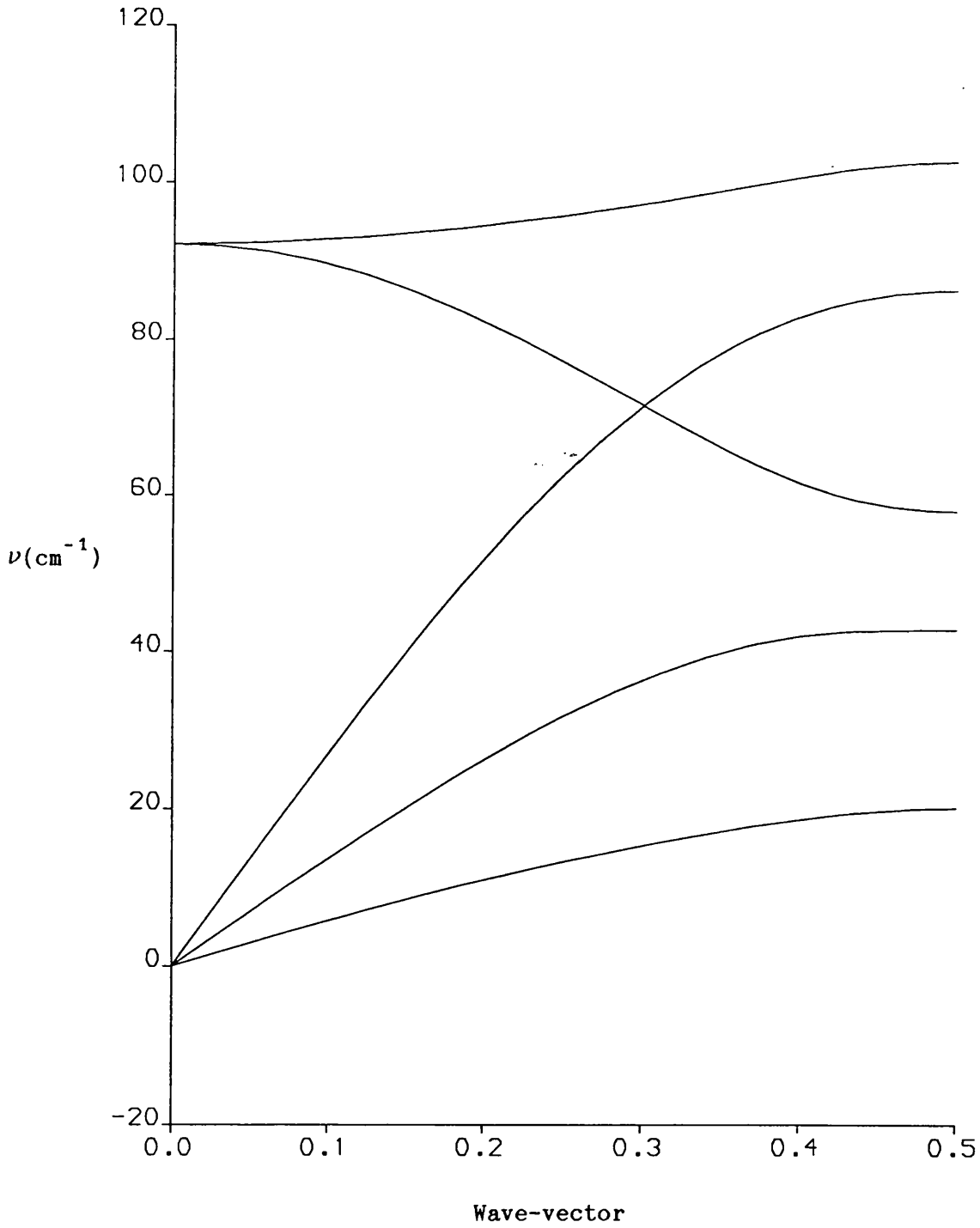

being the main failing of the molecular octupole and atomic multipole models for carbonyl sulphide.

7.8: Discussion

Within this chapter a number of different potentials have been examined, with varying degrees of success, to test their suitability as models for carbonyl sulphide. The focus of attention has been on a number of different forms for the multipolar component of the overall potential such that these different representations may be compared. In addition the anisotropic Berne-Pechukas potential has been investigated but this will be discussed at the end of this section.

The most important conclusion is that the molecular octupole of carbonyl sulphide needs to be successfully reproduced by an empirical potential. The two potentials which do provide satisfactory models for carbonyl sulphide (disregarding their inability to reproduce the compressibility, a fault common to all of the potentials) are the molecular octupole and the atomic multipole potentials, each of which reproduces the high value for the octupole moment. The atomic quadrupole potential fails to reproduce the molecular moment and does not provide a satisfactory model. The atomic charge + molecular octupole model, essentially the molecular octupole potential with a small modification, would be expected to improve the latter potential, as it also reproduces the molecular dipole and quadrupole moments. However the effect of the addition of the atomic charges is to destabilise the potential, not by a large amount but enough to prevent it from satisfying the required conditions for stability.

In general all of the potentials can be fitted with realistic values for the ϵ properties and all of the potentials yield a value for the compressibility of approximately 0.13 GPa, significantly below the

experimental value and the uniform failing of this set of potentials. In each case the lowest acoustic branch of the dispersion curves acts as the main indicator of the quality of the potential. In each direction it is always small and it is this branch which is found to become imaginary for the unsatisfactory potentials. The stability constants, which are closely related to the initial slopes of the acoustic branches of these dispersion curves support these results.

It is not apparent that the hybrid potentials are improved by increasing the complexity of the molecular multipole potential relative to the molecular octupole potential. The effects of the dipole and quadrupole moments are small and only the atomic multipole potential (which greatly overestimates the molecular quadrupole) provides results which are as satisfactory as those obtained for the molecular octupole potential (which negates the molecular quadrupole).

The anisotropic Berne-Pechukas molecule-molecule + molecular octupole potential retains the qualities of the molecular octupole potential but offers a significant improvement in the calculated value of the compressibility. It has to be considered as providing the best model for carbonyl sulphide of the various potentials considered within this chapter. Although the molecular octupole used within this potential, 12.296 Debye $Å^2$ is significantly higher than that used for the atom-atom + molecular octupole potential, 10.0 Debye $Å^2$ it is not significantly higher than the effective molecular octupole, 11.82 Debye $Å^2$ inherent to the atomic multipole potential. The improvement in the calculated compressibility for the Berne-Pechukas potential cannot be attributed to the molecular octupole and it is concluded that it must be due to the anisotropic molecule-molecule component of the hybrid potential. This conclusion forms the basis for the next chapter.

8.1: Introduction

In the previous chapter a number of potentials were introduced and considered as models for carbonyl sulphide. Attention was focussed on finding suitable forms for the multipolar interaction. A standard atom-atom potential was used in conjunction with the various multipolar components for all but the last potential. This final potential, the anisotropic Berne-Pechukas potential provided an improvement on the calculated compressibility and it was suggested that this might well be due to the change in the atom-atom/molecule-molecule component of the overall potential rather than any change in the multipolar model.

In more general terms it has already been discussed in Chapter 4 that the overall interaction between two molecules can be separated into three components, the electrostatic energy, the short-range repulsive energy and the dispersion energy. The previous chapter focussed on different forms for the electrostatic energy with no variation in the modelling of the repulsive and dispersive components. These two components are modelled by the two terms in the Lennard-Jones potential, whether it is utilised in an atom-atom or molecule-molecule form. This chapter will focus on the investigation of the Lennard-Jones potential, varying the exponents of its repulsive and dispersive components. A similar procedure is adopted as in the last chapter, with a standard multipolar model being used in conjunction with each Lennard-Jones potential. In this vein the repulsive and dispersive exponents are varied separately and the results presented such that the effect of varying each exponent may be critically examined.

Three sets of potentials are considered in this chapter. First, the effect of varying the repulsive exponent in the atom-atom + molecular octupole potential is examined, this potential being considered as the "basic" model for carbonyl sulphide. The same procedure is then examined for the anisotropic Berne-Pechukas potential, which was shown in the previous chapter to provide the best model for carbonyl sulphide. Finally the anisotropic Berne-Pechukas potential is considered with variation of the dispersive exponent.

8.2: Atom-Atom + Molecular Octupole Potential: Repulsive Variation

As discussed in the previous chapter the 12-6 Lennard-Jones atom-atom + molecular octupole potential satisfies all the required conditions of a model for carbonyl sulphide except the calculated value for the compressibility. Consequently the principal requirement of any improved potential is that it produces a higher value for the compressibility whilst still satisfying the other conditions for an empirical potential detailed previously.

Qualitatively it would seem likely that the variation of the exponents in the Lennard-Jones potential could effect a variation in the compressibility. The Lennard-Jones potential can be considered as forming an "energy well" and the steepness of the two sides are determined by the values of the two exponents. The compressibility of the crystal can be equated with the steepness of this energy well and it would be expected that lowering the exponents, hence reducing the steepness, would effectively increase the compressibility.

It has been mentioned in Chapter 4 that in general the repulsive exponent in atom-atom potentials is varied more frequently than the dispersive exponent. The dispersive exponent is rarely employed with a value other than six whilst the repulsive exponent is usually employed

in the range nine to thirteen. It is important to note that these are only general "guidelines". Much greater ranges for the exponents have been considered elsewhere and will be employed here. However in line with general philosophy, the first set of potentials to be considered investigate the effects of the variation of the repulsive exponent.

A series of four potentials is considered, centred on the atom-atom Lennard-Jones 12-6 potential considered in the previous chapter. In addition the results for the 14-6, 10-6 and 8-6 potentials are presented and discussed. The standard fitting procedure is applied to the four potentials, each being combined with a molecular octupole moment of 10.0 Debye $Å^2$. The fitted potential parameters are presented in table 8.1.

Table 8.1: Atom-Atom Lennard-Jones 14-6, 12-6, 10-6 and 8-6 + Molecular Octupole Potentials for OCS: Parameters

Atom Pair	ε/kcal mol^{-1}				R_0/Å
	14-6	12-6	10-6	8-6	
L-L	0.13728	0.06256	-0.02386	-0.12112	3.7
O-C	0.38941	0.33476	0.21808	-0.03632	3.9
O-S	0.03276	0.04929	0.07360	0.10916	3.9
C-S	0.11085	0.20619	0.36101	0.64291	3.9

Ω = 10.0 Debye $Å^2$

It can be seen that the ε parameters obtained by the fitting procedure follow a general trend, ε_{LL} and ε_{OC} decrease with the repulsive exponent while ε_{OS} and ε_{CS} increase. The atom-atom parameters for the 10-6 and 8-6 potentials are unrealistic, possessing at least one negative ε parameter. The dispersion curves have also been determined for this series of potentials and are presented in figures 8.1 to 8.8.

Figure 8.1: Atom-Atom Lennard-Jones 14-6 + Molecular Octupole Potential for OCS: Dispersion Curves Parallel to C_3

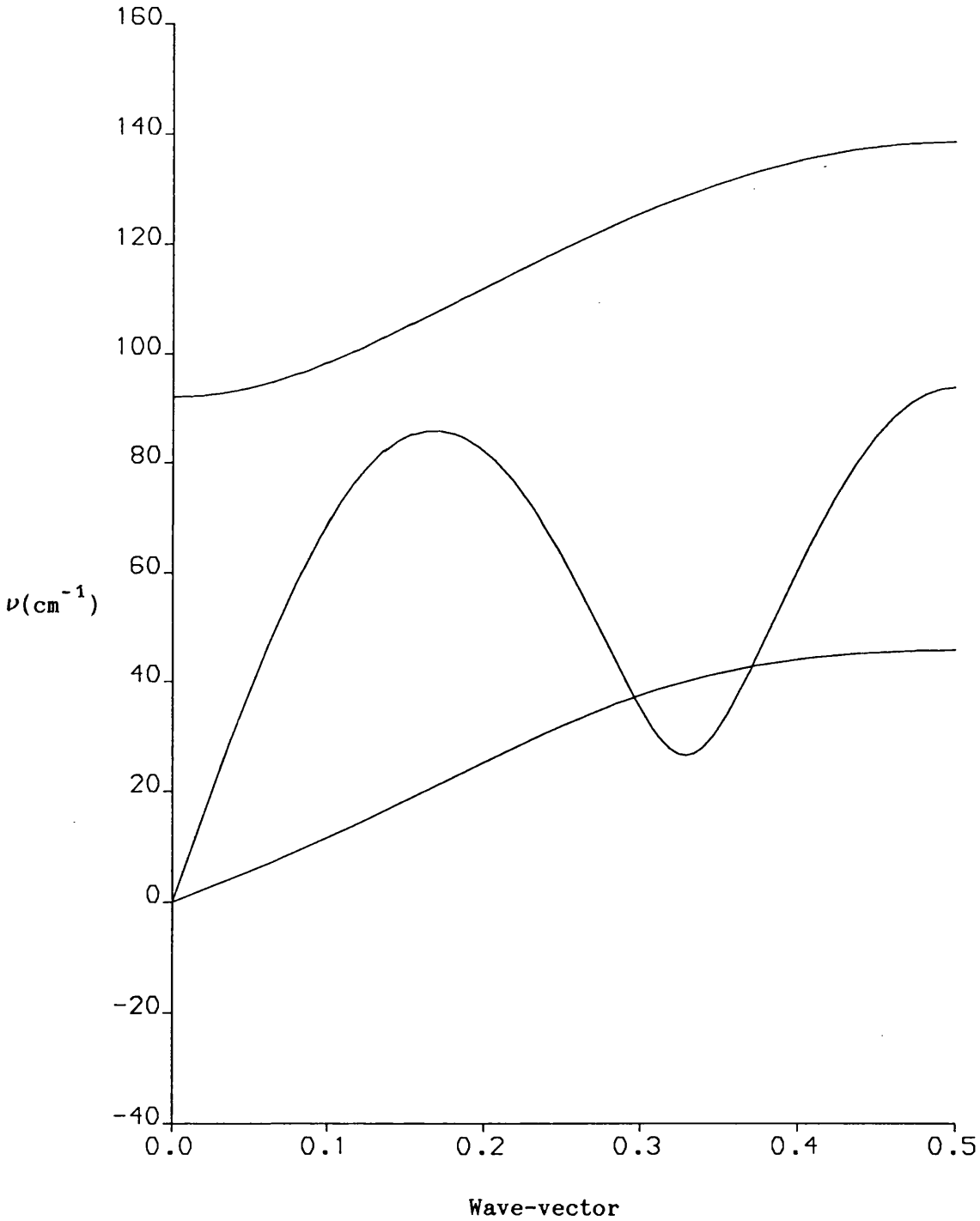

Figure 8.2: Atom-Atom Lennard-Jones 12-6 + Molecular Octupole Potential for OCS: Dispersion Curves Parallel to C_3

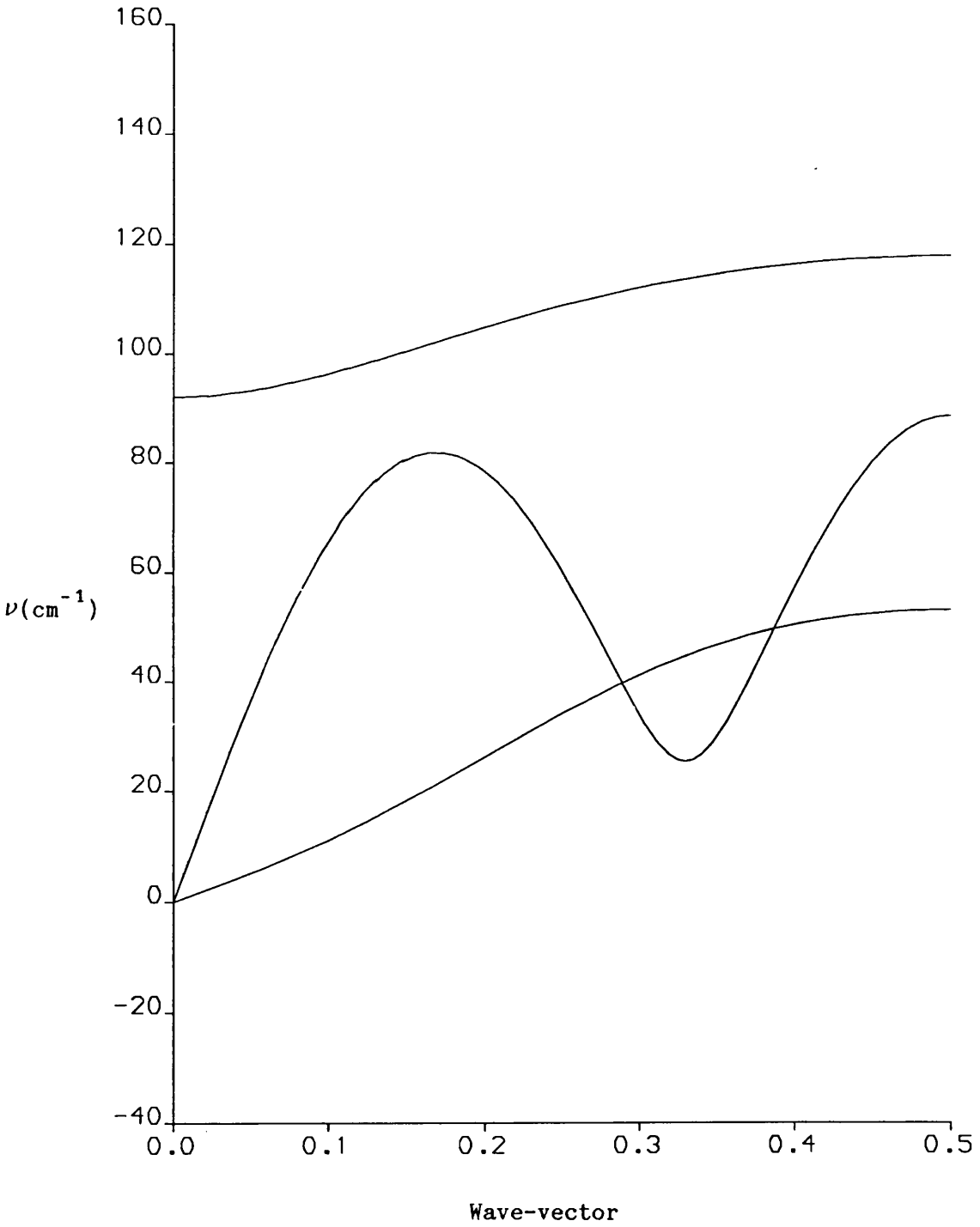

Figure 8.3: Atom-Atom Lennard-Jones 10-6 + Molecular Octupole Potential for OCS: Dispersion Curves Parallel to C_3

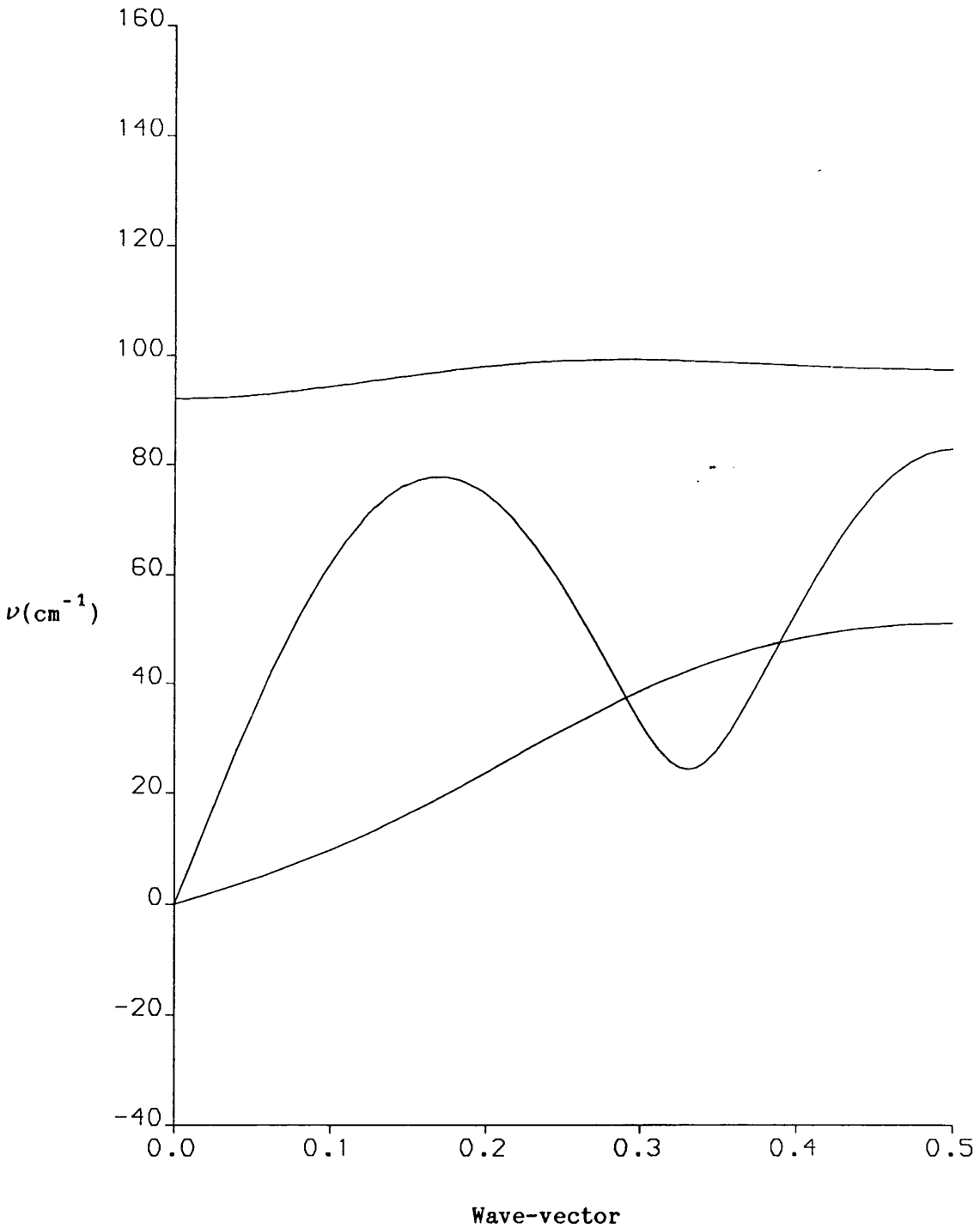

Figure 8.4: Atom-Atom Lennard-Jones 8-6 + Molecular Octupole Potential for OCS: Dispersion Curves Parallel to C_3

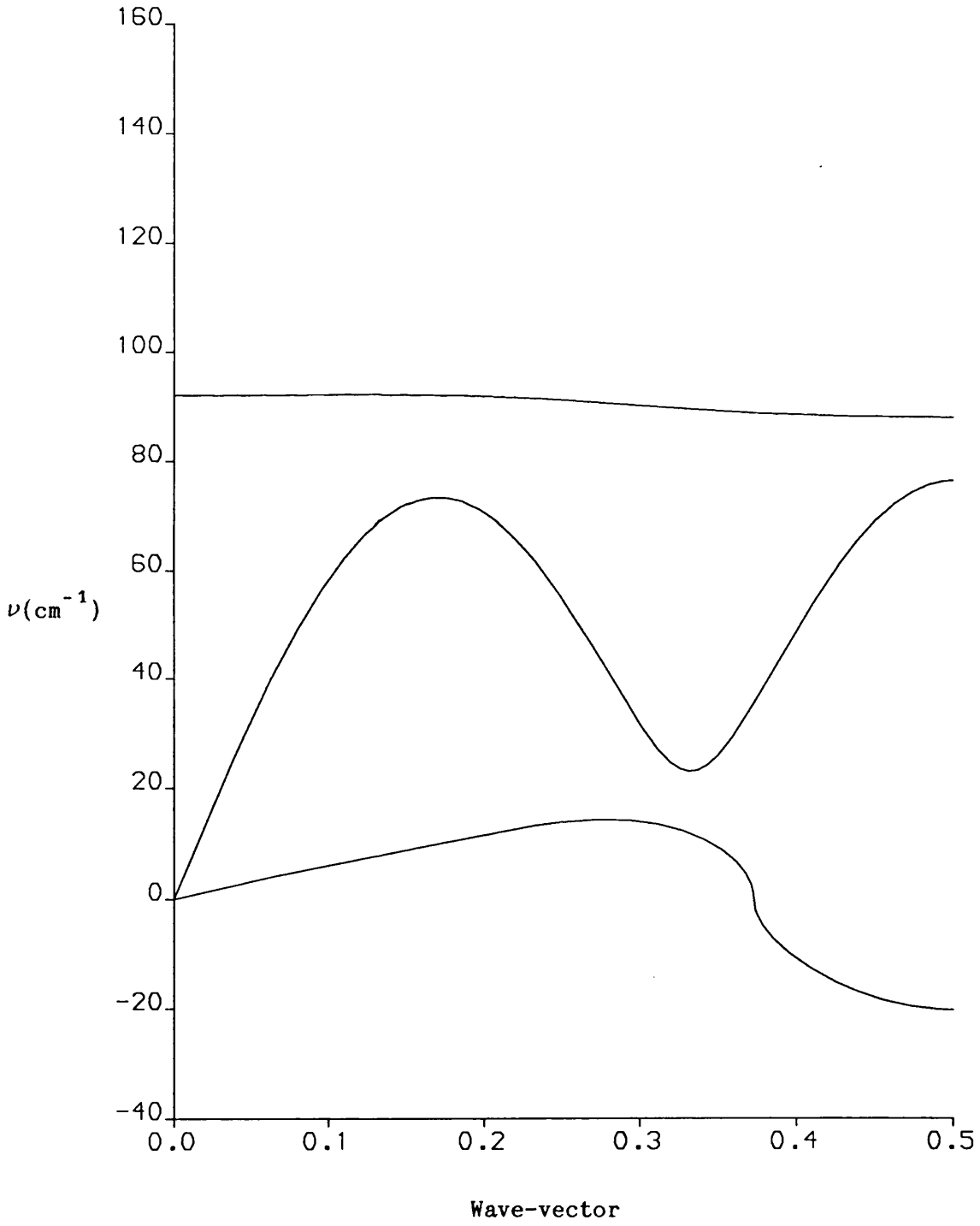

Figure 8.5: Atom-Atom Lennard-Jones 14-6 + Molecular Octupole Potential for OCS: Dispersion Curves Perpendicular to C_3

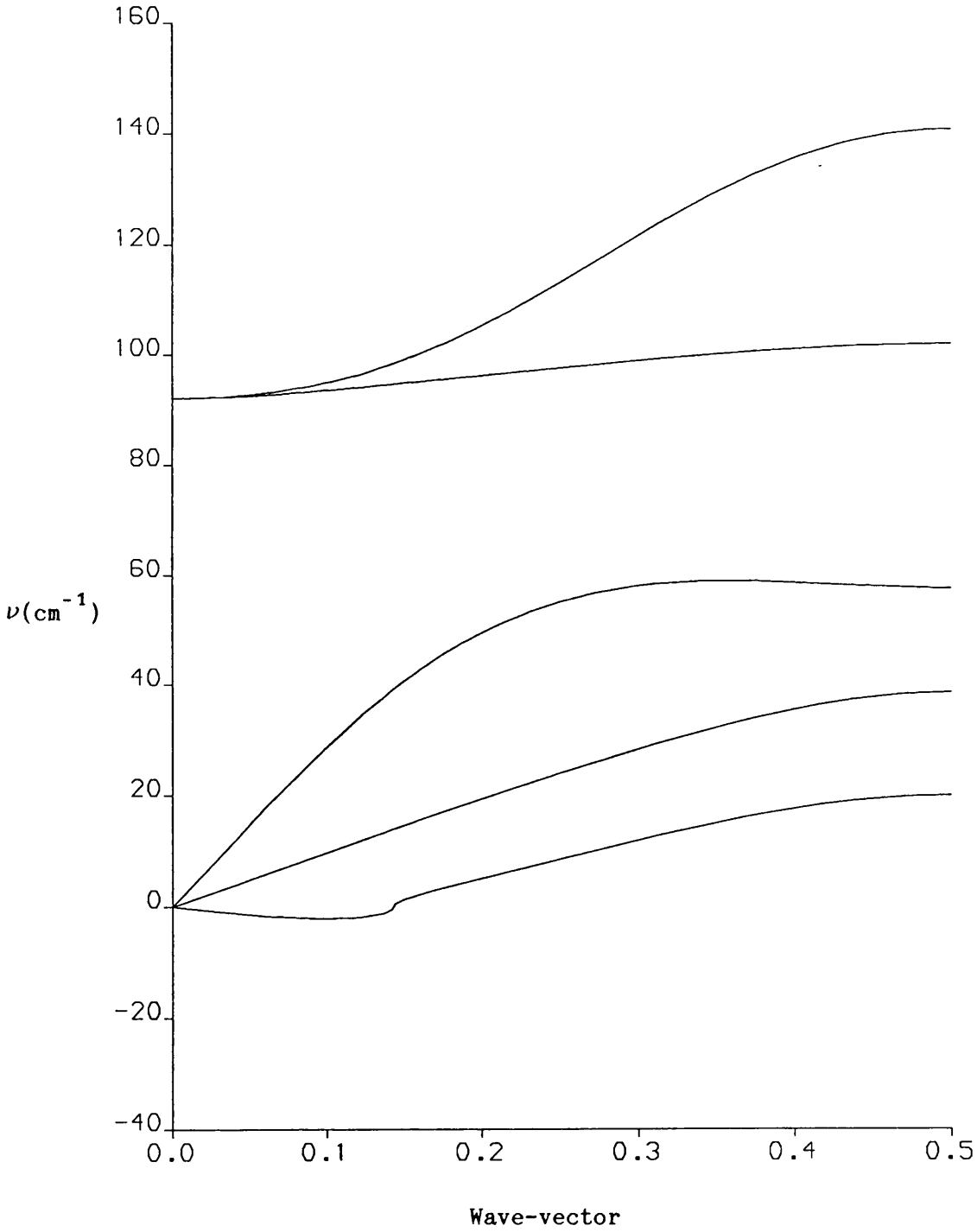

Figure 8.6: Atom-Atom Lennard-Jones 12-6 + Molecular Octupole Potential for OCS: Dispersion Curves Perpendicular to C_3

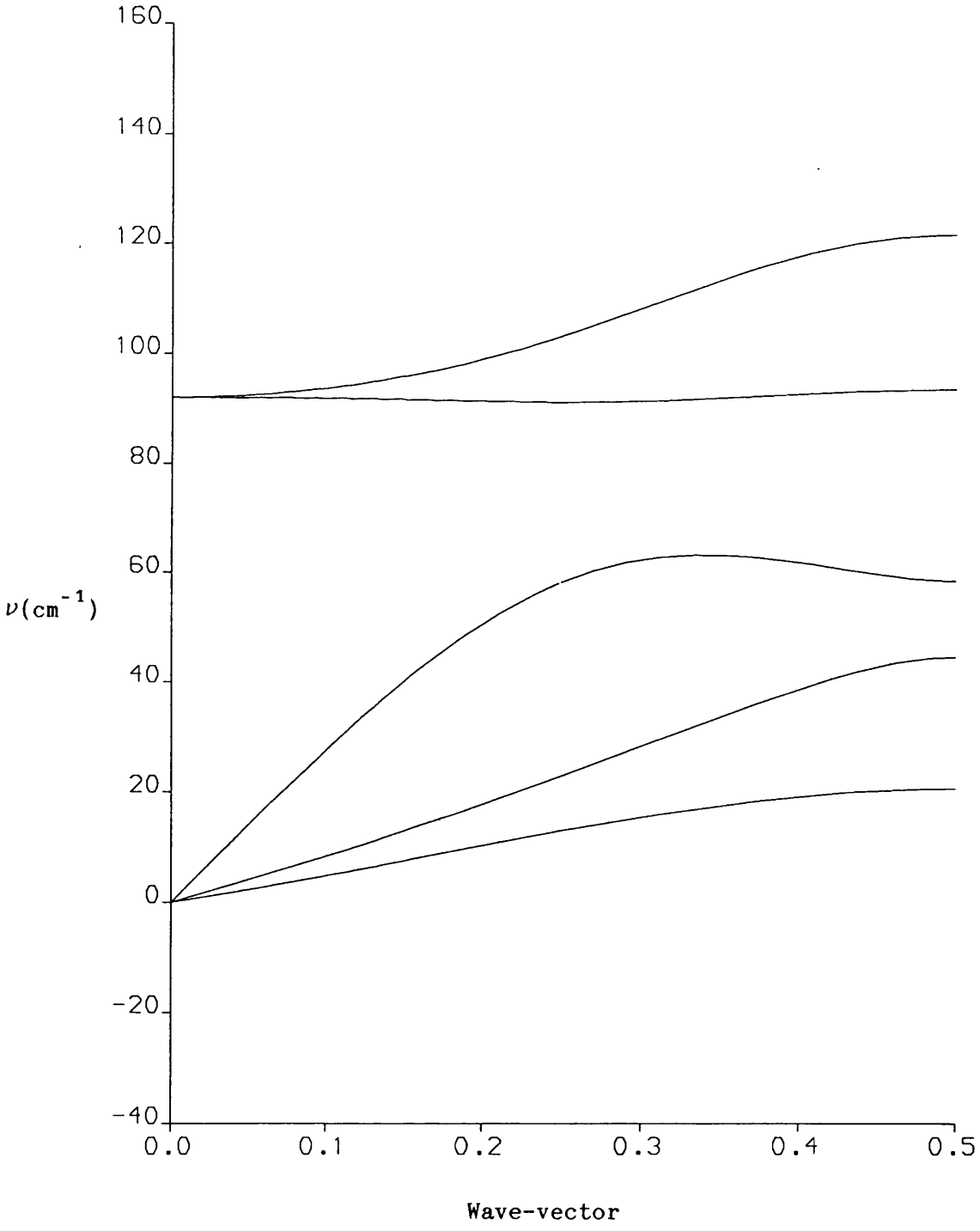

Figure 8.7: Atom-Atom Lennard-Jones 10-6 + Molecular Octupole Potential for OCS: Dispersion Curves Perpendicular to C_3

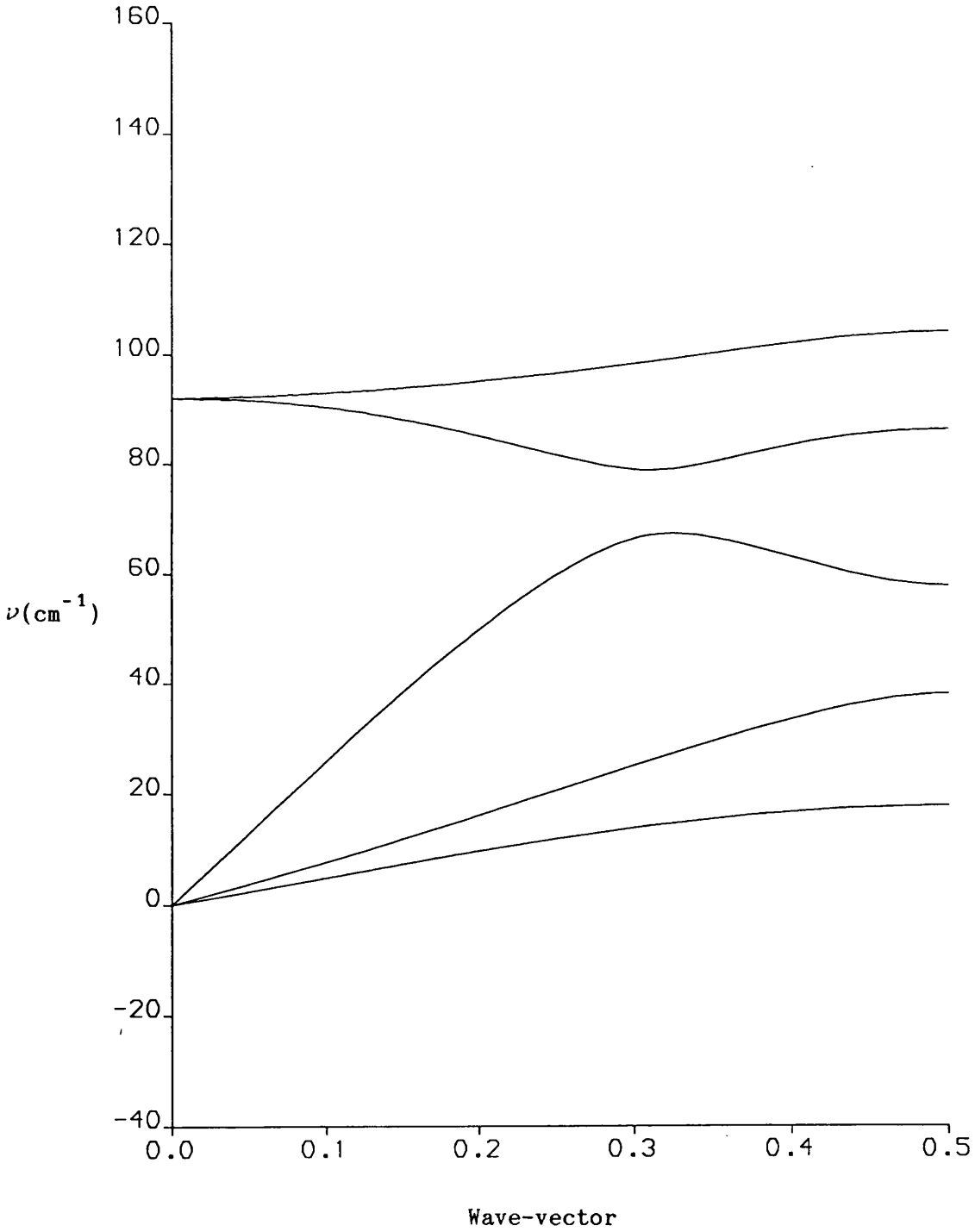

Figure 8.8: Atom-Atom Lennard-Jones 8-6 + Molecular Octupole Potential for OCS: Dispersion Curves Perpendicular to C_3

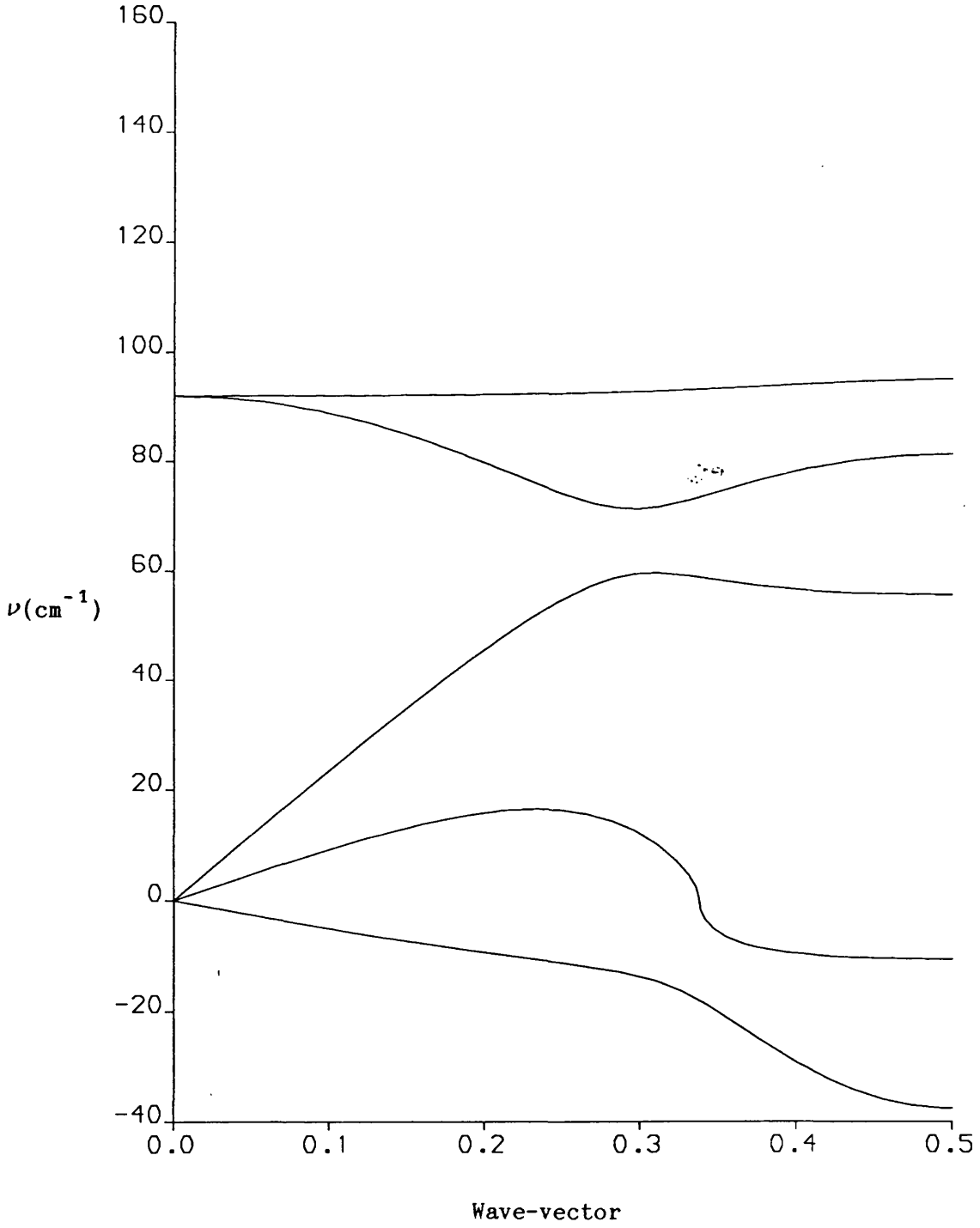

A number of trends are apparent in the dispersion curves, in the parallel direction the optical branch increases from 92 cm^{-1} to 140 cm^{-1} for the 14-6 potential but as the exponent is decreased this "upward" slope is also decreased, to the extent that the branch slowly drops for the 8-6 potential. The higher acoustic branch is relatively unaffected by variation of the exponent, though the magnitude of the frequency "maximum" around $\underset{\sim}{k} = 0.15$ decreases slightly as the exponent decreases. The lower acoustic branch is virtually identical for the 14-6, 12-6 and 10-6 potentials and yet remarkably different for the 8-6 potential. In this instance the initial slope is significantly lower and instead of continually rising it drops sharply at $\underset{\sim}{k} = 0.38$ and the branch becomes imaginary.

In the perpendicular direction similar trends are followed, the two optical branches exhibit the same behaviour as their (doubly degenerate) parallel counterparts, rising for the 14-6 potential and decreasing as the exponent decreases. The upper acoustic branch is also relatively unaffected, though the frequency of the maximum at $\underset{\sim}{k} = 0.3$ increases from the 14-6 to the 10-6 potential and then decreases for the 8-6, with the "hump" becoming more pronounced. The two lower acoustic branches also vary significantly. The upper of the two (the middle acoustic branch) mirrors its parallel counterpart, shallow but real for the 14-6, 12-6 and 10-6 potentials and sharply dropping into the imaginary region in the same wave-vector region for the 8-6 potential. The lowest acoustic branch exhibits significantly greater variation. For the 14-6 potential it is imaginary from $\underset{\sim}{k} = 0$ to $\underset{\sim}{k} = 0.15$, then turning real but small, a failing which it may recalled was characteristic of the atomic charge + molecule octupole potential. For the 12-6 and 10-6 potentials the branch is real throughout, yet for the 8-6 potential it is imaginary throughout,

starting small in magnitude with a significant drop at $\underset{\sim}{k}$ = 0.32, the wave-vector region when all the lower acoustic branches are seen to "fail" for the 8-6 potential.

Finally the elastic properties have been determined for this series of potentials. These are presented in table 8.2.

Table 8.2: Atom-Atom Lennard-Jones 14-6, 12-6, 10-6 and 8-6 + Molecular Octupole Potentials for OCS: Elastic Properties

Property	14-6	12-6	10-6	8-6
c_{11}/GPa	12.0160	10.5967	9.1099	7.5489
c_{12}/GPa	11.0364	9.3948	7.8046	6.3017
c_{13}/GPa	0.3377	-0.0111	-0.3356	-0.6556
c_{15}/GPa	0.6981	0.3052	-0.1854	-0.7711
c_{33}/GPa	34.1750	30.8875	27.5466	24.1320
c_{55}/GPa	0.6906	0.5352	0.4013	0.2411
S_3/GPa^2	787.5877	617.4872	465.7117	333.3831
S_4/GPa^2	-0.2982	0.4570	0.4551	-0.8885
$\varkappa_0$/GPa^{-1}	0.11434	0.13249	0.15750	0.19418

It may be seen that the magnitude of each of the elastic constants decreases as the repulsive exponent decreases. The stability constant S_4 is negative for both the 14-6 and 8-6 potentials, thus denying these two potentials elastic stability. The most important characteristic is the variation of the compressibility, $\varkappa_0$ which as expected increases as the exponent decreases. The variation is also significant, the calculated values for each successive potential being around 15-25% higher than for the previous potential. In comparison it should be recalled that the compressibilities for the various

atom-atom + multipole potentials considered in the previous chapter were all within 5% of each other. The variation is such that the value for the 8-6 potential is 88% of the experimental value (0.22 GPa^{-1}).

These results show that the variation of the repulsive exponent does offer significant improvement for the compressibility but the failings of the various potentials must also be recalled. The 14-6 potential is unsatisfactory because of its imaginary dispersion curve and its failure to satisfy the conditions for elastic stability. The 10-6 potential has no imaginary curves and satisfies elastic stability but has an unrealistic ϵ parameter. The 8-6 potential, although offering a great improvement in the compressibility has unrealistic ϵ parameters, imaginary dispersion curves and is elastically unstable. For this series of potentials only the 12-6 potential satisfies the basic requirements of an empirical potential.

Despite the fact that the variation of the repulsive exponent has failed to provide a satisfactory improvement on the atom-atom Lennard-Jones 12-6 + molecular octupole potential as a model for carbonyl sulphide, the results presented here indicate that the modelling of the compressibility can be improved by this method.

Atomic Charge + Molecular Octupole and Atomic Quadrupole Potentials

The other atom-atom hybrid potentials, the atomic charge + molecular octupole, atomic quadrupole and atomic multipole potentials which were described in the previous chapter have been investigated in a similar manner and the results obtained are not unexpected. The general trend that the compressibility increases as the repulsive exponent decreases is exhibited for all three sets of potentials.

For the first two sets, none of the fitted potentials satisfy the conditions for elastic stability. Each also exhibits imaginary dispersion curves. Overall they all prove to be unsatisfactory, each

set following the same internal trends as detailed above for the molecular octupole potential. Consequently each fails in comparison to its analogous molecular octupole potential for the reasons detailed in the previous chapter when the various multipolar potentials were considered.

Atomic Multipole Potentials

The atomic multipole potential differs from the two discussed above. It should be recalled that this potential proved to be as good but no better than the molecular octupole potential as a model for carbonyl sulphide. The compressibility for the atomic multipole 14-6, 12-6, 10-6 and 8-6 series of potentials follows the same trend as for the molecular octupole series, with the 8-6 potential yielding a near-identical value of 0.1939 GPa^{-1}. However the dispersion curves are better than their counterparts for the molecular octupole potential, no imaginary frequencies are apparent for any of the potentials and all four exhibit elastic stability, unlike the molecular octupole series for which the 14-6 and 8-6 potentials failed these requirements. However the 10-6 and 8-6 potentials atomic multipole potentials are unsatisfactory, for in each case the parameter ϵ_{LL} is found to be negative (the same failing as the 10-6 atom-atom + molecular octupole potential) and therefore the fitted potentials are unrealistic. Thus while the series of atomic multipole potentials exhibit less failings than the molecular octupole potentials the only models which satisfy the basic requirements of a hybrid potential are the 14-6 and 12-6 potentials, neither of which offers an improvement in the compressibility. Consequently the series of atomic multipole potentials is unable to provide an improved model for carbonyl sulphide.

8.3: Anisotropic Berne-Pechukas Molecule-Molecule + Molecular Octupole Potentials: Repulsive Variation

The problem encountered in the previous section was that whilst the reduction of the repulsive exponent effected an increase in the calculated compressibility it also caused a number of other properties to fluctuate. This variation was such that at least one of the conditions required of an empirical potential, realistic ϵ values, real dispersion curves or elastic stability, failed. Of all the potentials discussed in the previous chapter the best model for carbonyl sulphide was found to be provided by the anisotropic Berne-Pechukas potential. Therefore it is logical to examine the effects of varying the repulsive exponent for this potential.

Once again the same series of potentials are considered and the fitting procedure is successful for all four. The parameters obtained are presented in table 8.3.

Table 8.3: Anisotropic Berne-Pechukas Molecule-Molecule 14-6, 12-6, 10-6 and 8-6 + Molecular Octupole Potentials for OCS: Parameters

Potential	ϵ/kcal mol^{-1}	R_0/Å	Ω/Debye Å^2	χ
14-6	0.61087	4.0182	12.045	0.4145
12-6	0.58325	4.0654	12.296	0.4144
10-6	0.54951	4.1332	12.548	0.4138
8-6	0.50588	4.2374	12.776	0.4119

These parameters are seen to be physically realistic for all four potentials and the variation in their magnitudes is less than for the atom-atom + molecular octupole series. The dispersion curves for this set of potentials have also been determined and are presented in figures 8.9 to 8.16.

Figure 8.9: Anisotropic Berne-Pechukas Molecule-Molecule 14-6 +

Molecular Octupole Potential for OCS: Dispersion Curves Parallel to C_3

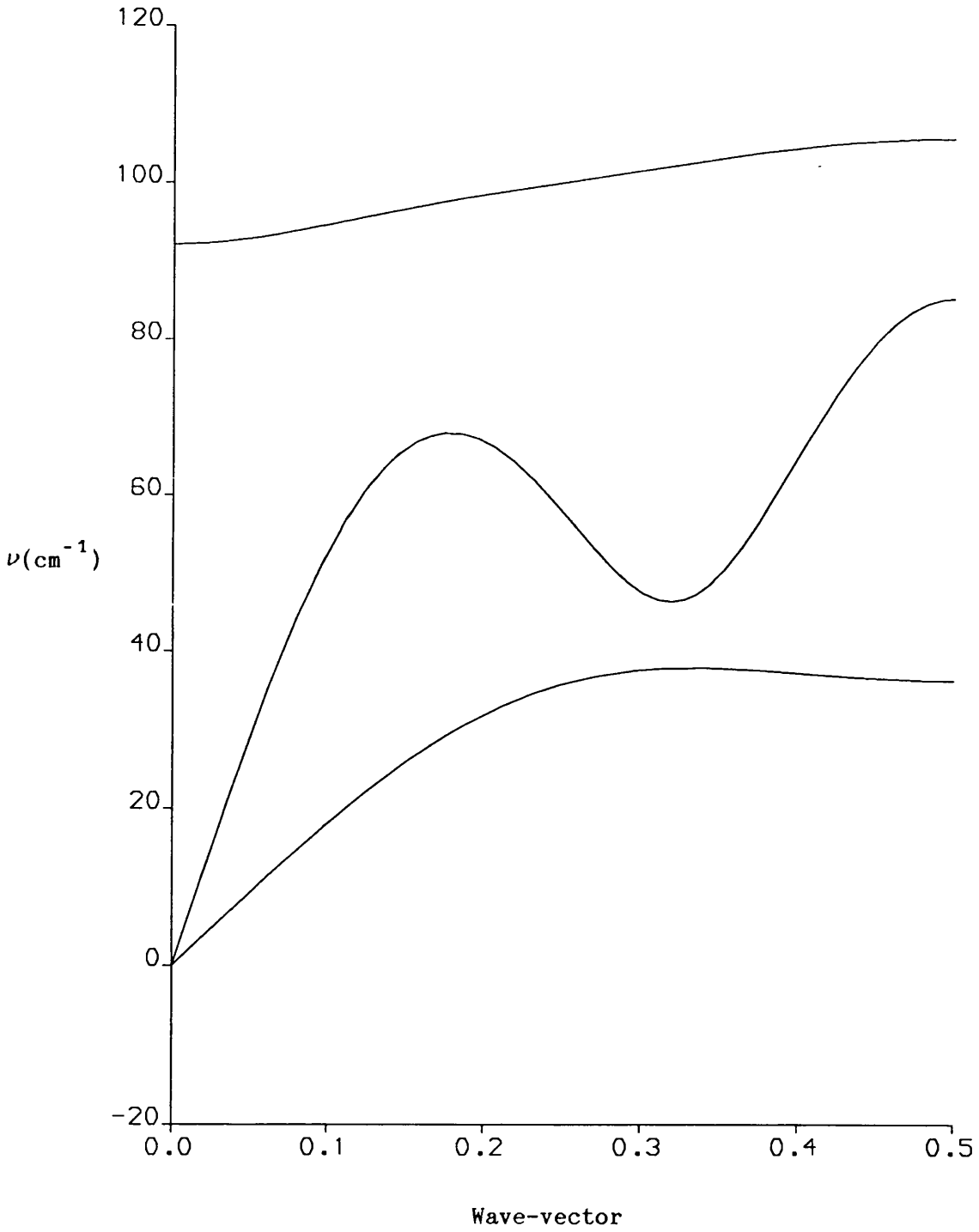

Figure 8.10: Anisotropic Berne-Pechukas Molecule-Molecule 12-6 + Molecular Octupole Potential for OCS: Dispersion Curves Parallel to C_3

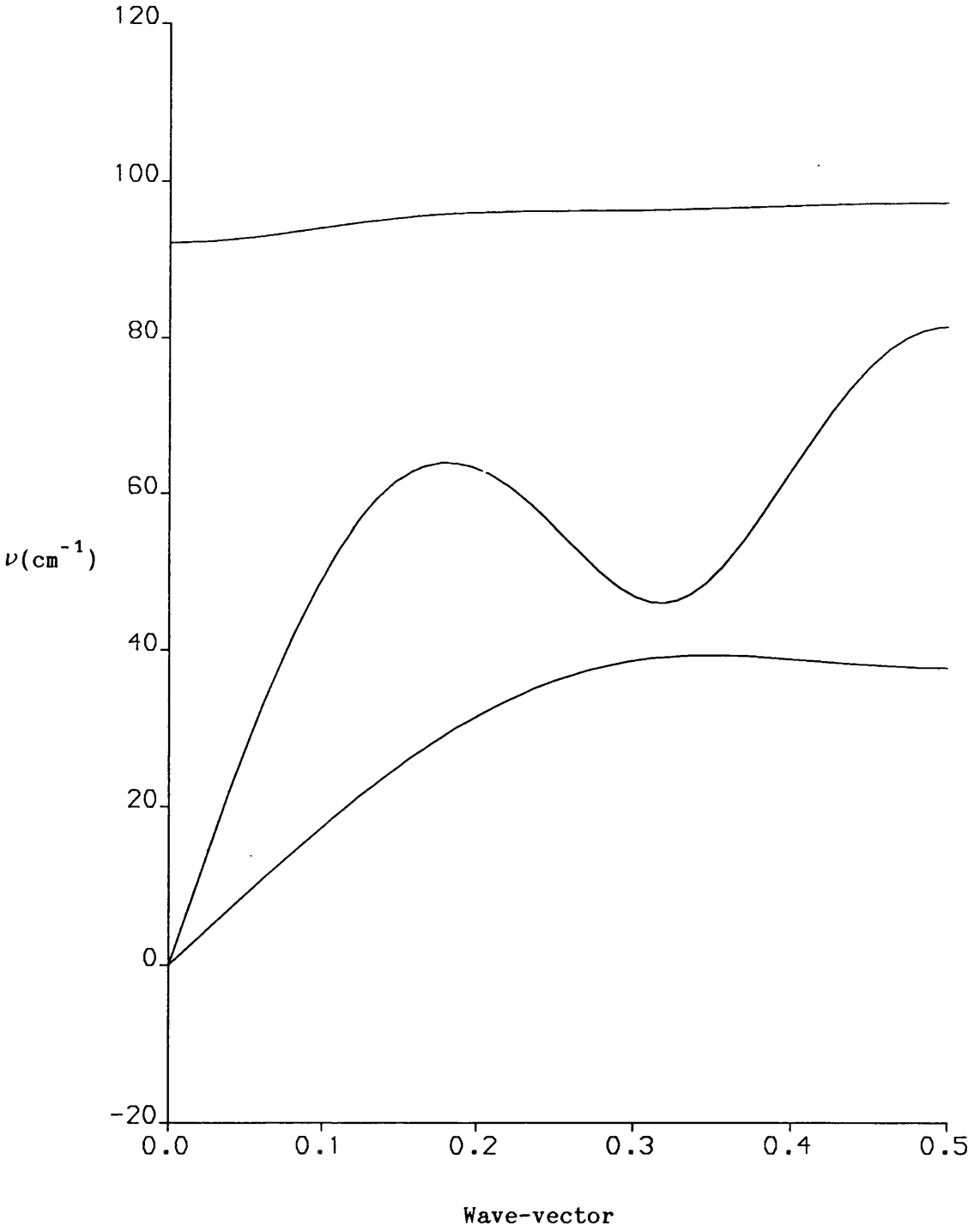

Figure 8.11: Anisotropic Berne-Pechukas Molecule-Molecule 10-6 + Molecular Octupole Potential for OCS: Dispersion Curves Parallel to C_3

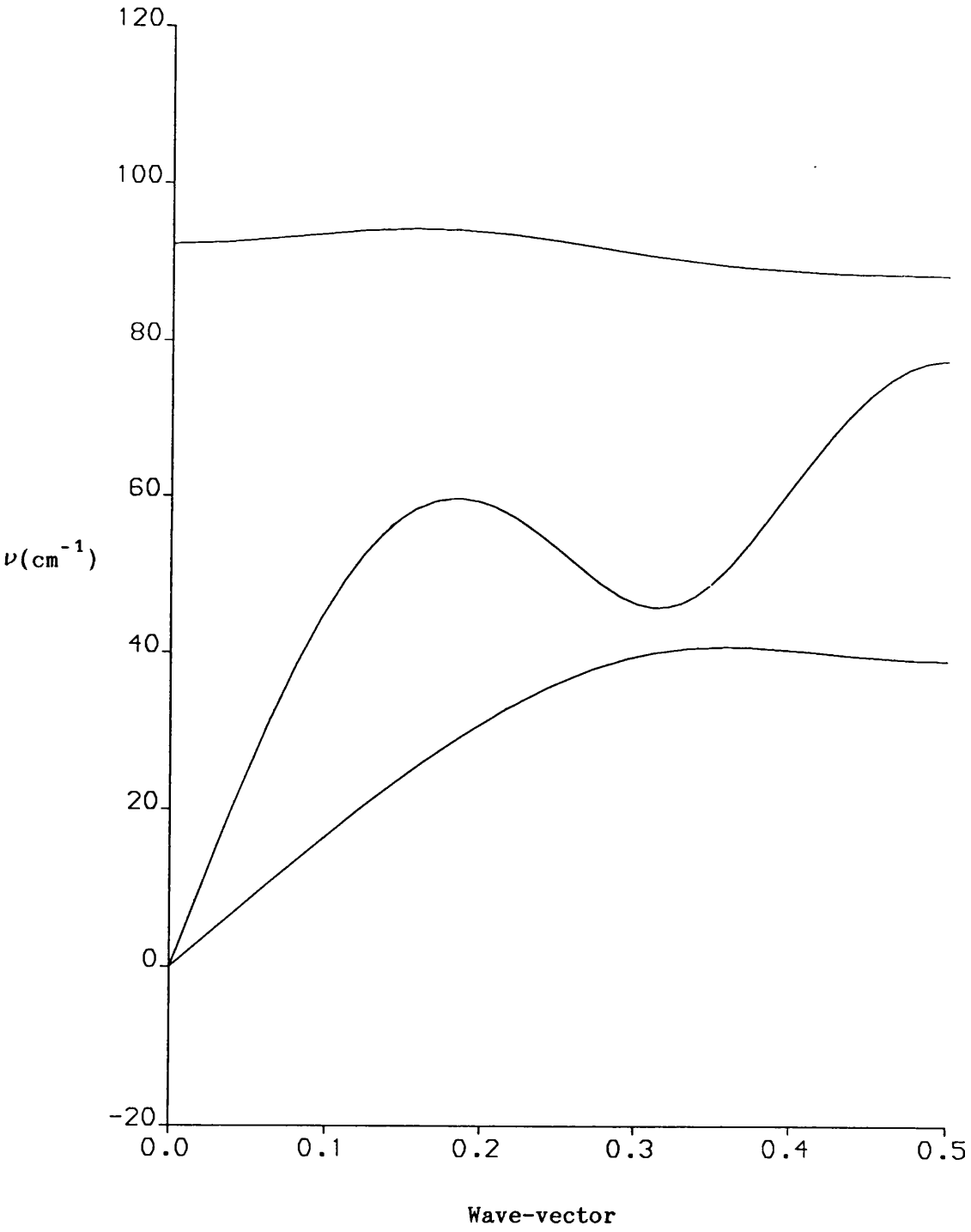

Figure 8.12: Anisotropic Berne-Pechukas Molecule-Molecule 8-6 + Molecular Octupole Potential for OCS: Dispersion Curves Parallel to C_3

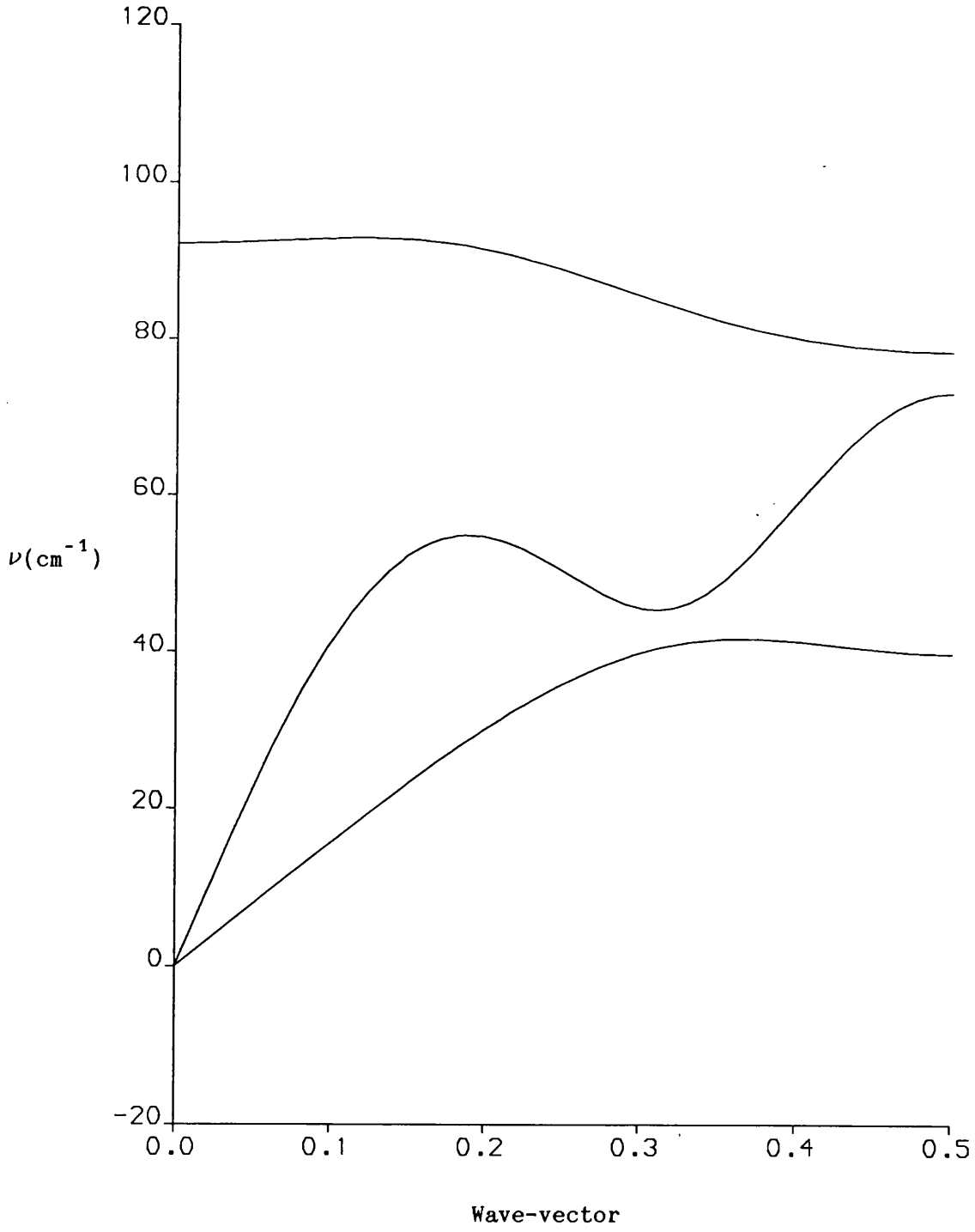

Figure 8.13: Anisotropic Berne-Pechukas Molecule-Molecule 14-6 + Molecular Octupole Potential for OCS: Disp. Curves Perpendicular to C_3

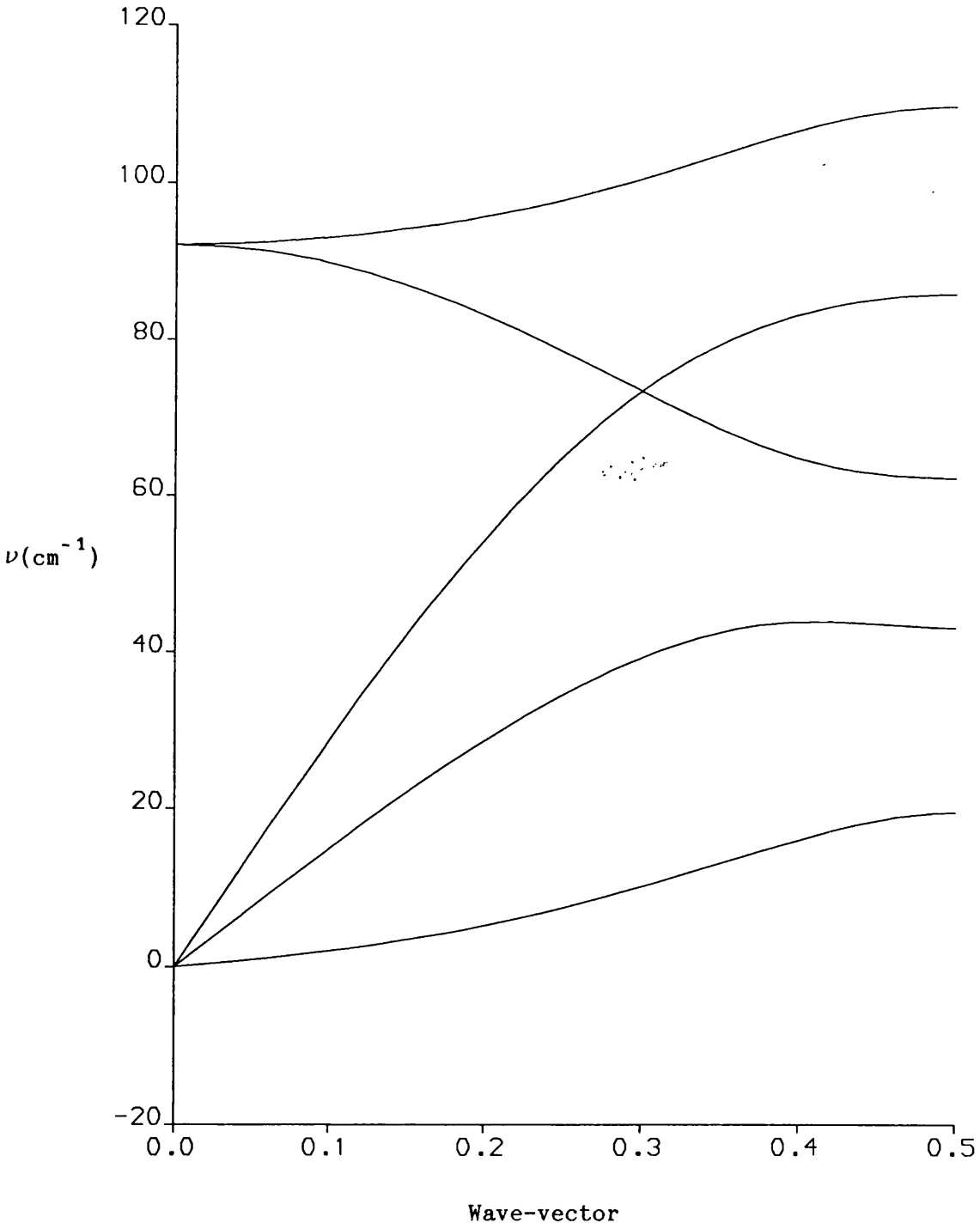

Figure 8.14: Anisotropic Berne-Pechukas Molecule-Molecule 12-6 + Molecular Octupole Potential for OCS: Disp. Curves Perpendicular to C_3

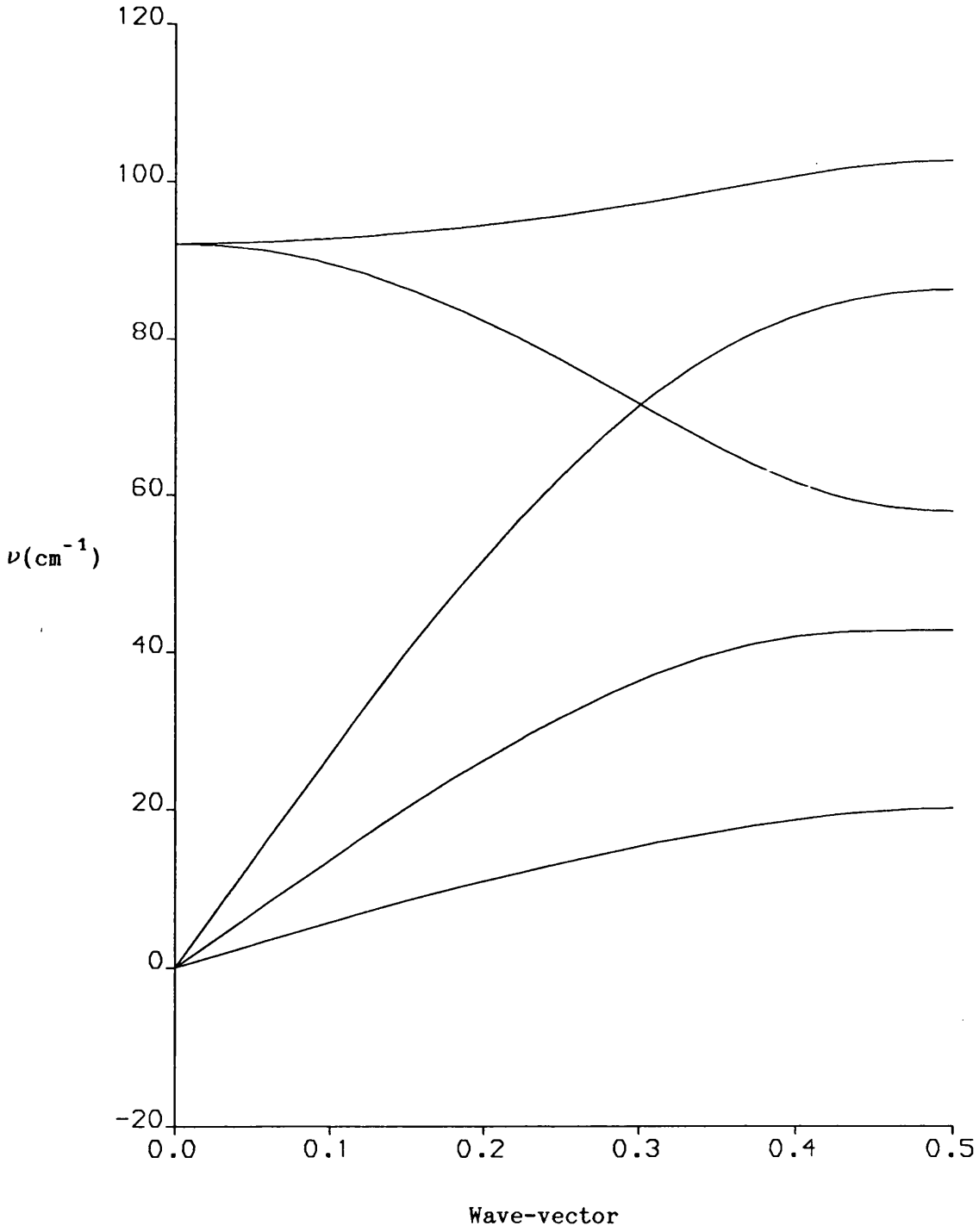

Figure 8.15: Anisotropic Berne-Pechukas Molecule-Molecule 10-6 +

Molecular Octupole Potential for OCS: Disp. Curves Perpendicular to C_3

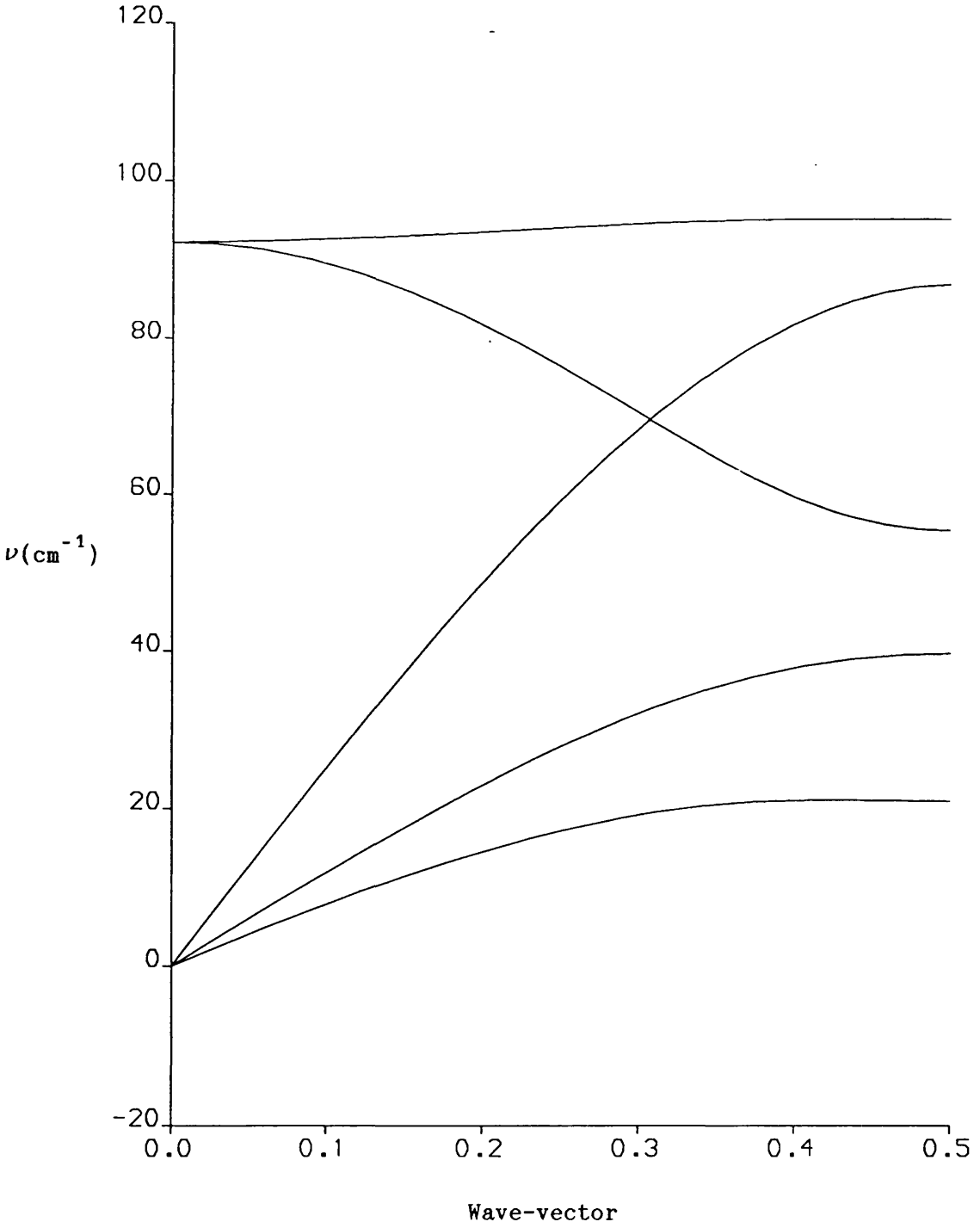

Figure 8.16: Anisotropic Berne-Pechukas Molecule-Molecule 8-6 +

Molecular Octupole Potential for OCS: Disp. Curves Perpendicular to C_3

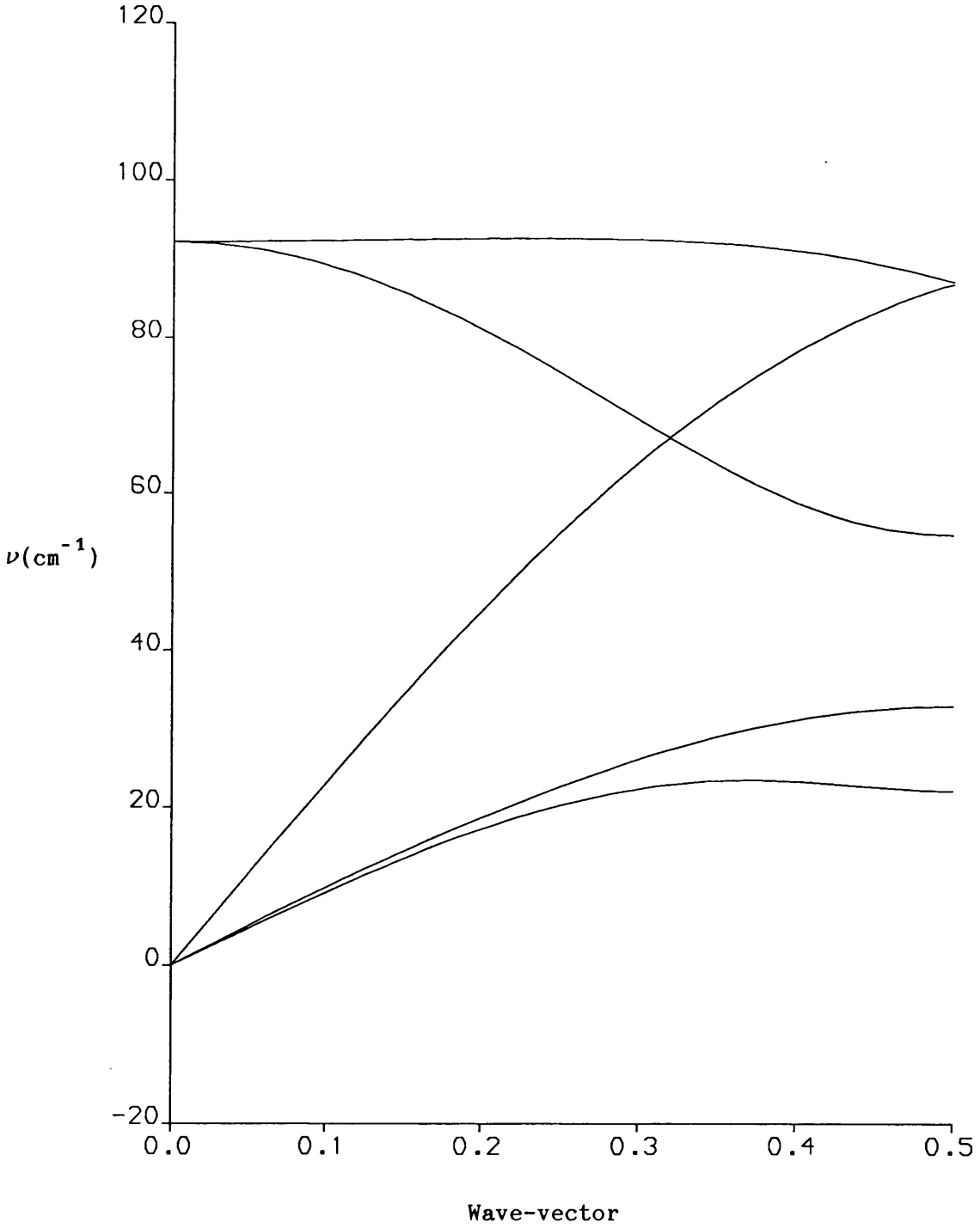

The most important characteristic of the dispersion curves is that there are no imaginary frequencies for any of the four potentials. In addition there are a number of other notable characteristics. The dispersion curves in each series are remarkably similar, the large variation exhibited by the series of atom-atom + molecular octupole potentials being much smaller for this set.

In the parallel direction the "falling" of the optical branch is apparent but nowhere near as pronounced for this series. The upper acoustic branch is near identical for all four potentials, exhibiting the same trend of having a frequency "maximum" around $\underset{\sim}{k} = 0.18$, which decreases as the exponent is decreased. The lower acoustic branch, generally found to be the branch which acts as a "pointer" to the quality of the curves and a branch which varied greatly for the atom-atom + molecular octupole potential, is virtually identical throughout this series, the frequency rising to 40 cm^{-1} and remaining steady, a relatively stable value for this particular branch.

In the perpendicular direction similar trends are observed. The optical branches are similar, the highest dropping as the exponent is decreased. The variation of the acoustic branches is small, though the middle branch drops as the exponent decreases. The lower acoustic branch, the "pointer" in the perpendicular direction is also very stable, although it only rises to 20 cm^{-1} it remains steady at that frequency and does not drop significantly as the exponent decreases.

The dispersion curves exhibit the same basic characteristic as the potential parameters obtained by the fitting procedure, namely that the variation in the parameters/properties obtained is significantly smaller for the series of anisotropic Berne-Pechukas potentials than for their atom-atom + molecular octupole counterparts. The final test of this series of potentials is to determine their elastic properties

and these are presented in table 8.4.

Table 8.4: Anisotropic Berne-Pechukas Molecule-Molecule 14-6, 12-6, 10-6 and 8-6 + Mol. Octupole Potentials for OCS: Elastic Properties

Property	14-6	12-6	10-6	8-6
c_{11}/GPa	11.1809	9.9026	8.5528	7.1064
c_{12}/GPa	8.8508	7.4252	6.0722	4.7994
c_{13}/GPa	0.7113	0.4195	0.1375	-0.1325
c_{15}/GPa	1.4470	1.0007	0.5054	-0.0218
c_{33}/GPa	19.5433	17.0027	14.4190	11.7582
c_{55}/GPa	1.9077	1.7342	1.5501	1.3533
S_3/GPa^2	390.473	294.267	210.602	139.955
S_4/GPa^2	0.2575	2.2935	3.3343	3.1211
κ_0/GPa^{-1}	0.14411	0.16874	0.20353	0.25688

The first characteristic of these elastic properties is that each of the potentials fulfils the requirements for elastic stability. The compressibility shows a great variation with the exponent and the value for the 8-6 potential is actually higher than the experimental value (0.22 GPa^{-1}), the first potential discussed which yields this result. The variation in the magnitude of the compressibility shows the same general trend as for the atom-atom + molecular octupole potential, each successive potential yielding a value 15-25% higher.

The advantages of this potential over the atom-atom + molecular octupole potential are two-fold, first the anisotropic Berne-Pechukas potentials yield higher values for the compressibilities than their counterparts. Secondly the variation in the fitted parameters and the frequencies of the dispersion curves is significantly smaller for the

Berne-Pechukas potentials, such that all four potentials satisfy the basic requirements of an empirical potential, yet the variation in the compressibility is not restrained by the same extent. The original problem discussed at the start of this section, of the potentials being too "sensitive" is effectively solved by this model. The series of Berne-Pechukas potentials can be considered as being far more "stable" than any of the other potentials and as such provide the best model for carbonyl sulphide. For the potentials presented in this section the compressibility for the 10-6 potential is slightly below the experimental value while for the 8-6 potential it is slightly above. The 9-6 potential would be expected to give the best estimate and this potential is discussed in the next section.

8.4: Anisotropic Berne-Pechukas Molecule-Molecule + Molecular Octupole Potentials: Dispersive Variation

It has been discussed that both the repulsive and dispersive exponents in the atom-atom/molecule-molecule potentials may be varied. The effects of varying the repulsive exponent for the potentials presented in the previous chapter have been discussed in the previous sections with the dispersive exponent kept fixed as six. It is expected that the general treatment applied to repulsive variation should also apply to dispersive variation and this is investigated in this section. As before a fixed value for the repulsive exponent is chosen and a fixed multipolar model is employed. In line with the conclusions of the previous section the standard potential is chosen to be the anisotropic Berne-Pechukas molecule-molecule 9-6 potential. In addition, the 9-7, 9-5 and 9-4 potentials are considered.

All four potentials are successfully fitted in the normal manner and the parameters obtained are given in table 8.5.

Table 8.5: Anisotropic Berne-Pechukas Molecule-Molecule 9-7, 9-6, 9-5 and 9-4 + Molecular Octupole Potentials for OCS: Parameters

Potential	ϵ/kcal mol^{-1}	R_0/Å	Ω/Debye Å^2	χ
9-7	0.57501	4.1131	12.482	0.41443
9-6	0.53031	4.1782	12.633	0.41304
9-5	0.47625	4.2680	12.793	0.41090
9-4	0.41291	4.3934	12.961	0.40817

As with the series of potentials for the variation of the repulsive exponent all of the parameters obtained here are realistic and the effect of reducing the dispersive exponent is the same on each property; ϵ and χ decrease while R_0 and Ω increase. The degree of variation is comparable, though it should be noted that in this series the dispersive powers differ by one, whereas the series of repulsive powers differed by two. The variation of χ, the degree of anisotropy is significantly greater for this series.

The dispersion curves have also been calculated for this series of potentials and these are presented in figures 8.17 to 8.24. They do not differ strikingly from the n-6 series of dispersion curves, all of the four potentials produce curves without imaginary frequencies and the variation from one set of curves to the next in the series is relatively small. The lower acoustic branch in the parallel direction remains real, with a stable frequency in the region of 40 cm^{-1} for each of the potentials. Similarly the lowest acoustic branch in the perpendicular direction also remains real, in the region of 20 cm^{-1}. The curve which shows the greatest variation for these potentials is the middle acoustic branch in the perpendicular direction, approaching a frequency of 40 cm^{-1} for the 9-7 potential but dropping to 20 cm^{-1} for the 9-4 potential, almost crossing the lower branch.

Figure 8.17: Anisotropic Berne-Pechukas Molecule-Molecule 9-7 + Molecular Octupole Potential for OCS: Dispersion Curves Parallel to C_3

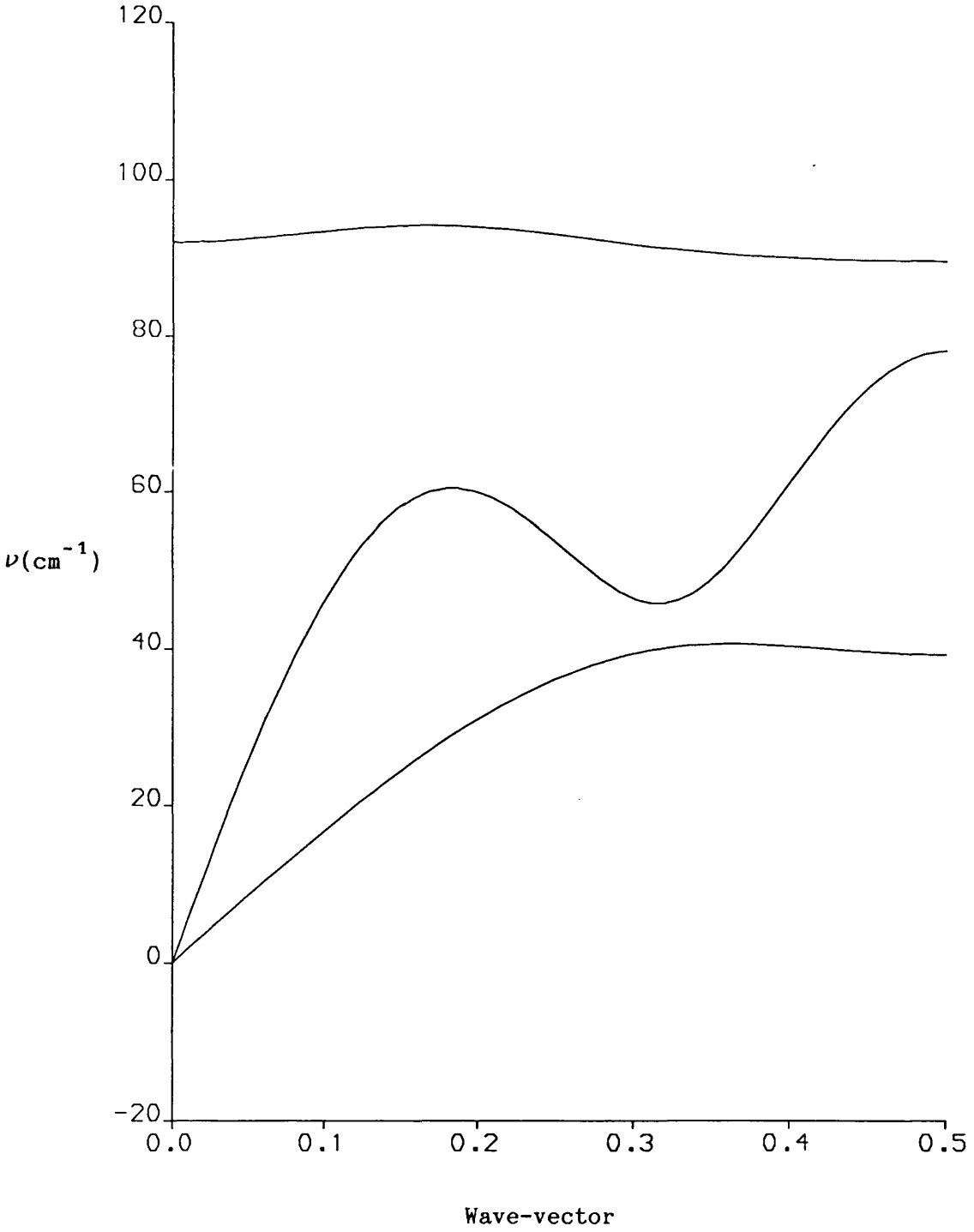

Figure 8.18: Anisotropic Berne-Pechukas Molecule-Molecule 9-6 + Molecular Octupole Potential for OCS: Dispersion Curves Parallel to C_3

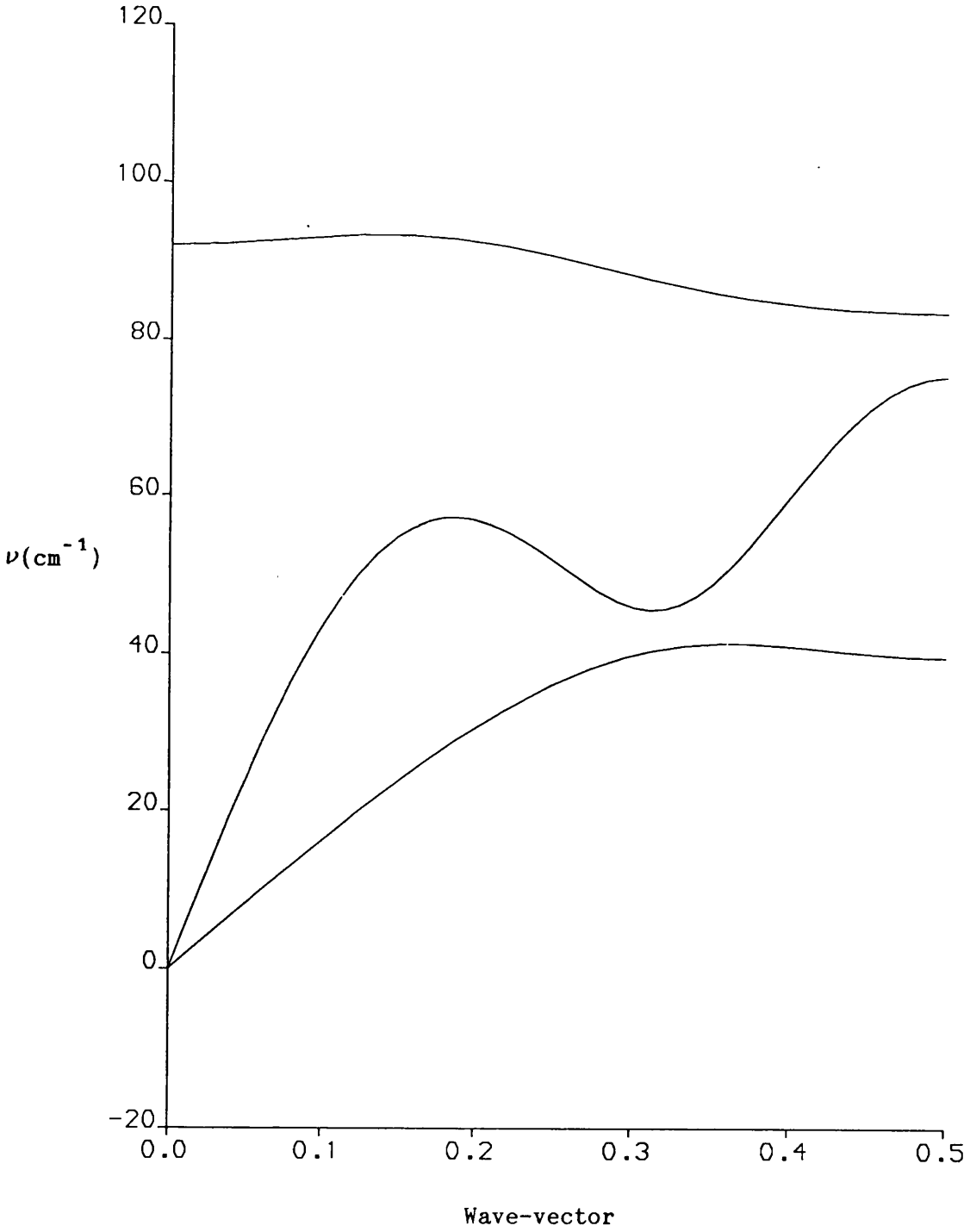

Figure 8.19: Anisotropic Berne-Pechukas Molecule-Molecule 9-5 +

Molecular Octupole Potential for OCS: Dispersion Curves Parallel to C_3

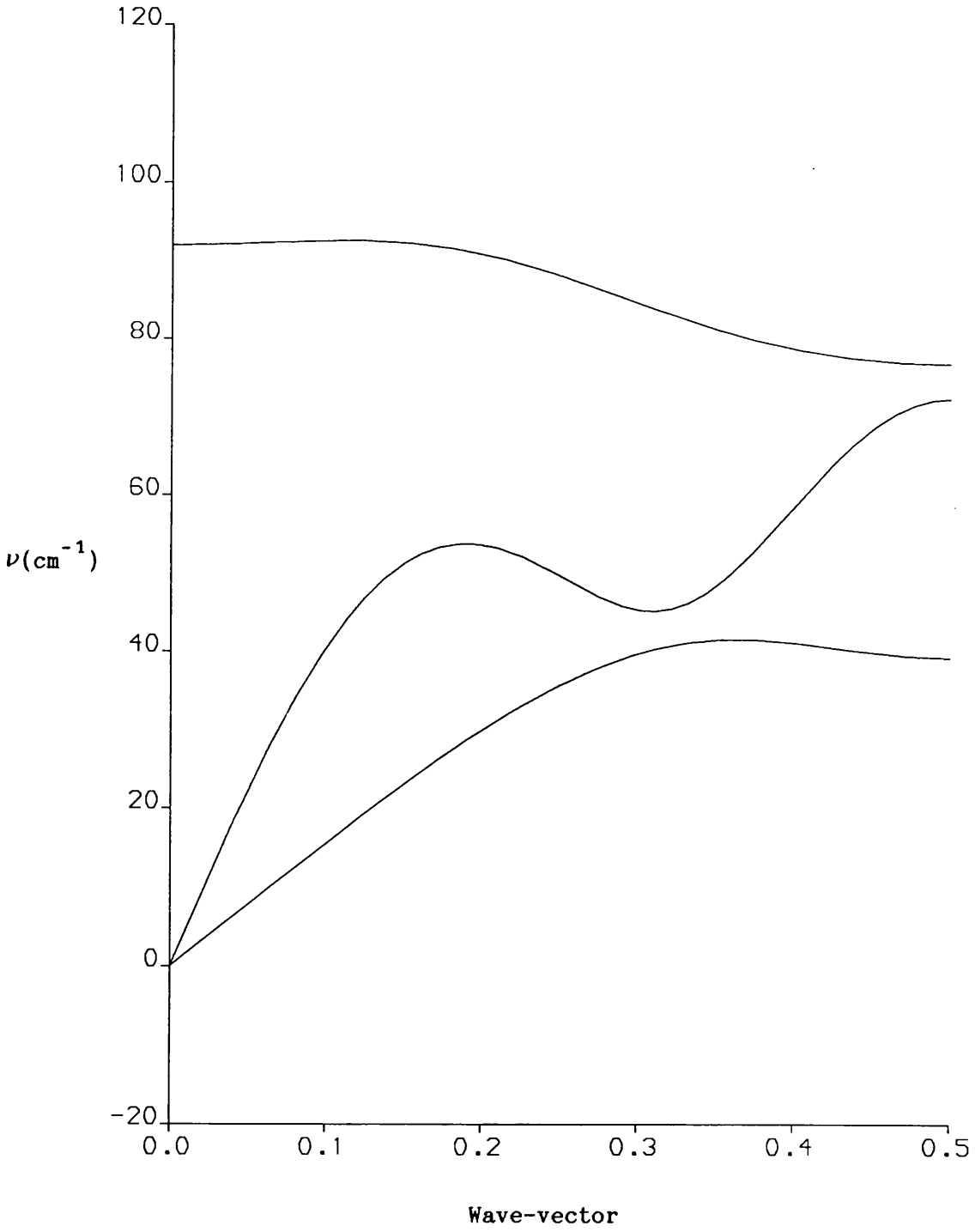

Figure 8.20: Anisotropic Berne-Pechukas Molecule-Molecule 9-4 + Molecular Octupole Potential for OCS: Dispersion Curves Parallel to C_3

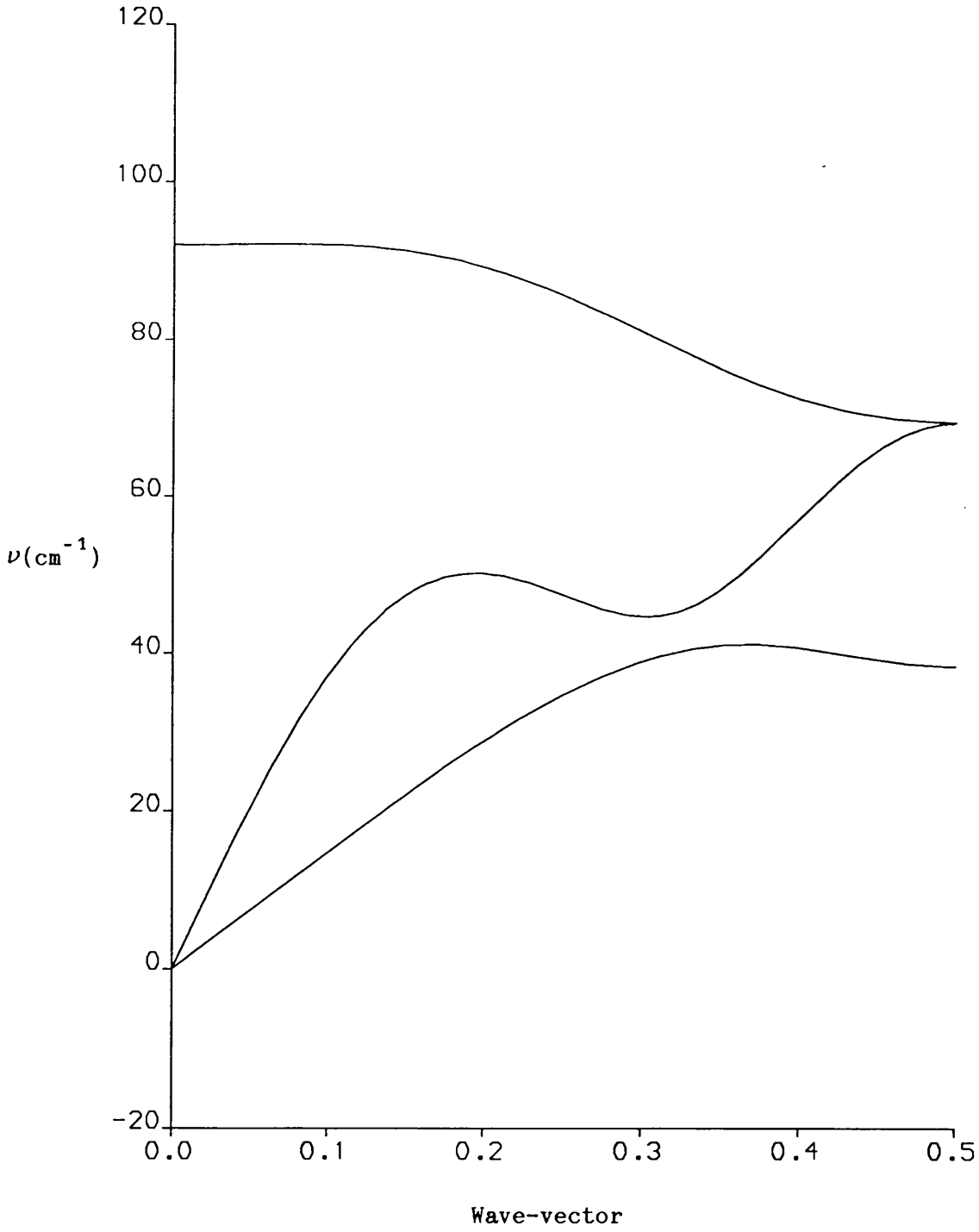

Figure 8.21: Anisotropic Berne-Pechukas Molecule-Molecule 9-7 + Molecular Octupole Potential for OCS: Disp. Curves Perpendicular to C_3

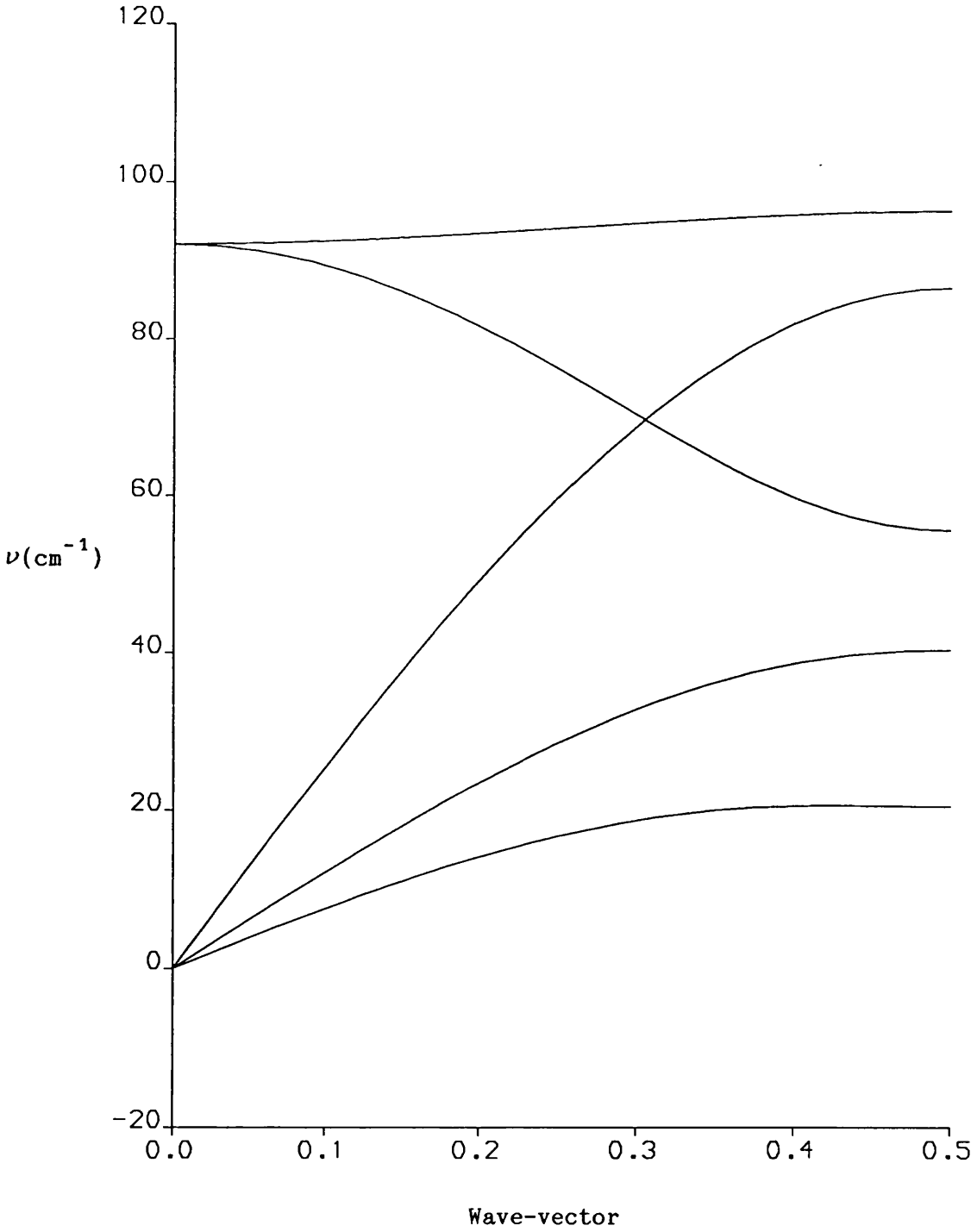

Figure 8.22: Anisotropic Berne-Pechukas Molecule-Molecule 9-6 + Molecular Octupole Potential for OCS: Disp. Curves Perpendicular to C_3

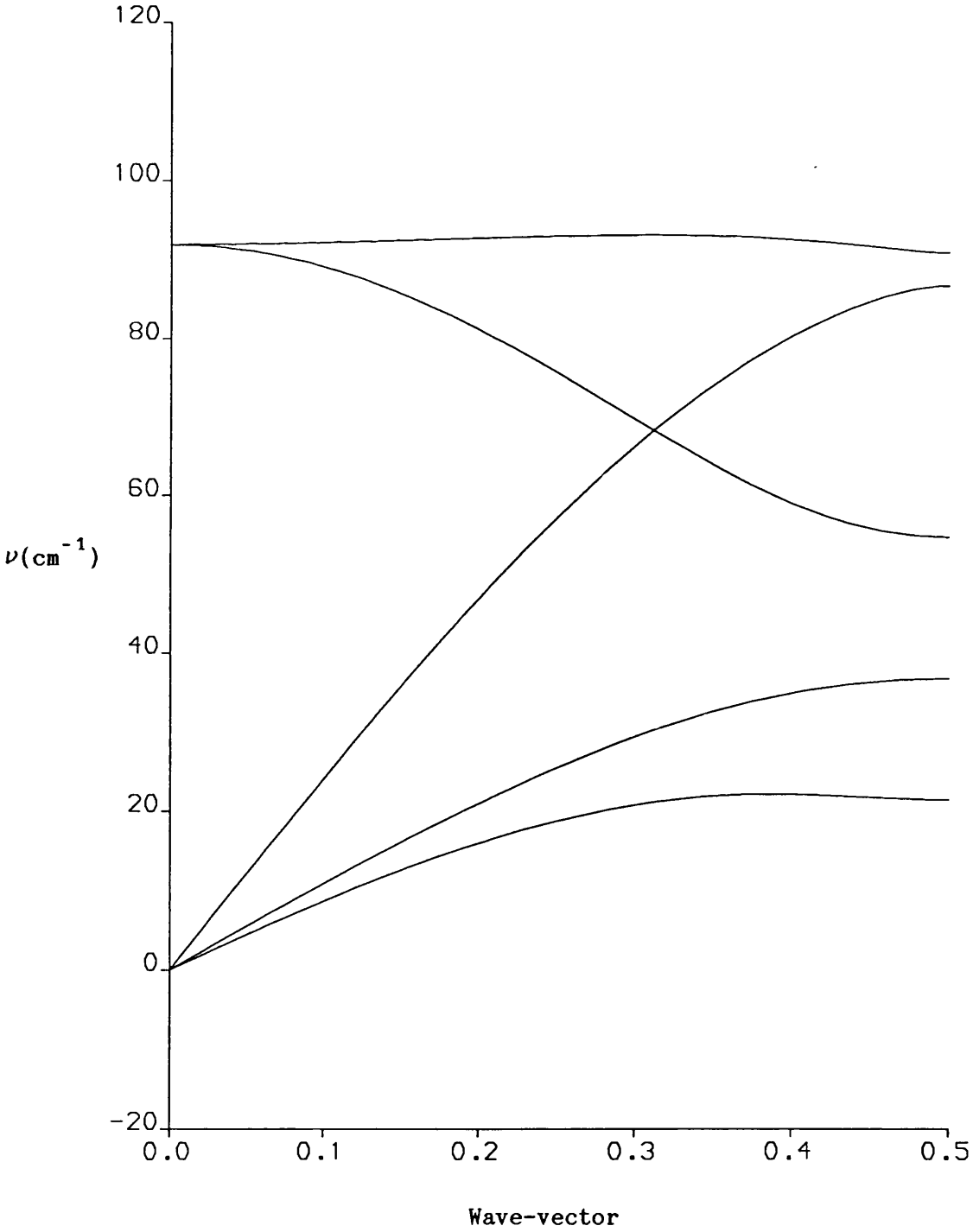

Figure 8.23: Anisotropic Berne-Pechukas Molecule-Molecule 9-5 +

Molecular Octupole Potential for OCS: Disp. Curves Perpendicular to C_3

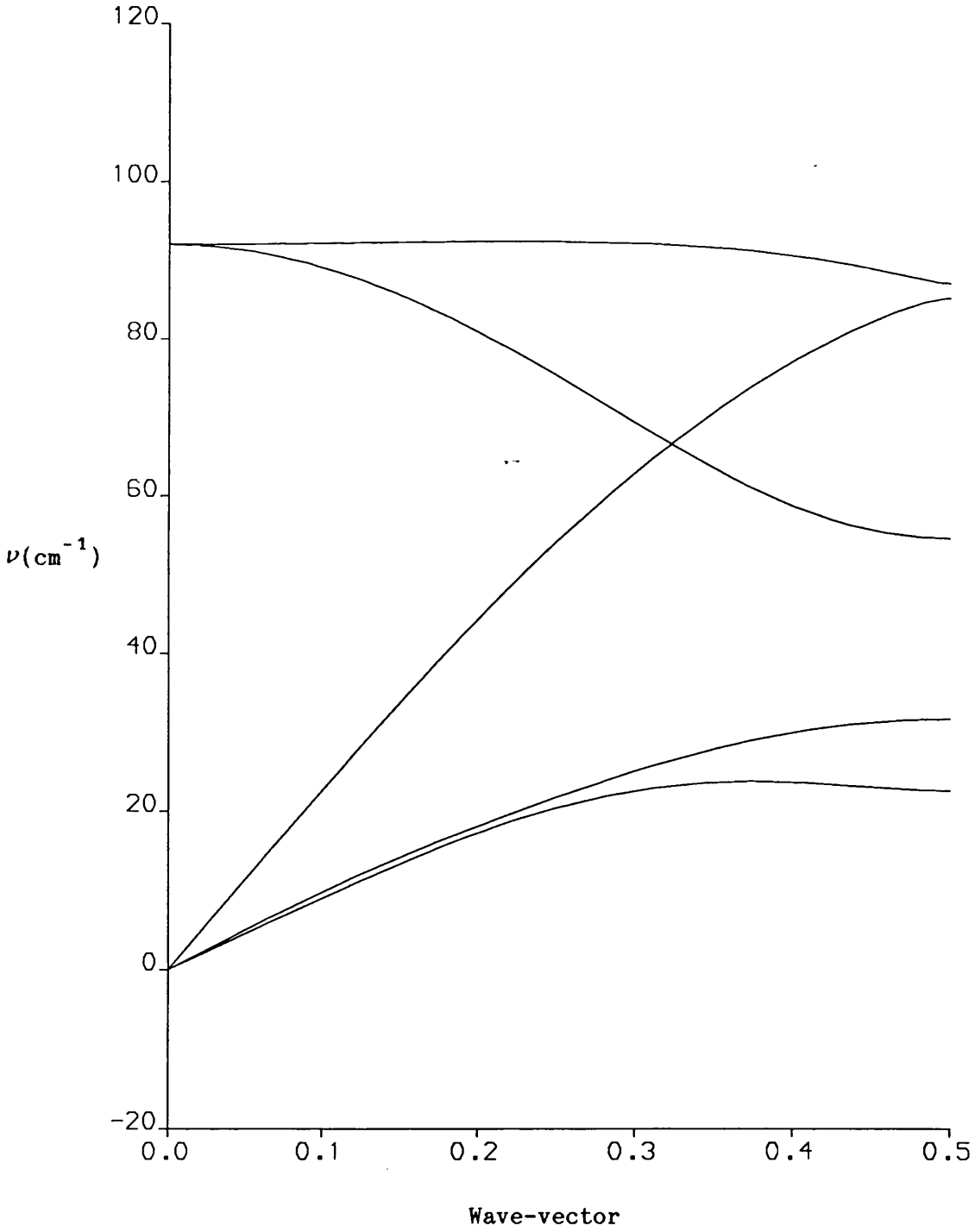

Figure 8.24: Anisotropic Berne-Pechukas Molecule-Molecule 9-4 + Molecular Octupole Potential for OCS: Disp. Curves Perpendicular to C_3

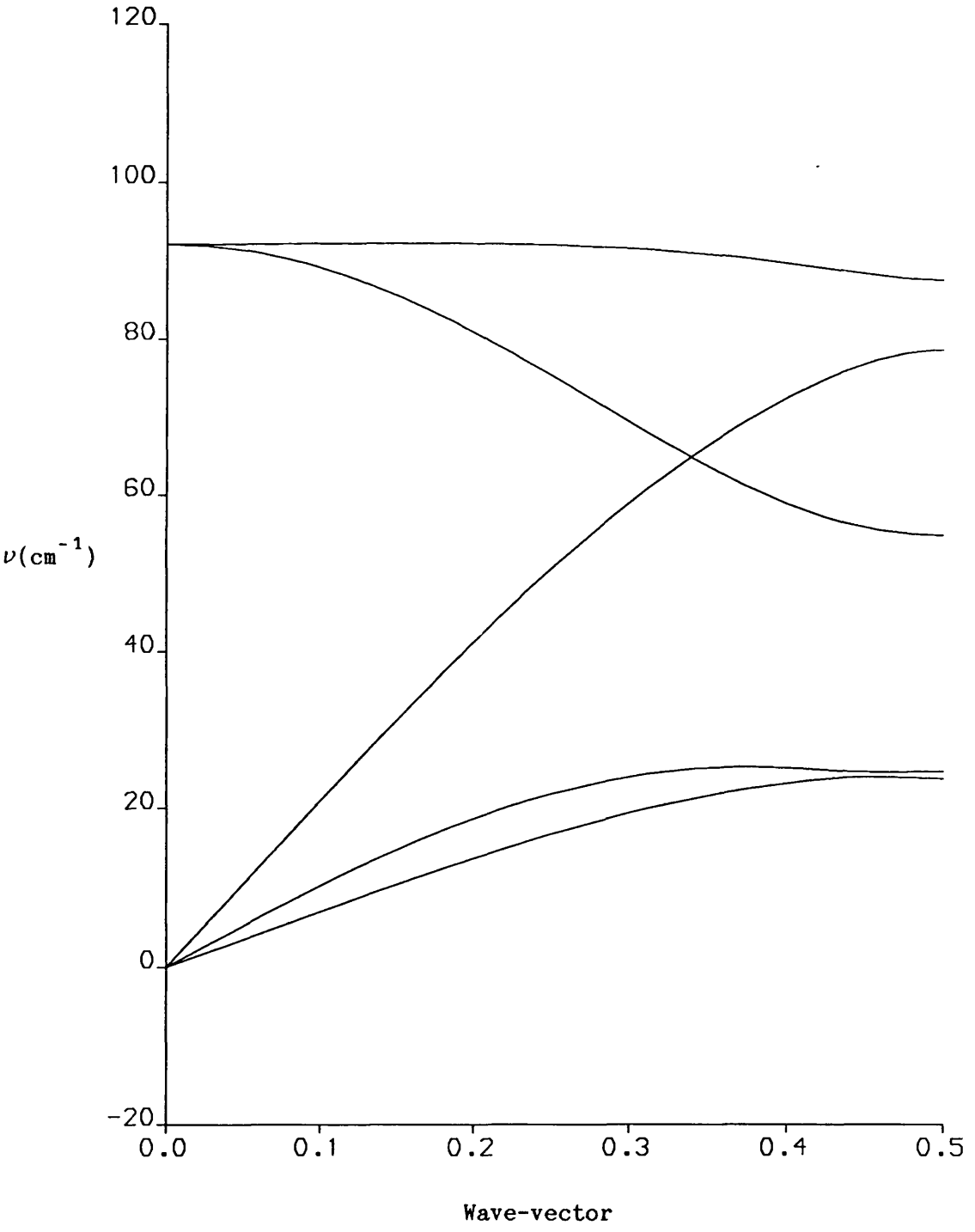

In general the potential parameters and dispersion curves for this series of potentials exhibit the same trends as for those considered in the previous section. The elastic properties have also been determined and these are given in table 8.6.

Table 8.6: Anisotropic Berne-Pechukas Molecule-Molecule 9-7, 9-6, 9-5 and 9-4 + Molecular Octupole Potentials for OCS: Elastic Properties

Property	9-7	9-6	9-5	9-4
c_{11}/GPa	8.7598	7.8344	6.8816	5.8980
c_{12}/GPa	6.2647	5.4202	4.6310	3.8990
c_{13}/GPa	0.1826	0.0079	-0.1701	-0.3614
c_{15}/GPa	0.5809	0.2502	-0.0839	-0.4153
c_{33}/GPa	14.8852	13.0768	11.2685	9.4932
c_{55}/GPa	1.5751	1.4524	1.3209	1.1697
S_3/GPa^2	223.579	173.327	129.672	92.743
S_4/GPa^2	3.2551	3.3812	2.9587	1.9933
χ_0/GPa^{-1}	0.19709	0.22718	0.26783	0.32594

Once again all of the potentials satisfy the conditions for elastic stability and the great variation in the compressibility is observed, the 9-4 potential yielding a value almost 50% larger than the experimental value. The 9-6 potential yields a value for the compressibility which is in excellent agreement with the original estimate from experiment. It is also interesting to note that the value of the stability constant S_4 for the 9-6 potential is the highest for any of the potentials presented in either this or the previous chapter. Indeed, unlike the other three stability constants which tend to decrease consistently with the exponent (whether

repulsive or dispersive), S_4 generally exhibits a maximum. It would appear that as a rough guide for the comparison of potentials, not only is S_4 required to be positive but that the higher its value the better the potential proves to be as a model for carbonyl sulphide.

8.5: Discussion

In this chapter the effects of varying the exponents for the repulsive and dispersive terms in the hybrid potential have been systematically investigated. It has been shown that the variation of these exponents produces a significant variation in the compressibility, with the reduction of either exponent increasing the calculated compressibility. However, for all of the atom-atom potentials considered it is found that the improvement in the compressibility is obtained to the detriment of other properties, in particular the energy-well parameters and the acoustic frequencies. The dispersion curves are found to be very sensitive to this variation and often it leads to imaginary frequencies. The anisotropic Berne-Pechukas potentials exhibit all of the beneficial qualities of the atom-atom potentials but without the associated failures. All of the Berne-Pechukas potentials which have been considered, satisfy the conditions required of such a model and this permits attention to be focussed on the attempt to find a potential whose parameters yield an accurate value for the compressibility. This potential is found to be the anisotropic Berne-Pechukas molecule-molecule 9-6 potential, combined with a molecular octupole of 12.633 Debye $Å^2$.

9.1: Introduction

In the previous chapters the molecular crystal of carbonyl sulphide has been considered and a number of empirical potentials have been proposed as suitable models. These potentials have been shown to have varying degrees of success but overall it has been shown that a large number of lattice properties can be reproduced by relatively simplistic potentials. The next test for this general model is to apply it to a different crystal, one which is similar to carbonyl sulphide to see if it is able to reproduce the crystal's properties with an equal degree of success. The crystal chosen is cyanogen iodide (ICN) which has the same crystal structure as carbonyl sulphide.

9.2: Lattice Properties of Cyanogen Iodide

The lattice structure of cyanogen iodide has been determined by Ketelaar and Zwartsenberg[36] using X-ray diffraction and is rhombohedral, space group C_{3v}^5 (R3m) with one molecule per unit cell. The two unit cell parameters are the unit cell length, a = 4.44 Å, slightly longer than for carbonyl sulphide and the unit cell angle, $\alpha = 101.4^{\circ}$, also larger than for carbonyl sulphide and representing a more "open" crystal structure. The bond lengths have not been determined directly but Deakin[26] has provided suitable values of r(C-N) = 1.18 Å and r(C-I) = 2.03 Å which are consistent with diffraction data. The sublimation energy has been determined by Ketelaar and Kruyer[37] at -14.31 kcal mol^{-1}. No experimental estimate of the Debye temperature is available and so the lattice energy is assumed to be equal to the value above. The far-infrared and Raman spectra of cyanogen iodide have both been measured by Savoie and

Pezolet[38] and yield a consistent value for the single fundamental band in the lattice vibration region at 136 cm^{-1}. The Raman spectrum has been measured more recently by Sun and Anderson[39] and it is their value for this band, 127 cm^{-1} which is used as the value for the fundamental frequency used in the potential fitting calculations.

The molecular dipole moment of cyanogen iodide has been determined using microwave spectroscopy by Townes and Schawlow[40] at μ = 3.71 Debye. Ewing, Tigelaar and Flygare[41] have investigated the Zeeman effect in cyanogen iodide and have obtained a value of the molecular quadrupole moment, Θ = -7.33 Debye Å. Both of these moments are significantly larger than the corresponding moments for carbonyl sulphide and they correspond to a molecule with a large degree of dipolar and quadrupolar character. No experimental value for the octupole moment is available but ab initio calculations suggest a value in the range 37-43 Debye $Å^2$. This value is approximately four times higher than the octupole moment of carbonyl sulphide and is therefore consistent with the relative magnitudes of the dipole and quadrupole moments of cyanogen iodide and carbonyl sulphide.

As with carbonyl sulphide there are no available experimental values for the elastic constants of cyanogen iodide. Nor is any estimate of the compressibility available. However the elastic constants may still be usefully determined so that the conditions for elastic stability may be investigated. It will be shown that the lack of a value for the compressibility to act as a test for an empirical potential does not prove critical for the modelling of cyanogen iodide.

9.3: Model Potentials for Cyanogen Iodide

With the known values for the lattice energy and the torsional frequency of vibration plus the two conditions for zero stress, the procedure used for fitting an empirical potential for carbonyl sulphide may be applied to cyanogen iodide in an identical manner.

The first model investigated is the atom-atom potential without any electrostatic component. This potential proves to be as unsatisfactory for modelling the lattice properties of cyanogen iodide as it did for carbonyl sulphide. The same flaws are found, the fitting procedure always yields at least one negative ϵ parameter and at least two imaginary dispersion curves are observed. The result is expected, it has been previously shown that carbonyl sulphide could not be successfully modelled without an electrostatic component in the hybrid potential and cyanogen iodide exhibits greater multipolar character than carbonyl sulphide.

It has been discussed that for carbonyl sulphide the effects of the molecular dipole and quadrupole moments were relatively insignificant and that the octupole moment was the first moment whose contributions to the specimen lattice properties was of significance. This does not apply to cyanogen iodide. The dipole and quadrupole moments are significantly higher than for carbonyl sulphide and calculation confirms that they cannot be neglected in an electrostatic model of cyanogen iodide. The simplest "successful" potential for carbonyl sulphide was found to be the atom-atom + molecular octupole potential. The analogue of this potential has been investigated for cyanogen iodide, with the multipolar component comprising the molecular dipole, quadrupole and octupole moments. The values for the dipole and quadrupole used are the experimental values, while the value for the octupole moment is taken to be 37.0 Debye $Å^2$.

The standard fitting procedure is adopted for this potential, calculating the contributions of the three multipole moments to the specimen lattice properties and fitting the four atom-atom potential parameters so that the correct values for the lattice properties are reproduced. The parameters obtained are presented in table 9.1.

Table 9.1: Atom-Atom Lennard-Jones 12-6 + Molecular Multipole Potential for ICN: Parameters

Atom Pair	ϵ/kcal mol^{-1}	R_0/Å
like-like	-0.46105	4.1
N-C	1.39700	4.3
N-I	0.21945	4.3
C-I	0.21945	4.4

μ = 3.71 Debye, Θ = -7.33 Debye Å, Ω = 37.0 Debye Å^2

The parameter ϵ_{LL} is seen to be negative and therefore physically unrealistic. This flaw, the presence of an unrealistic ϵ parameter, is found to occur for all variations of this potential. Variation of the repulsive or dispersive exponents in the atom-atom component does not yield a set of four physically realistic parameters. The fitting procedure for these variants may produce a positive value for ϵ_{LL} but one of the other ϵ parameters is then found to be negative. This result contrasts with carbonyl sulphide, for which this form of potential did yield satisfactory values for the atom-atom parameters. The dispersion curves for this potential have also been determined and these are presented in figures 9.1 and 9.2. Once again the results can be compared with those for carbonyl sulphide. The dispersion curves in the parallel direction are real and have the same basic characteristics as those of carbonyl sulphide, although the lower

Figure 9.1: Atom-Atom Lennard-Jones 12-6 + Molecular Multipole Potential for ICN: Dispersion Curves Parallel to C_3

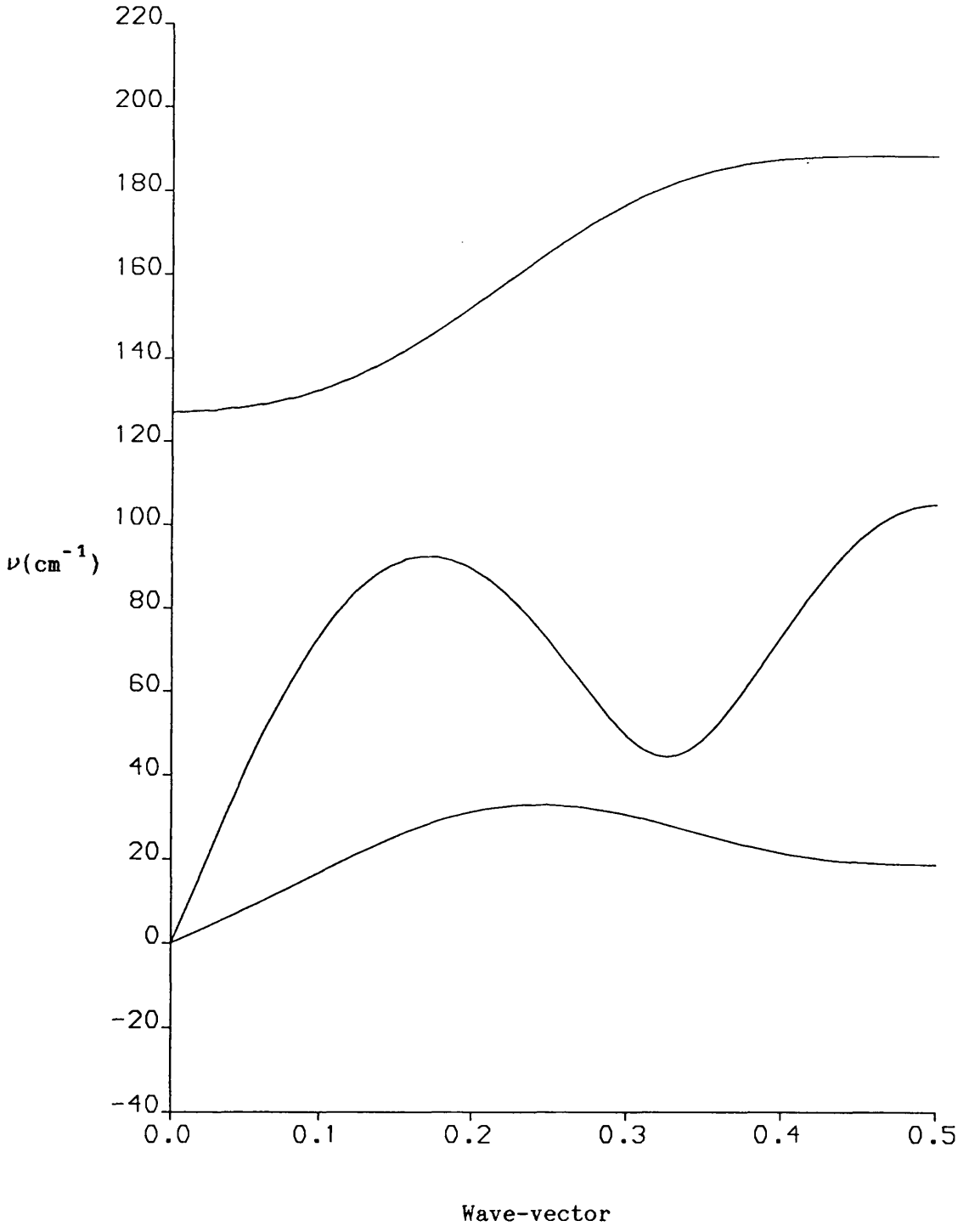

Figure 9.2: Atom-Atom Lennard-Jones 12-6 + Molecular Multipole Potential for ICN: Dispersion Curves Perpendicular to C_3

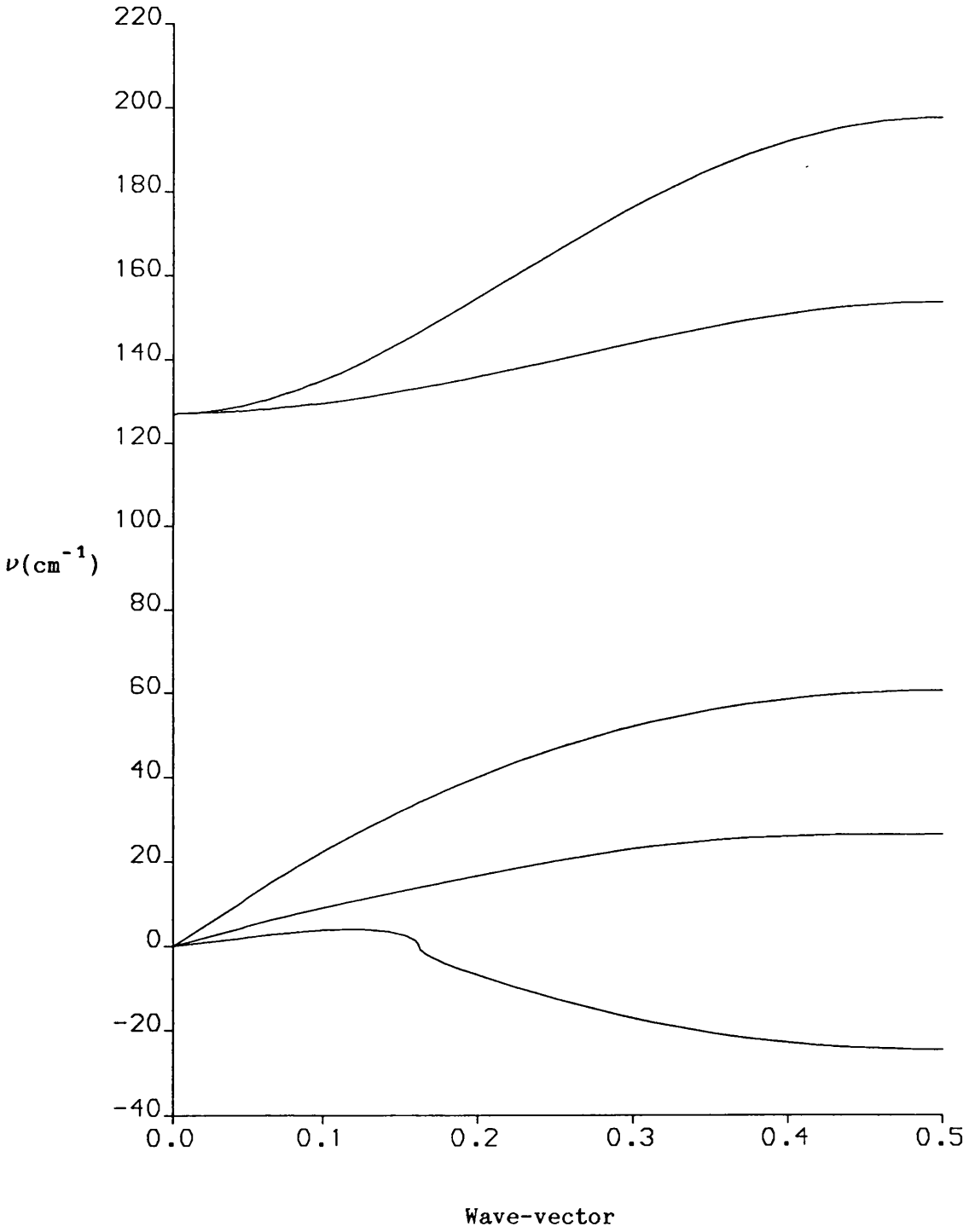

acoustic branch is significantly smaller in magnitude. In the perpendicular direction the same pattern is followed, except that the lower acoustic branch becomes imaginary at $\underset{\sim}{k} = 0.16$, this branch resembling the equivalent branch for the atom-atom 8-6 + molecular octupole potential for carbonyl sulphide. Variation of the exponents does not improve the dispersion curves either, all hybrid potentials yielding imaginary frequencies. Finally the elastic properties have also been determined and these are presented in table 9.2.

Table 9.2: Atom-Atom Lennard-Jones 12-6 + Molecular Multipole Potential for ICN: Elastic Properties

$c_{11} = 18.365$ GPa	$c_{12} = 15.990$ GPa
$c_{13} = -1.585$ GPa	$c_{15} = -1.094$ GPa
$c_{33} = 80.491$ GPa	$c_{55} = 2.736$ GPa
$S_3 = 397.314$ GPa^2	$S_4 = 0.591$ GPa^2
$\chi_0 = 0.0736$ GPa^{-1}	

The results show that this potential does at least exhibit elastic stability (the requirement being that c_{33}, c_{55}, S_3 and S_4 are all positive). As has been discussed there is no experimental value available for comparison with the calculated compressibility but it seems likely that at a third of the value for the compressibility of carbonyl sulphide this calculated value is also an underestimate.

Overall the results do not compare well with carbonyl sulphide. The hybrid potential obtained does not satisfy the conditions required, possessing an unrealistic ϵ parameter and imaginary frequencies. The atomic charge + molecular octupole, atomic quadrupole and atomic multipole models for the electrostatic interaction have also been investigated and as with carbonyl sulphide they offer no improvement

on the molecular multipole potential, each exhibiting at least one unrealistic ϵ parameter and imaginary dispersion curves. The anisotropic Berne-Pechukas potential has also been investigated and exhibits similar failings, with an unrealistic value for the molecular octupole moment generated by the fitting procedure.

9.4: Discussion

It can be seen that the hybrid potentials utilised with great success for modelling the lattice properties of carbonyl sulphide are far less successful when applied to cyanogen iodide despite the apparent similarities in their crystal structures. It would seem that these two molecular crystals are not as alike as originally proposed and the main differences between them are probably due to their differing charge distributions. The experimentally determined dipole and quadrupole moments for carbonyl sulphide are relatively small and the molecule is dominated by its large calculated octupole moment. Cyanogen iodide also has a large calculated octupole moment but the experimental values for the dipole and quadrupole moments are also high and cannot be discounted as they were for carbonyl sulphide.

In each case only the dipole and quadrupole moments have been measured experimentally but values for the higher molecular moments (up to twentieth order) as well as values for atomic moments, calculated using the Stone partition method, have been determined from ab initio calculations using the CADPAC[35] package, details of which are given in Appendix A. The values of the first six molecular multipole moments obtained by this method are presented in table 9.3. For carbonyl sulphide TZPPP basis sets are used for all three atoms while for cyanogen iodide TZPP basis sets are used for carbon and nitrogen and an SV4PPP basis set used for iodine.

Table 9.3: Molecular Multipole Moments for OCS and ICN obtained by Ab Initio Calculation

Multipole Moment	OCS	ICN
μ / Debye	0.846	3.707
Θ / Debye Å	-1.713	-7.509
Ω / Debye $Å^2$	13.534	41.609
Φ / Debye $Å^3$	2.435	-94.795
M^5/ Debye $Å^4$	32.279	316.172
M^6/ Debye $Å^5$	25.275	-976.563

Using these values for the higher moments (but retaining the experimental values for the dipole and quadrupole) the contributions of each term in the multipolar expansion, up to sixth order, to the lattice energy and the torsional frequency of vibration is given in table 9.4, along with the combined totals of the interactions up to third and sixth order. It must be noted that the molecular multipole expansion taken to higher terms does not give a good representation of the total interaction and any conclusions which are to be drawn from the calculations should be qualitative only.

The contributions for the various components to the lattice energy and torsional frequency for carbonyl sulphide are seen to have reasonable values and the octupole is seen to be an important feature of the multipolar expansion. This result is consistent with its domination of the electrostatic potentials discussed in the previous chapters, for which it should be recalled the primary requirement was that the molecular octupole should be reasonably modelled.

In contrast the values obtained for cyanogen iodide become rapidly unrealistic for the higher moments such that, for example, physically unreasonable high lattice energies are obtained.

Table 9.4: Contributions of Molecular Multipole Terms to the Lattice Energy and Torsional Frequency of Vibration for OCS and ICN

M(I) - M(J) Interaction	Lat.Energy/ kcal mol^{-1}		Torsional Freq./ cm^{-1}	
	OCS	ICN	OCS	ICN
1 - 1	0.0721	1.9289	5.560*i*	20.502*i*
2 - 2	-0.0388	-1.7614	7.444	35.771
3 - 3	-1.4263	-14.3612	65.441	147.992
4 - 4	-0.0051	-5.4286	5.098	119.128
5 - 5	0.2808	2.2622	46.993*i*	95.055*i*
6 - 6	0.0743	30.7158	28.782*i*	417.121*i*
1 - 3	0.5922	6.7476	29.098*i*	70.002*i*
1 - 5	-0.1975	-5.8379	24.354	94.356
2 - 4	-0.0412	8.6456	11.116	114.834*i*
2 - 6	0.0136	-3.4595	8.368*i*	95.102
3 - 5	0.4399	12.7157	47.583*i*	182.331*i*
4 - 6	-0.0276	-3.4916	14.745	118.090
Total (3rd)	-0.8008	-0.7476	58.825	133.641
Total (6th)	-0.2636	28.6751	30.830*i*	406.822*i*

Considering the multipolar expansion further, it should be noted that the higher order multipole moments are dominated by parts of the electron distribution which are relatively far from the molecular centre. The apparent breakdown of the multipolar expansion suggested by the above calculation may then be due to significant overlap of the free molecule wavefunctions in the crystal. The potentials used within this thesis do not take account of overlap directly and the theories which underlie them apply to zero or small overlap of the wavefunctions.

The geometry of the cyanogen iodide crystal would suggest that the overlap would be greatest along the linear chains of molecules, namely along the three-fold axis with the "short" atom-atom contact distance previously mentioned. Although carbonyl sulphide has the same structure as cyanogen iodide and both have this anomalous short contact, its lattice energy is relatively low, being almost exactly the same as that of carbon dioxide. The usual qualitative observation is that an increase in mass of a molecule leads to an increase in the lattice energy of the crystal, a trend not observed from carbon dioxide to carbonyl sulphide. However the lattice energy of cyanogen iodide is relatively high, being about the same as that of the heavier iodine molecule. These two comparisons suggest that the carbonyl sulphide molecules are more weakly bound within the crystal than cyanogen iodide molecules.

An additional piece of evidence to support this view comes from the Raman and infrared spectra of the two molecules. It has already been mentioned that a single fundamental band is observed which is assigned to a vibration in which all of the molecules tilt in phase away from the crystal three-fold axis. The corresponding force constant k, which is related to the frequency ν and the molecular moment of inertia I, by $\nu = (k/I)^{1/2}/2\pi$, gives a measure of the strength of the interaction between molecules in a linear chain. The moments of inertia of the two molecules have been calculated and are found to be 82.474 amu $Å^2$ for carbonyl sulphide and 162.378 amu $Å^2$ for cyanogen iodide. The fundamental frequencies are recalled as being 92 cm^{-1} and 127 cm^{-1} respectively. Using these values the force constants may be calculated and it is found that the ratio (k_{ICN}/k_{OCS}) has the value 3.75, further supporting the view that the binding in cyanogen iodide is considerably stronger than in carbonyl sulphide.

A final piece of indirect evidence comes from the dimer of carbonyl sulphide which has been recently investigated by Randall, Wilkie, Howard and Muenter[42]. They have shown that it has a non-polar structure, being a planar complex with the two molecular axes parallel and making an angle close to 90° with the line joining the two centres of mass. Deakin and Walmsley[43] have performed calculations on the dimer using the same type of potentials employed within this thesis and these agree with the observed structure but also indicate that there is a strong secondary minimum for a parallel polar structure.

This suggestion of a not very strongly favoured dimer structure is indirectly indicated by thermodynamic crystal properties detailed in the Handbook of Chemistry and Physics[44]. At atmospheric pressure solid carbonyl sulphide melts at 135 K while the liquid boils at 223 K. In contrast carbon dioxide sublimes at 195 K and has no liquid phase. This parallels with the previous remark about the relative magnitudes of their lattice energies, that of carbonyl sulphide being relatively low. Cyanogen iodide is more like carbon dioxide in this respect and sublimes at 318 K.

All of these arguments suggest that a successful model for cyanogen iodide should include the effect of overlap more directly, a requirement not necessary for carbonyl sulphide. As an intermediate step which can be undertaken with a simple extension of the methods developed for carbonyl sulphide the induction interaction, previously neglected, can be taken into account. This is considered in the next chapter.

10.1: Introduction

In the previous chapter a number of reasons for the failure of the extension of the various hybrid potentials, developed for carbonyl sulphide, to the superficially similar cyanogen iodide crystal were discussed. It was concluded that for cyanogen iodide the effects of electron overlap were more significant than for carbonyl sulphide and that a relatively simple first step in considering the overlap would be to determine the induction energy. In chapter 4 the induction energy was introduced as being one of the second order terms in the perturbation series of the ground-state energy of a pair of molecules, a term which it was assumed could be neglected. In this chapter the induction energy of the two molecules concerned is determined and this assumption will be examined.

10.2: Theory of Induction Energy

Every molecule which has a permanent charge distribution will have an associated electric field and electric field gradients. Any other molecule which lies within this electric field will be subject to its effects and the interaction between the two will cause a shift in the energy of the molecule, referred to as the induction energy.

If a pair of molecules are considered in isolation the induction energy of molecule B due to the charge distribution inherent in molecule A is given by:

$$u_{ind}^{(B)} = -\frac{1}{2}\alpha_{\alpha\beta}^{(B)}F_{\alpha}^{(B)}F_{\beta}^{(B)} - \frac{1}{3}A_{\alpha,\beta\gamma}^{(B)}F_{\alpha}^{(B)}F_{\beta\gamma}^{(B)} - \frac{1}{6}C_{\alpha\beta,\gamma\delta}^{(B)}F_{\alpha\beta}^{(B)}F_{\gamma\delta}^{(B)} - \ldots\ldots \qquad (10.2.1)$$

where $F_{\alpha}^{(B)}$ and $F_{\alpha\beta}^{(B)}$ are the electric field and electric field gradient

at the origin in molecule B due to the permanent charge distribution of molecule A. If there are more than two molecules present then $F_{\alpha}^{(B)}$ and $F_{\alpha\beta}^{(B)}$ are the cumulative field and field gradients due to all of the other molecules. $\alpha_{\alpha\beta}^{(B)}$ is the static dipole polarizability, $A_{\alpha,\beta\gamma}^{(B)}$ is the static dipole-quadrupole polarizability and $C_{\alpha\beta,\gamma\delta}^{(B)}$ is the static quadrupole polarizability of molecule B. It should be noted that the convention has been used whereby repeated Greek subscripts represent summation over all cartesian axes.

The electric field and first electric field gradient at the centre of molecule B may be expressed in terms of the permanent multipole moments of all the other molecules within the crystal as follows:

$$F_{\alpha}^{(B)} = - \sum_{A} \frac{\partial}{\partial R_{\alpha}^{AB}} \phi^{(A)} \qquad (10.2.2)$$

$$F_{\alpha\beta}^{(B)} = - \sum_{A} \frac{\partial^2}{\partial R_{\alpha}^{AB} \partial R_{\beta}^{AB}} \phi^{(A)} \qquad (10.2.3)$$

where $\phi^{(A)}$ is the multipole potential and R^{AB} the distance between the centres of mass of molecules A and B. In terms of the external axis system this potential is given by:

$$\phi^{(A)} = q - \mu_{\gamma} T_{\gamma}(R^{AB}) + \frac{1}{3} \Theta_{\gamma\delta} T_{\gamma\delta}(R^{AB}) - \frac{1}{15} \Omega_{\gamma\delta\varepsilon} T_{\gamma\delta\varepsilon}(R^{AB}) + \frac{1}{105} \Phi_{\gamma\delta\varepsilon\tau} T_{\gamma\delta\varepsilon\tau}(R^{AB}) - .. \qquad (10.2.4)$$

where $T_{\gamma\delta\varepsilon}(R^{AB})$ are the tensors considered in previous chapters.

Induction Energy for Rhombohedral Crystals

The expressions used for the determination of the induction energy may be considerably simplified for rhombohedral crystals such as carbonyl sulphide and cyanogen iodide. Firstly, in each case all of the multipole moments are polarized along the molecular (z) axis and

so expression (10.2.4) may be differentiated with respect to R_α^{AB} and R_β^{AB} to give the electric field and the first electric field gradient:

$$F_\alpha^{(B)} = -q \sum_A T_\alpha(R^{AB}) + \mu_z \sum_A T_{\alpha z}(R^{AB}) - \frac{1}{3}\Theta_{zz} \sum_A T_{\alpha zz}(R^{AB}) + \frac{1}{15}\Omega_{zzz} \sum_A T_{\alpha zzz}(R^{AB}) - \frac{1}{105}\Phi_{zzzz} \sum_A T_{\alpha zzzz}(R^{AB}) + .. \quad (10.2.5)$$

$$F_{\alpha\beta}^{(B)} = -q \sum_A T_{\alpha\beta}(R^{AB}) + \mu_z \sum_A T_{\alpha\beta z}(R^{AB}) - \frac{1}{3}\Theta_{zz} \sum_A T_{\alpha\beta zz}(R^{AB}) + \frac{1}{15}\Omega_{zzz} \sum_A T_{\alpha\beta zzz}(R^{AB}) - \frac{1}{105}\Phi_{zzzz} \sum_A T_{\alpha\beta zzzz}(R^{AB}) + .. \quad (10.2.6)$$

These expressions are further simplified by the symmetry of the crystals concerned. With the crystals being assumed to be infinite the reference molecule (B) may be considered as lying at the centre of the crystal and this has two consequences. Tensors of the form $T_{xzz..}(R^{AB})$ and $T_{yzz..}(R^{AB})$ are essentially mathematically odd functions and as such their summations over the infinite lattice are zero. Similarly the odd-powered tensors of the form $T_{zzz..}(R^{AB})$ are also odd functions and their summations disappear. With these simplifications the only non-zero component of the electric field is as follows:

$$F_z^{(B)} = \mu_z \sum_A T_{zz}(R^{AB}) + \frac{1}{15}\Omega_{zzz} \sum_A T_{zzzz}(R^{AB}) + \ldots \quad (10.2.7)$$

Further relations simplify the electric field-gradient components. Tensors of the form $T_{xyzz..}(R^{AB})$ are also odd functions and their summations disappear. Furthermore the cartesian fixed axis system may be conveniently defined such that tensors of the form $T^{(n)}_{xxzz..}(R^{AB})$, $T^{(n)}_{yyzz..}(R^{AB})$ and $T^{(n)}_{zzzz..}(R^{AB})$ are related by the relation:

$$T^{(n)}_{xxzz..}(R^{AB}) = T^{(n)}_{yyzz..}(R^{AB}) = -\frac{1}{2} T^{(n)}_{zzzz..}(R^{AB}) \qquad (10.2.8)$$

Noting that the total molecular charge is zero the only non-zero components of the electric field-gradient are given by:

$$F^{(B)}_{zz} = -\frac{1}{3}\Theta_{zz}\sum_{A} T_{zzzz}(R^{AB}) - \frac{1}{105}\Phi_{zzzz}\sum_{A} T_{zzzzzz}(R^{AB}) + ..$$

$$F^{(B)}_{xx} = F^{(B)}_{yy} = -\frac{1}{2} F^{(B)}_{zz} \qquad (10.2.9)$$

Using the two simplified relations for the non-zero components of the electric field and electric field-gradient (10.2.7) and (10.2.9), the required components of the electric field and the electric field-gradient may be calculated for each molecule and using (10.2.1) the induction energies determined.

10.3: Calculation of Induction Energies

The electric fields and electric field-gradients for carbonyl sulphide and cyanogen iodide are calculated for molecular multipole moments up to fourth order. The contribution of higher order terms is relatively low for both molecules and as has been discussed in the previous chapter there is some degree of doubt concerning the magnitude of these higher moments, particularly for cyanogen iodide.

Carbonyl Sulphide

The values for the molecular dipole and quadrupole moments of carbonyl sulphide are those determined experimentally and these are supplemented by the values for the octupole and hexadecapole moments quoted in the previous chapter and determined by ab initio calculation. The values for the various tensor summations and the contributions of each of the terms to the electric field and the

electric field are detailed in tables 10.1 and 10.2.

Table 10.1: Electric Field Components for OCS

n	$M^{(n)}$ / Debye $Å^{(n-1)}$	$T^{(n+1)}_{zz..}$ / $Å^{-(n+1)}$	$F^{(B)}_{z}$ / Debye $Å^{-3}$
1	0.71512	-1.9594×10^{-2}	-1.4012×10^{-2}
2	-0.79	0	0
3	13.534	-3.4558×10^{-2}	-3.1172×10^{-2}
4	2.435	0	0
Total	NA	NA	-4.5184×10^{-2}

Table 10.2: Electric Field-Gradient Components for OCS

n	$M^{(n)}$ / Debye $Å^{(n-1)}$	$T^{(n+2)}_{zz..}$ / $Å^{-(n+1)}$	$F^{(B)}_{zz}$ / Debye $Å^{-4}$
1	0.71512	0	0
2	-0.79	-3.4558×10^{-2}	-9.1004×10^{-3}
3	13.534	0	0
4	2.435	7.1346×10^{-2}	-1.6547×10^{-3}
Total	NA	NA	-1.0755×10^{-2}

To determine the induction energy, values for the various components of the polarizability tensors are also required. These have also been determined by ab initio calculation and the full tensors are quoted in Appendix A. However the symmetry of the polarizability tensors and various relations previously detailed permit the contributions of the polarizabilities detailed in equation (10.2.1) to be simplified such that the total induction energy (up to the quadrupole-quadrupole polarizability term) is given by:

$$u_{ind}^{(B)} = -\frac{1}{2}\alpha_{zz}^{(B)}F_z^{(B)}F_z^{(B)} - \frac{1}{2}A_{z,zz}^{(B)}F_z^{(B)}F_{zz}^{(B)} - \frac{3}{8}C_{zz,zz}^{(B)}F_{zz}^{(B)}F_{zz}^{(B)}$$

(10.3.1)

The contributions of each term to the induction energy may now be determined and these are presented in table 10.3.

Table 10.3: Induction Energy for OCS

Component	Polarizability	$u_{ind}^{(B)}$ / kcal mol^{-1}
α_{zz}	7.0277 Å^3	-0.10328
$A_{z,zz}$	-0.8324 Å^4	0.00291
$C_{zz,zz}$	7.0264 Å^5	-0.00439
Total	NA	-0.10476

The induction energy for carbonyl sulphide is clearly seen to be dominated by the dipole-dipole polarizability term. More importantly it should be noted that at -0.10 kcal mol^{-1} the induction energy as calculated here is only 1.6% of the total lattice energy for carbonyl sulphide (-6.72 kcal mol^{-1}), a small contribution which suggests that its earlier neglect is justifiable.

Cyanogen Iodide

The same procedure is adopted for the determination of the induction energy of cyanogen iodide. As with carbonyl sulphide the dipole and quadrupole moments used are those determined experimentally and the octupole and hexadecapole moments used are those provided by ab initio calculation. The values for the various tensor summations and the contributions of each of the terms to the electric field and the electric field are detailed in tables 10.4 and 10.5.

Table 10.4: Electric Field Components for ICN

n	$M^{(n)}$ / Debye $Å^{(n-1)}$	$T^{(n+1)}_{zz..}$ / $Å^{-(n+1)}$	$F^{(B)}_{z}$ / Debye $Å^{-3}$
1	3.71	-1.9475×10^{-2}	-7.2254×10^{-2}
2	-7.33	0	0
3	41.609	-1.8227×10^{-2}	-5.0560×10^{-2}
4	-94.795	0	0
Total	NA	NA	-1.2281×10^{-1}

Table 10.5: Electric Field-Gradient Components for ICN

n	$M^{(n)}$ / Debye $Å^{(n-1)}$	$T^{(n+2)}_{zz..}$ / $Å^{-(n+1)}$	$F^{(B)}_{zz}$ / Debye $Å^{-4}$
1	3.71	0	0
2	-7.33	-1.8227×10^{-2}	-4.4535×10^{-2}
3	41.609	0	0
4	-94.795	4.1493×10^{-2}	3.7462×10^{-2}
Total	NA	NA	-7.0724×10^{-3}

The components of the polarizability tensors have also been determined by ab initio calculation, using the TZPP/SV4PPP basis set and the full tensors are quoted in Appendix A. The contributions of each term to the induction energy are presented in table 10.6.

Table 10.6: Induction Energy for ICN

Component	Polarizability	$u^{(B)}_{ind}$ / kcal mol^{-1}
α_{zz}	9.2277 $Å^3$	-1.00187
$A_{z,zz}$	-15.3934 $Å^4$	0.09625
$C_{zz,zz}$	21.9485 $Å^5$	-0.00593
Total	NA	-0.91155

As with carbonyl sulphide the induction energy is dominated by the dipole-dipole term but for cyanogen iodide it is much higher. For cyanogen iodide the induction energy is approximately nine times higher than for carbonyl sulphide, despite the lattice energy of cyanogen iodide being approximately only twice as high. The value for the induction energy is 6.4% of the lattice energy for cyanogen iodide, a relatively significant contribution.

10.4: Discussion

The induction energies calculated here should only be considered as a first attempt at investigating the contribution of overlap to the lattice properties of carbonyl sulphide and cyanogen iodide. Only the zeroth order term in the potential expansion, the energy, itself has been considered. These calculations do support the conclusions of the previous chapter. For carbonyl sulphide the induction energy is small whereas for cyanogen iodide it is significantly higher. It should also be noted that the main contribution to the induction energy in each case comes from the dipole-dipole polarizability interacting with the electric field. For carbonyl sulphide the greatest contributor to the field is the molecular octupole, the dipolar contribution being less than half as significant. Conversely for cyanogen iodide the most important contribution comes from the molecular dipole moment.

These results support the view that for carbonyl sulphide to be successfully modelled the induction energy may be neglected but that this simplification cannot be applied to cyanogen iodide. Although initially the two molecular crystals appear to be similar there are significant differences in the charge distributions of the two and the potentials which were found to be successful for modelling carbonyl sulphide are inadequate for simple extension to cyanogen iodide.

A.1: Introduction

One of the main problems which has been discussed in this thesis for both carbonyl sulphide and cyanogen iodide is the lack of experimental data available for the electrostatic properties of the two molecules. To overcome this, the experimental values have been supplemented by results obtained from ab initio calculations. This follows the work of Deakin[26] who has discussed a number of ab initio basis sets. The primary objective of these calculations is to obtain representative values for higher molecular moments (for both molecules only the dipole and quadrupole moments are available from experimental measurements), distributed multipole analyses[33,34] and components of various molecular polarizability tensors.

All of the calculations discussed here have been performed using CADPAC, the Cambridge Analytic Derivatives Package developed by Amos et al[35]. CADPAC consists of a suite of computer programs which perform Hartree-Fock self-consistent-field linear-combination-of-atomic-orbitals molecular-orbital (HF-SCF-LCAO-MO) ab initio calculations. Default settings are provided which are appropriate for calculations on a wide range of molecules and the package may be used without specialist knowledge of the techniques used.

The basis sets used are composed of contracted Gaussian-type orbitals (CGTO's) which represent each Slater type orbital (STO). Each Hartree-Fock atomic orbital (AO) is represented by a given number of STO's. The CGTO basis sets are normally described in terms of the number of STO's which are used to represent each AO. A basis set in which the AO is represented by a single STO is described as being a minimal (M) or single-zeta (SZ) basis set. An AO represented by two

STO's is described as double-zeta (DZ) and by three STO's as triple-zeta (TZ). These sets may also be combined and often a basis set is used in which the core AO's are represented by a single (minimal) STO and the valence AO's by two (double-zeta) STO's; such a basis set is known as a split-valence (SV) basis set. A basis set can be further improved by the addition of one or more polarization functions and the inclusion of each of these is indicated by the addition of the letter P to the above nomenclature. A generalised CGTO basis set is described in the form (ls, mp, nd...) where the letters l, m, n... represent the number of s, p, d... type CGTO's.

The basis sets used have been obtained from the compilation by Poirier, Kari and Csizmadia[45]. This provides suitable basis sets for oxygen, carbon, sulphur, nitrogen and iodine although polarization functions have not been included. Suitable values for these have been obtained by Ahlrichs and Taylor[46] yielding the single polarization (P) functions with exponent η for first and second row atoms. The use of the "even-scaling" rule[47,48] enables the single polarization function to be replaced by two polarization functions (PP) with exponents $1/2\eta$ and 2η or by three polarization functions (PPP) with exponents $1/4\eta$, η and 4η. These values are given in table A.1.

Table A.1: Values for the Exponentials for the Ab Initio Single, Double and Triple Polarization Functions for C, N, O and S

atom	η	$1/2\eta$	2η	$1/4\eta$	η	4η
C	0.72	0.6944	1.44	0.3472	0.72	2.88
N	0.98	0.5102	1.96	0.2551	0.98	3.92
O	1.28	0.3906	2.56	0.1953	1.28	5.12
S	0.542	0.9225	1.084	0.4613	0.542	2.178

A.2: Ab Initio Calculations for Carbonyl Sulphide

For carbonyl sulphide two types of basis sets have been used. Split-valence basis sets reported by Dunning and Hay[49] provide sets of (3s2p) CGTO's for carbon and oxygen and a (6s4p) CGTO set for sulphur. Dunning[50] has published more sophisticated triple-zeta basis sets for carbon and oxygen using (5s3p) CGTO's. McLean and Chandler[51] have published a (6s5p) triple-zeta basis set for sulphur. The bond lengths used are the equilibrium values determined by Amos and Battaglia[52]; r(C-O) = 1.165 Å and r(C-S) = 1.558 Å.

Ab initio calculations using these basis sets lead to values for the dipole and quadrupole moments for carbonyl sulphide, both of which are experimentally determined quantities. Comparison with the dipole moment is generally good but the calculated values for the quadrupole moment are generally too high, the closest value being that obtained from the TZPPP basis sets. It is generally found that the triple-zeta (TZ) basis sets yield better results than the split-valence (SV) basis sets and that the more sophisticated polarization functions also yield better values for the dipole and quadrupole moments.

The total ground-state energies also follow this trend, their values being lower for more sophisticated basis sets. The calculated values for the higher multipole moments are dependent upon the basis set but the variation is relatively small. The components of the polarizability tensors follow the same pattern but the distributed multipole analyses are very sensitive to variation of the basis set. Representative values for these calculated properties are given below, table A.2 gives the calculated molecular multipole moments for the TZPPP basis set (used in Chapter 9), table A.3 gives the polarizability tensors for the TZPPP basis set (used in Chapter 10 for the calculation of the induction energy) and table A.4 gives the

results of the distributed multipole analysis for the TZP basis set (used in Chapter 7 for the atomic multipole model). Discussion of these values may be found in the appropriate chapters.

Table A.2: Molecular Multipole Moments for OCS - Ab Initio Calculations using TZPPP Basis Sets

μ	= 8.4620×10^{-1} Debye	Θ	= -1.7128×10^{0} Debye Å
Ω	= 1.3534×10^{1} Debye Å^2	Φ	= 2.4351×10^{0} Debye Å^3
M^5	= 3.2278×10^{1} Debye Å^4	M^6	= 2.5274×10^{1} Debye Å^5
M^7	= 4.5397×10^{1} Debye Å^6	M^8	= 1.0233×10^{2} Debye Å^7
M^9	= -2.7821×10^{1} Debye Å^8	M^{10}	= 4.0450×10^{2} Debye Å^9
M^{11}	= -5.3584×10^{2} Debye Å^{10}	M^{12}	= 1.6180×10^{2} Debye Å^{11}

Table A.3: Molecular Polarizabilities for OCS - Ab Initio Calculations using TZPPP Basis Sets

$\alpha_{\alpha\beta}$; Å^3

	x	y	z
x	2.8300	0.0000	0.0000
y	0.0000	2.8300	0.0000
z	0.0000	0.0000	7.0277

$A_{\alpha,\beta\gamma}$; Å^4

	xx	yy	zz	xy	xz	yz
x	0.0000	0.0000	0.0000	0.0000	0.7049	0.0000
y	0.0000	0.0000	0.0000	0.0000	0.0000	0.7049
z	0.4162	0.4162	-0.8324	0.0000	0.0000	0.0000

$C_{\alpha\beta,\gamma\delta}$; Å^5

	xx	yy	zz	xy	xz	yz
xx	2.4574	1.0558	-3.5132	0.0000	0.0000	0.0000
yy	1.0558	2.4574	-3.5132	0.0000	0.0000	0.0000
zz	-3.5132	-3.5132	7.0264	0.0000	0.0000	0.0000
xy	0.0000	0.0000	0.0000	0.7008	0.0000	0.0000
xz	0.0000	0.0000	0.0000	0.0000	3.7998	0.0000
yz	0.0000	0.0000	0.0000	0.0000	0.0000	3.7998

Table A.4: Distributed Multipole Analysis for OCS - Ab Initio Calculations using TZP Basis Sets

atom type	q(e)	μ(Debye)	Θ(Debye Å)
O	-0.4736	-0.1621	-0.0228
C	0.6189	-0.9654	-0.2888
S	-0.1453	0.3930	1.9108

A.3: Ab Initio Calculations for Cyanogen Iodide

For cyanogen iodide two separate types of basis sets are required. The (3s2p) split-valence and (5s3p) triple-zeta basis sets used for carbonyl sulphide may be used for carbon and nitrogen atoms in cyanogen iodide but a different set of CGTO's are required for the much larger iodine atom. Andzelm, Klobukowski and Radzio-Andzelm[53] have provided suitable basis sets for the halogens and recommend two particular types, a minimal basis set consisting of (5s4p2d) CGTO's known as an M4 basis set and a split-valence basis set consisting of (6s5p2d) CGTO's known as an SV4 basis set. The bond lengths used have been determined using microwave spectroscopy by Cazzoli, Degli Esposti and Favera[54] at r(C-N) = 1.16044 Å and r(C-I) = 1.99209 Å. As with the split-valence basis sets used for carbon, oxygen, nitrogen and sulphur, polarization functions are available which permit further improvement of the SV4 basis set. With the use of these relatively simple polarization functions values for the molecular dipole and quadrupole moments may be obtained which are in excellent agreement with the experimental values. Representative values for the ground-state energy of the molecule plus the first three molecular multipole moments are given in table A.5, where the basis sets for carbon and nitrogen are given first followed by the iodine basis set.

Table A.5: Molecular Properties for ICN - Ab Initio Calculations

Basis sets	E/hartrees	μ/Debye	Θ/DebyeÅ	Ω/DebyeÅ^2
SVP / SV4PPP	-7005.2900	3.3242	-5.9489	37.9571
TZP / SV4PPP	-7005.4009	3.6911	-7.6024	42.6599
TZPP/ SV4PPP	-7005.4048	3.7068	-7.5096	41.6081

The calculated values for the dipole moment and quadrupole moment compare well with experimental values, 3.71 Debye and -7.33 Debye Å respectively and the difference in the quality of the split-valence (SV) and triple-zeta (TZ) basis sets for C and N is clear. Further improvement of the triple-zeta basis sets for C and N by using a double polarization function leads to further improvement in the results. It should also be noted that the improvement of the quality of the basis set for I, using a triple-polarization function (again using the "even-scaling" rule to generate three values for the exponents of the polarization functions, namely 4η, η and $1/4\eta$) also further improves the results and it is concluded that the use of these more complex basis sets, whilst significantly more costly in terms of computation time, is worthwhile for the excellent results obtained.

As with carbonyl sulphide the calculations have been performed to obtain values for a number of properties which have not been measured experimentally. Representative values for these properties are given below, in each case using the TZPP/SV4PPP basis set. Table A.6 gives the calculated molecular multipole moments, table A.7 gives the polarizability tensors and table A.8 gives the results of the distributed multipole analysis.

Table A.6: Molecular Multipole Moments for ICN - Ab Initio Calculations using TZPP/SV4PPP Basis Sets

μ	$= 3.7067\times10^{0}$ Debye	Θ	$= -7.5091\times10^{0}$ Debye Å
Ω	$= 4.1608\times10^{1}$ Debye Å^2	Φ	$= -9.4792\times10^{1}$ Debye Å^3
M^5	$= 3.1616\times10^{2}$ Debye Å^4	M^6	$= -9.7653\times10^{2}$ Debye Å^5
M^7	$= 3.1604\times10^{3}$ Debye Å^6	M^8	not available
M^9	not available	M^{10}	$= -1.0848\times10^{5}$ Debye Å^9
M^{11}	$= 3.4881\times10^{5}$ Debye Å^{10}	M^{12}	$= -1.1112\times10^{6}$ Debye Å^{11}

Table A.7: Molecular Polarizabilities for ICN - Ab Initio Calculations using TZPP/SV4PPP Basis Sets

$\alpha_{\alpha\beta}$; Å^3

	x	y	z
x	4.0243	0.0000	0.0000
y	0.0000	4.0243	0.0000
z	0.0000	0.0000	9.2277

$A_{\alpha,\beta\gamma}$; Å^4

	xx	yy	zz	xy	xz	yz
x	0.0000	0.0000	0.0000	0.0000	-2.4086	0.0000
y	0.0000	0.0000	0.0000	0.0000	0.0000	-2.4086
z	7.6967	7.6967	-15.3934	0.0000	0.0000	0.0000

$C_{\alpha\beta,\gamma\delta}$; Å^5

	xx	yy	zz	xy	xz	yz
xx	6.7296	4.2447	-10.9743	0.0000	0.0000	0.0000
yy	4.2447	6.7296	-10.9743	0.0000	0.0000	0.0000
zz	-10.9743	-10.9743	21.9485	0.0000	0.0000	0.0000
xy	0.0000	0.0000	0.0000	1.2425	0.0000	0.0000
xz	0.0000	0.0000	0.0000	0.0000	7.6745	0.0000
yz	0.0000	0.0000	0.0000	0.0000	0.0000	7.6745

Table A.8: Distributed Multipole Analysis for ICN - Ab Initio Calculations using TZPP/SV4PPP Basis Sets

atom type	q(e)	μ(Debye)	Θ(Debye Å)
I	0.2292	-0.3515	-0.1840
C	0.0508	0.1851	-0.6194
N	-0.2800	0.1207	3.8856

References

[1] M.Born and K.Huang, "Dynamical Theory of Crystal Lattices", Oxford, 1954.

[2] S.Califano (editor), Lattice Dynamics and Intermolecular Forces, Proceedings of the International School of Physics "Enrico Fermi", Course LV (Academic Press, New York, 1975); [a] S.H.Walmsley.

[3] S.Califano, V.Schettino and N.Neto, "Lattice Dynamics of Molecular Crystals", Springer-Verlag, Berlin, 1981.

[4] V.Schettino and S.Califano, J.Mol.Struct, 100 (1983) 459.

[5] J.Lascombe (editor), Dynamics of Molecular Crystals, Proceedings of the 41st International Meeting of the Societe Francaise de Chemie, Division de Chemie Physique (Elsevier, Amsterdam, 1987); [a] S.H.Walmsley.

[6] S.H.Walmsley, Chem.Phys.Lett, 114 (1985) 217.

[7] S.H.Walmsley, Intern.Rev.Phys.Chem, 5 (1986) 185.

[8] M.Born and T.von Karman, Physik Z, 13 (1912) 297.

[9] H.B.Huntingdon, Solid State Physics 7 (1958) 214.

[10] A.E.H.Love, "Mathematical Theory of Elasticity", p.38. Dover, New York, 1944.

[11] S.Bhagavantam, "Crystal Symmetry and Physical Properties", p.132. Academic Press, London & New York, 1966.

[12] A.Bondi, "Physical Properties of Molecular Crystals, Liquids, and Glasses", John Wiley, New York, 1968.

[13] A.D.Buckingham in "Intermolecular Interactions: From Diatomics to Biopolymers", ed.(B.Pullman), John Wiley, New York, 1978.

[14] A.I.Kitaigorodsky, "Molecular Crystals and Molecules", Academic Press, London, 1966.

[15] B.J.Berne and P.Pechukas, J.Chem.Phys, 56 (1972) 4213.

[16] S.H.Walmsley, Chem.Phys.Lett, 49 (1977) 390.

[17] J.Corner, Proc.Roy.Soc, A192 (1948) 275.

[18] N.Neto, R.Righini, S.Califano and S.H.Walmsley, Chem.Phys, 29 (1978) 167.

[19] J.D.Kemp and W.F.Giauque, J.Am.Chem.Soc, 59 (1937) 79.

[20] S.Aung and H.L.Strauss, J.Chem.Phys, 58 (1973) 2724.

[21] L.Vegard, Z.Krist, 77 (1931) 411.

[22] J.S.W.Overell, G.S.Pawley and B.M.Powell, Acta Cryst, B 38 (1982) 1121.

[23] V.Chandrasekharan and S.H.Walmsley, Mol.Phys, 33 (1977) 573.

[24] A.Anderson and S.H.Walmsley, Mol.Phys, 7 (1964) 583.

[25] J.E.Cahill, K.L.Treuil, R.E.Miller and G.E.Leroi, J.Chem.Phys, 49 (1968) 3320.

[26] A.A.Deakin, PhD Thesis, University of London (1988).

[27] R.Stevenson, J.Chem.Phys, 27 (1957) 673.

[28] A.A.Deakin and S.H.Walmsley, Chem.Phys, 136 (1989) 105.

[29] F.H.de Leeuw and A.Dymanus, Chem.Phys.Lett, 7 (1970) 288.

[30] F.H.de Leeuw and A.Dymanus, J.Mol.Spectr, 48 (1973) 427.

[31] M.R.Battaglia, A.D.Buckingham, D.Neumark, R.K.Pierens and J.H.Williams, Mol.Phys, 43 (1981) 1015.

[32] J.Bentley in "Chemical Applications of Atomic and Molecular Electrostatic Potentials", eds.(P.Politzer and D.G.Truhlar), Plenum Press, New York, 1981.

[33] A.J.Stone, Chem.Phys.Lett, 83 (1981) 233.

[34] A.J.Stone and M.Alderton, Mol.Phys, 56 (1985) 1047.

[35] R.D.Amos, CADPAC: Cambridge Analytic Derivatives Package, Publication CCP1/84/4 (Science and Engineering Research Council, Daresbury Laboratory, Daresbury, Warrington, WA4 4AD; 1984).

[36] J.A.Ketelaar and J.W.Zwartsenberg, Rec.Trav.Chim, 58 (1939) 449.

[37] J.A.Ketelaar and S.Kruyer, Rec.Trav.Chim, 62 (1943) 550.

[38] R.Savoie and M.Pezolet, Can.J.Chem, 49 (1971) 2459.

[39] T.S.Sun and A.Anderson, J.Raman Spectr, 2 (1974) 573.

[40] C.H.Townes and A.L.Schawlow, Microwave Spectroscopy, McGraw-Hill, New York, 1955.

[41] J.J.Ewing, H.L.Tigelaar and W.H.Flygare, J.Chem.Phys, 56 (1972) 1957.

[42] R.W.Randall, J.M.Wilkie, B.J.Howard and J.S.Muenter, Mol.Phys, 69 (1990) 839.

[43] A.A.Deakin and S.H.Walmsley, J.Mol.Struct, 247 (1991) 89.

[44] "Handbook of Chemistry and Physics", ed.(R.C.Weast), CRC Press, Cleveland, Ohio.

[45] R.Poirier, R.Kari and I.G.Csizmadia, "Handbook of Gaussian Basis Sets: A Compendium for Ab Initio Molecular Orbital Calculations", Elsevier, Amsterdam, 1985.

[46] R.Ahlrichs and P.R.Taylor, J.Chim.Phys, 78 (1981) 315.

[47] R.C.Raffenetti, J.Chem.Phys, 58 (1973) 4452.

[48] J.S.Binkley and J.A.Pople, Intern.J.Quantum Chem, 9 (1975) 229.

[49] T.H.Dunning Jr. and P.J.Hay, "Methods of Electronic Structure Theory, Modern Theoretical Chemistry, Vol.3", ed.(H.F.Schaefer III), Plenum Press, New York, 1977.

[50] T.H.Dunning Jr, J.Chem.Phys, 55 (1971) 716.

[51] A.D.McLean and G.S.Chandler, J.Chem.Phys, 72 (1980) 5639.

[52] R.D.Amos and M.R.Battaglia, Mol.Phys, 36 (1978) 1517.

[53] J.Andzelm, M.Klobukowski and E.Radzio-Andzelm, J.Comput.Chem, 5 (1984) 146.

[54] G.Cazzoli, C.Degli Esposti and P.G.Favera, J.Mol.Struct, 48 (1978) 1.